

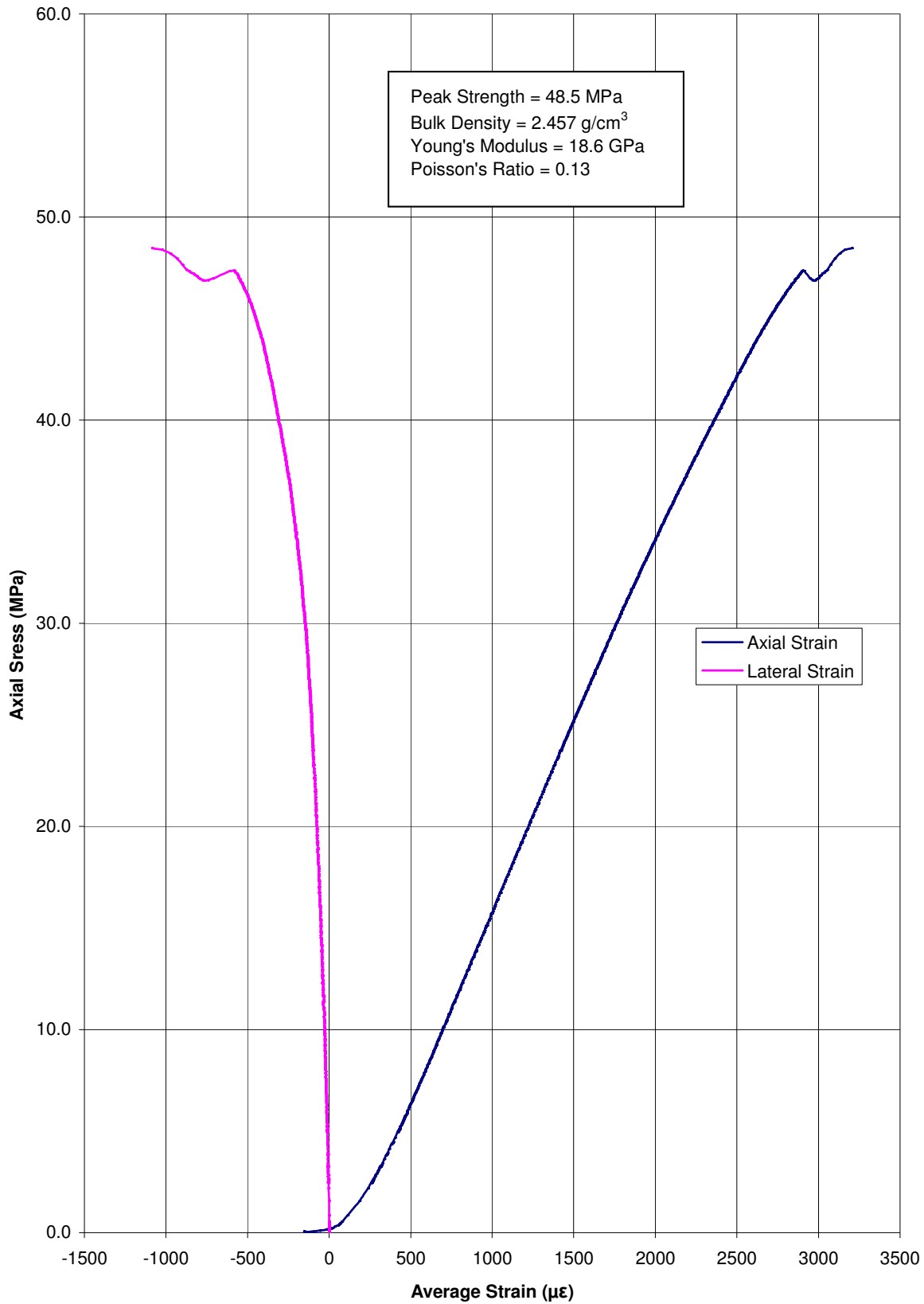
SAMPLE: END09-07-02



Length: 78.89 mm
Diameter: 45.31 mm
Density: 2.457 g/cm³
Peak Strength: 48.5 MPa
Young's Modulus: 18.6 GPa
Poisson's Ratio: 0.13
Failure Cause: Microfracture



END09-07-02 Stress vs. Strain



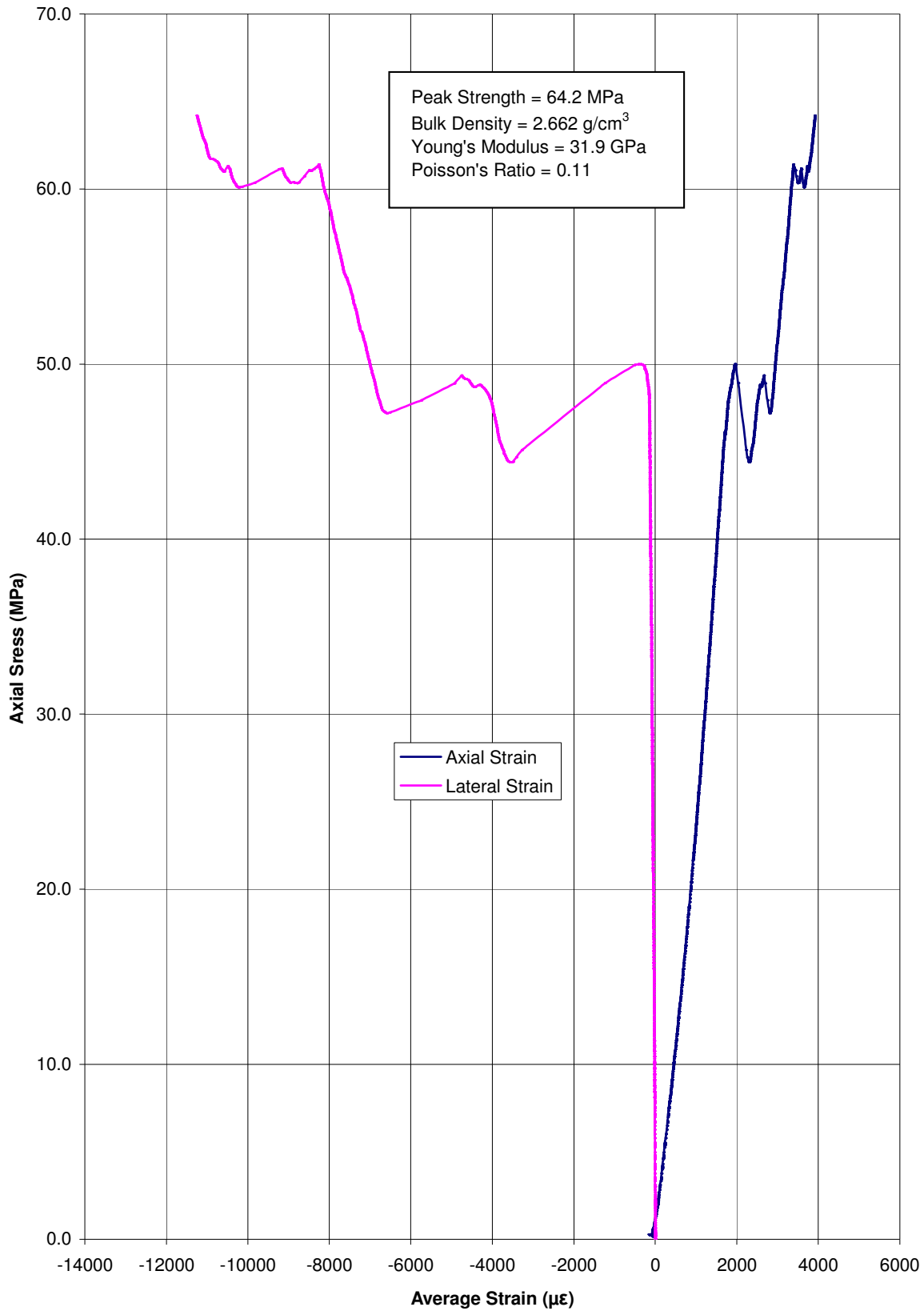
SAMPLE: END09-07-03



Length: 99.18 mm
Diameter: 45.08 mm
Density: 2.662 g/cm³
Peak Strength: 64.2 MPa
Young's Modulus: 31.9 GPa
Poisson's Ratio: 0.11
Failure Cause: Intact Rock



END09-07-03 Stress vs. Strain



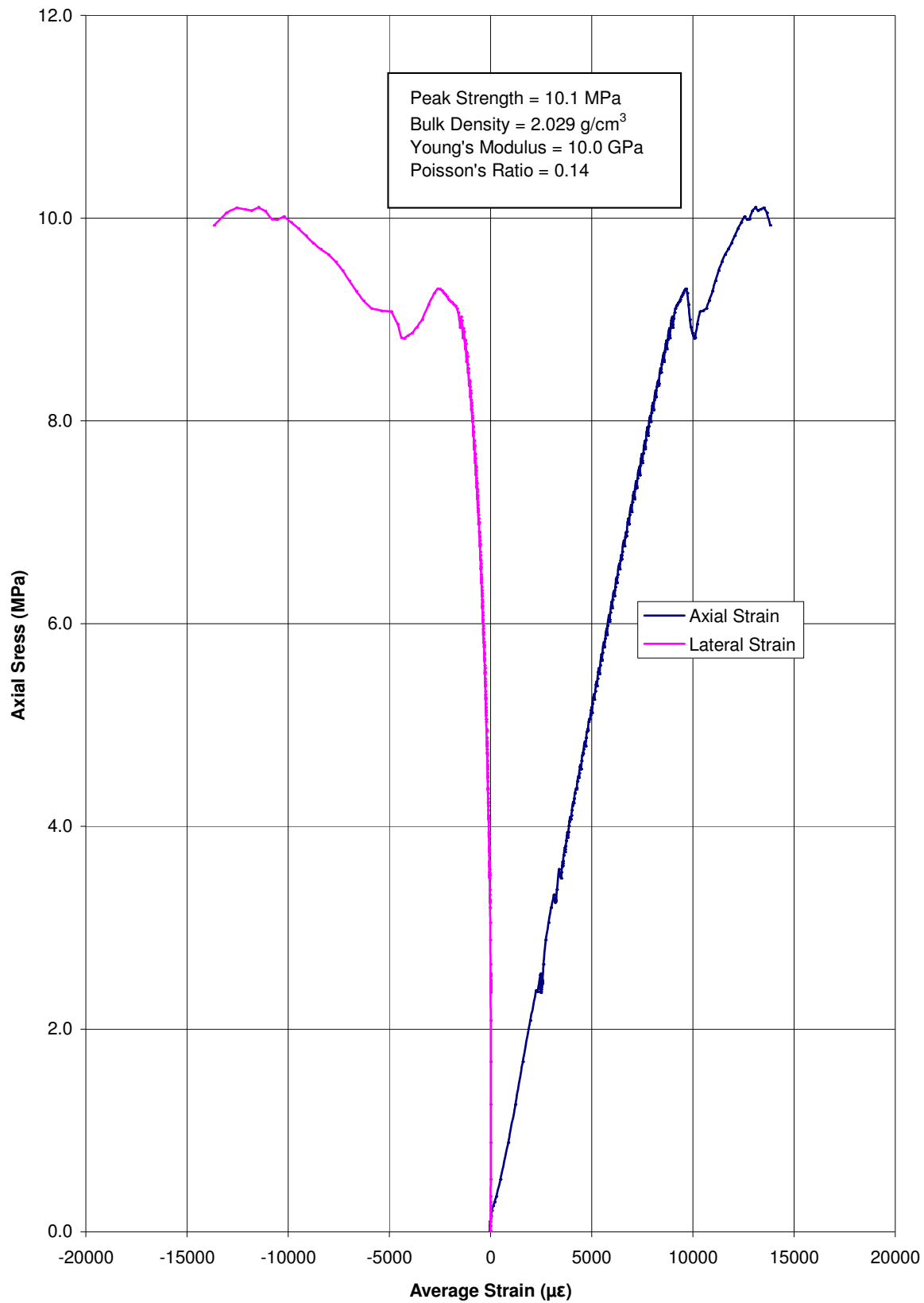
SAMPLE: END09-11-02



Length: 100.51 mm
Diameter: 47.25 mm
Density: 2.029 g/cm³
Peak Strength: 10.1 MPa
Young's Modulus: 10.0 GPa
Poisson's Ratio: 0.14
Failure Cause: Intact Rock



END09-11-02 Stress vs. Strain



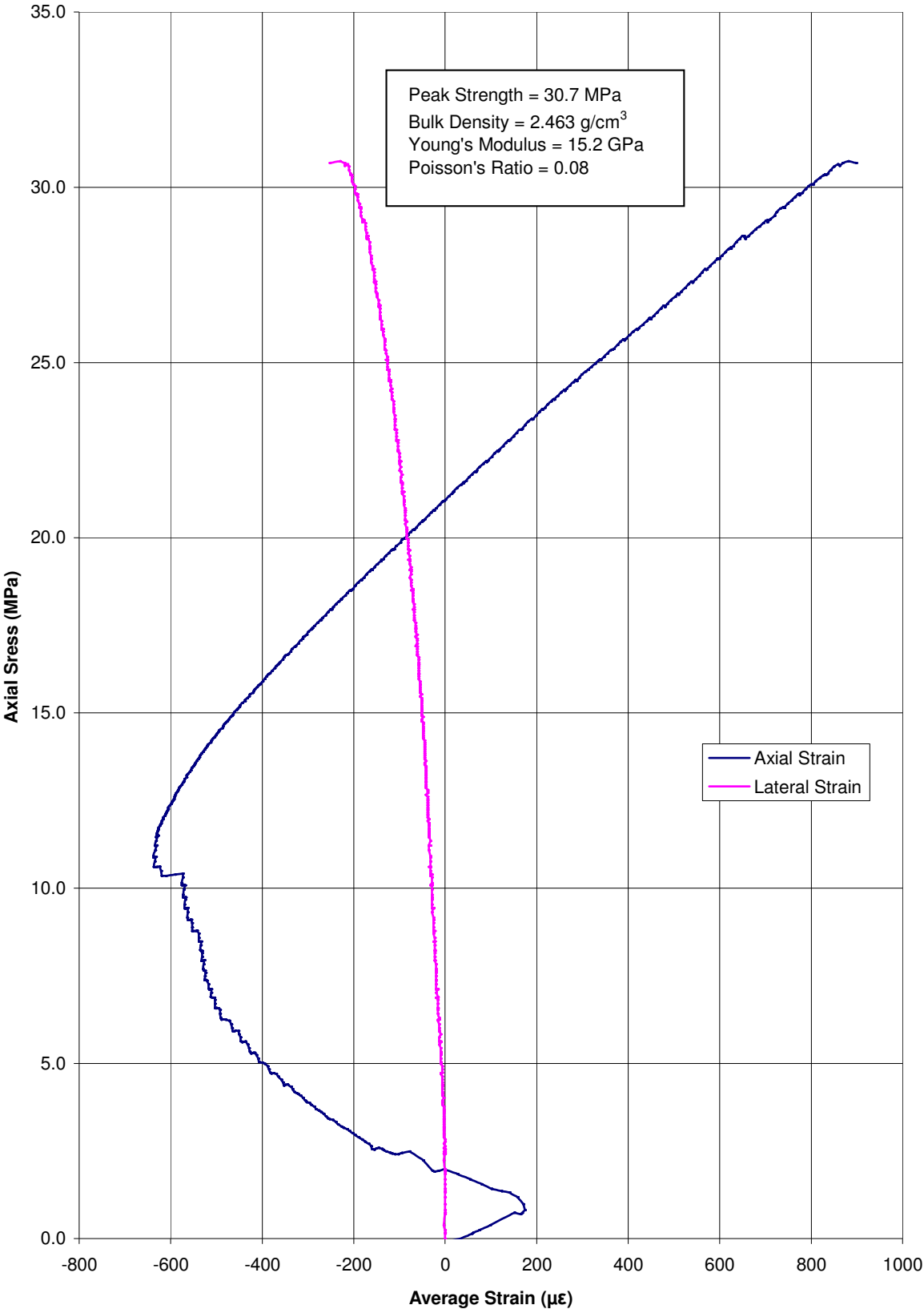
SAMPLE: END09-11-03



Length: 112.01 mm
Diameter: 47.7 mm
Density: 2.463 g/cm³
Peak Strength: 30.7 MPa
Young's Modulus: 15.2 GPa
Poisson's Ratio: 0.08
Failure Cause: Intact Rock



END09-11-03 Stress vs. Strain



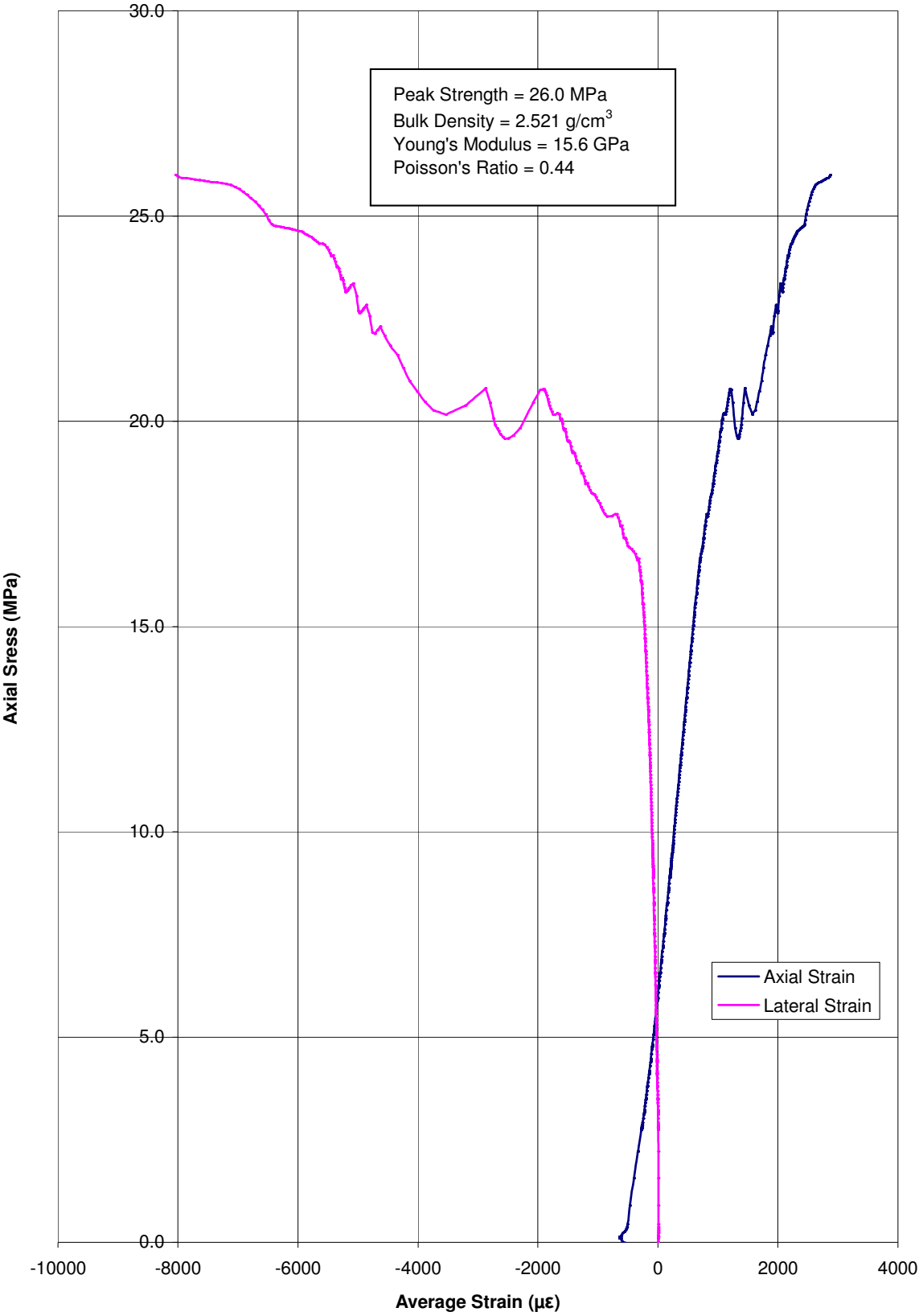
SAMPLE: END09-11-04



Length: 113.6 mm
Diameter: 47.47 mm
Density: 2.521 g/cm³
Peak Strength: 26.0 MPa
Young's Modulus: 15.6 GPa
Poisson's Ratio: 0.44
Failure Cause: Intact Rock



END09-11-04 Stress vs. Strain



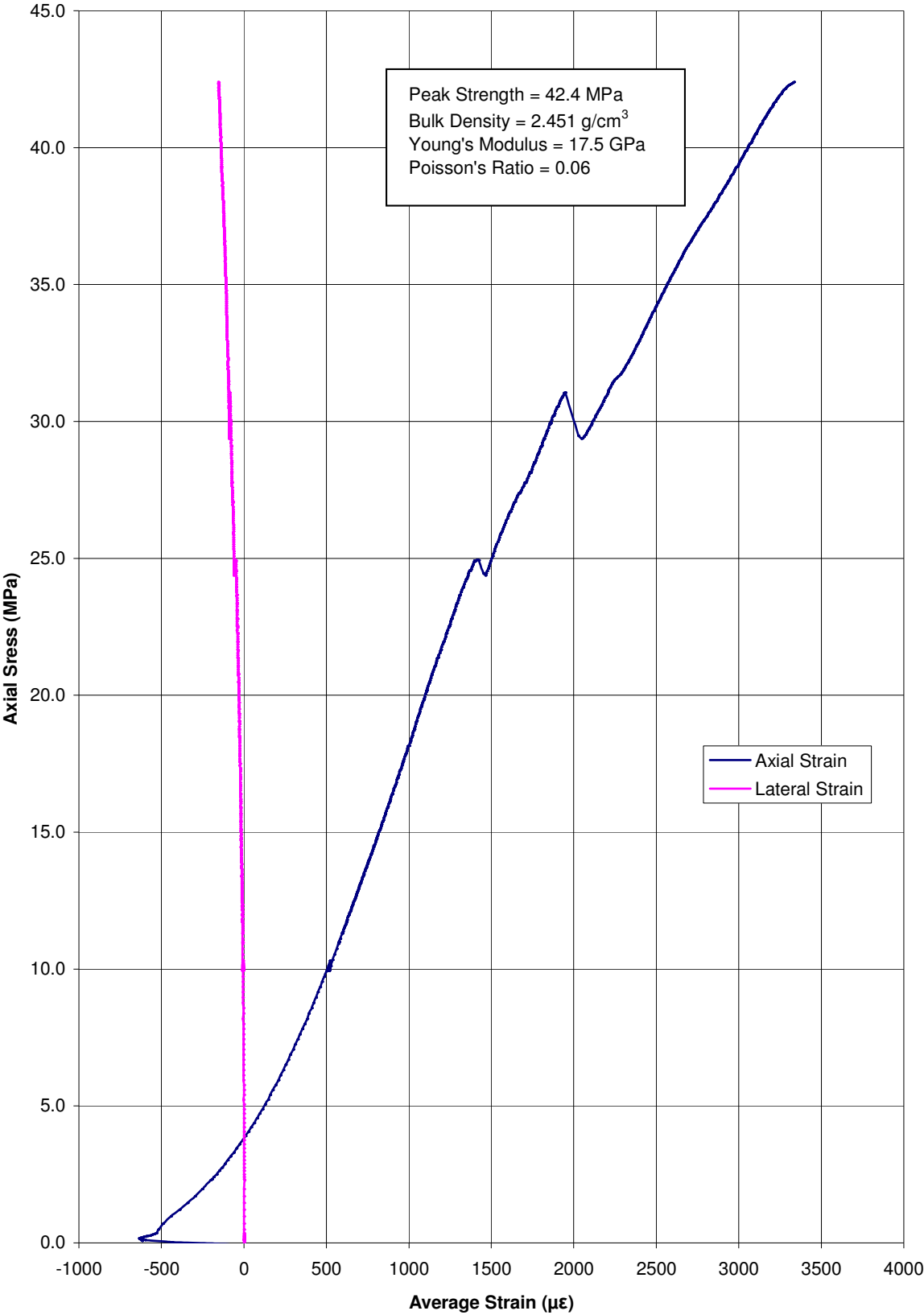
SAMPLE: END09-11-06



Length: 112.26 mm
Diameter: 47.51 mm
Density: 2.451 g/cm³
Peak Strength: 42.4 MPa
Young's Modulus: 17.5 GPa
Poisson's Ratio: 0.06
Failure Cause: Microfracture



END09-11-06 Stress vs. Strain



SAMPLE: END09-11-09



Length: 103.02 mm

Diameter: 47.06 mm

Density: 2.202 g/cm³

Peak Strength: 28.7 MPa

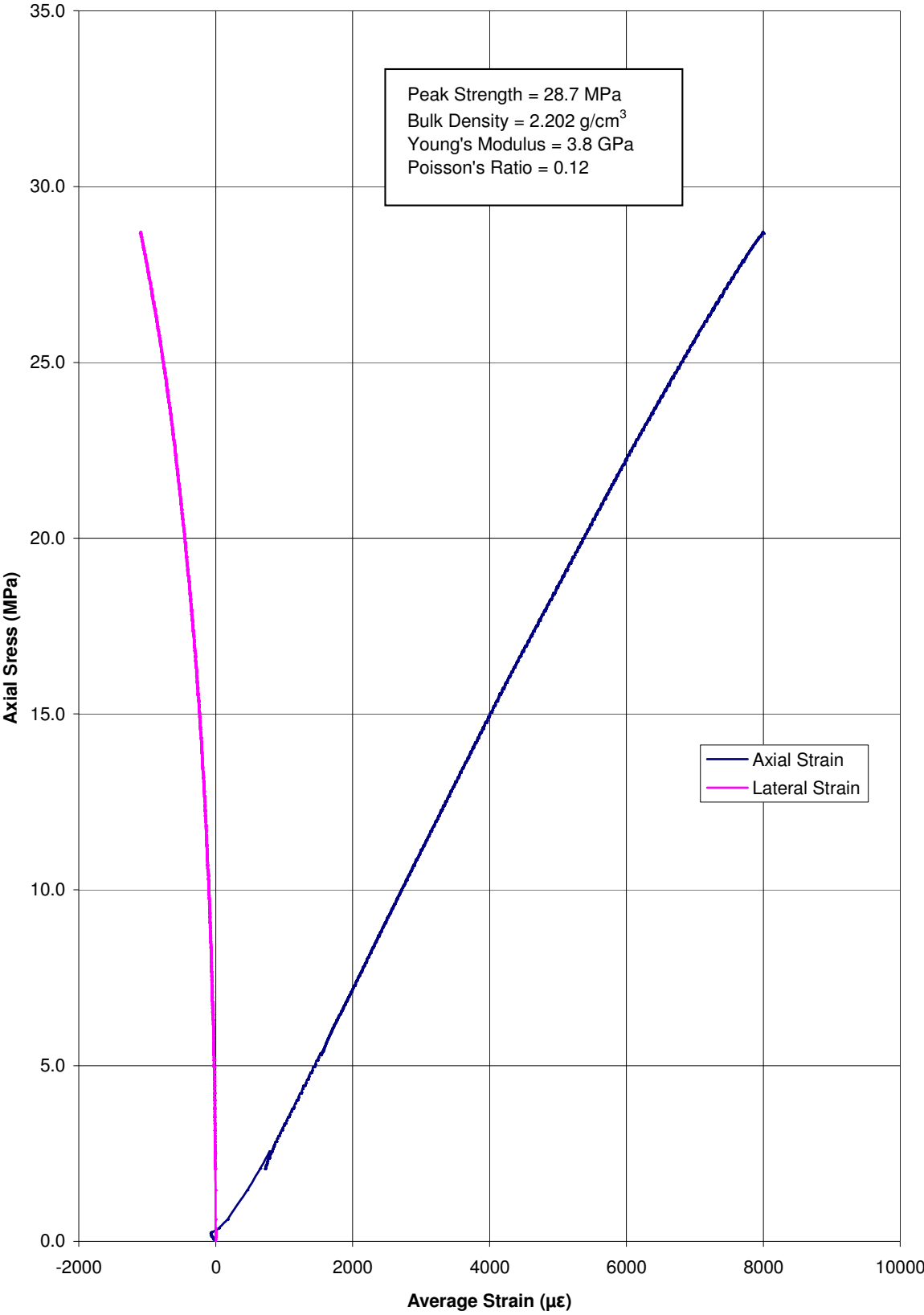
Young's Modulus: 3.8 GPa

Poisson's Ratio: 0.12

Failure Cause: Intact Rock



END09-11-09 Stress vs. Strain



SAMPLE: END09-12-04



Length: 94.16 mm

Diameter: 47.78 mm

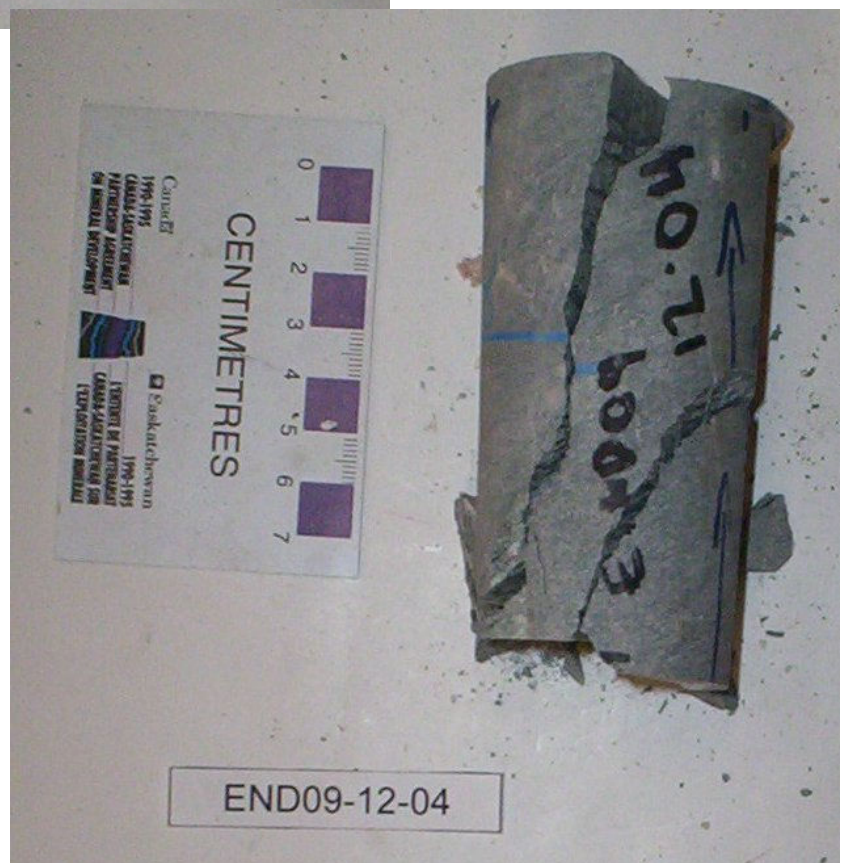
Density: 2.491 g/cm³

Peak Strength: 38.5 MPa

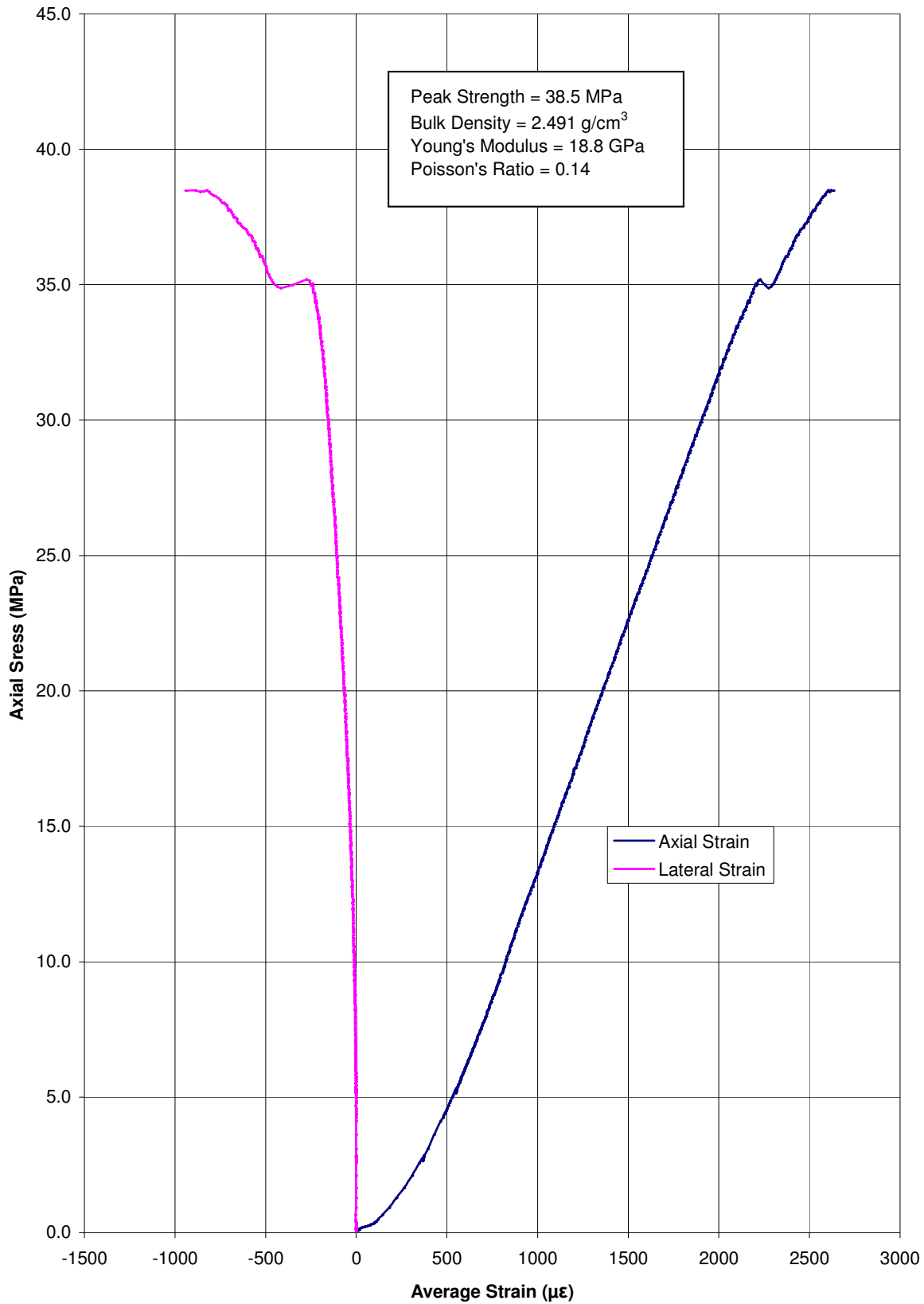
Young's Modulus: 18.8 GPa

Poisson's Ratio: 0.14

Failure Cause: Intact Rock



END09-12-04 Stress vs. Strain



SAMPLE: END09-12-06



Length: 97.82 mm

Diameter: 47.75 mm

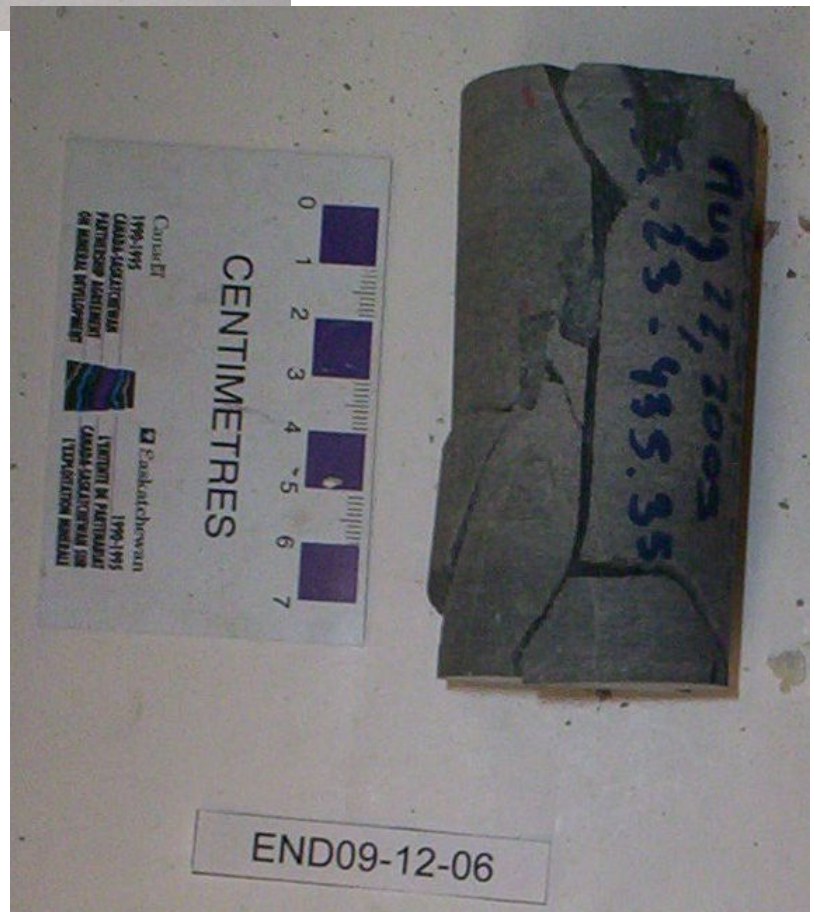
Density: 2.601 g/cm³

Peak Strength: 119.6 MPa

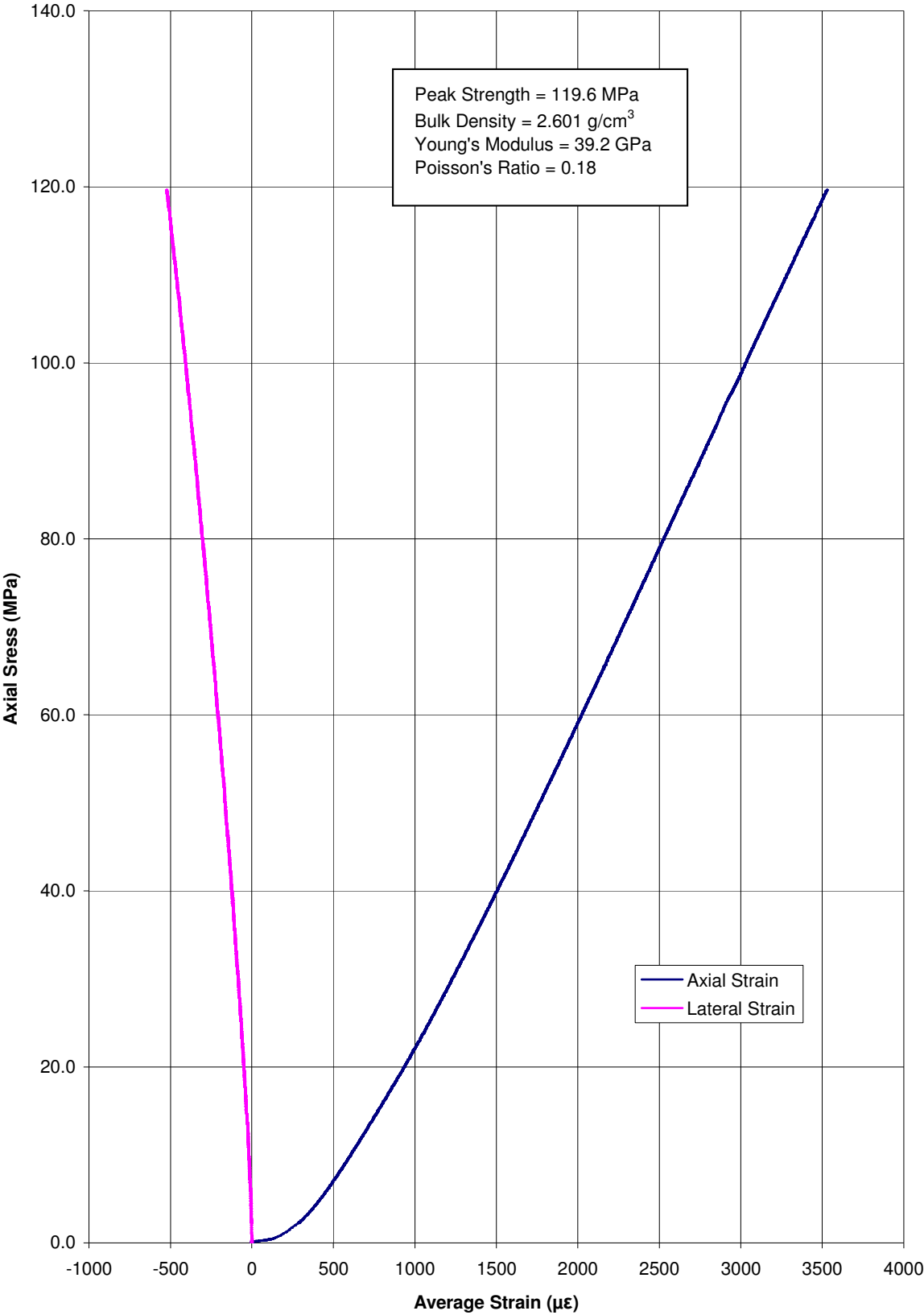
Young's Modulus: 39.2 GPa

Poisson's Ratio: 0.18

Failure Cause: Intact Rock



END09-12-06 Stress vs. Strain



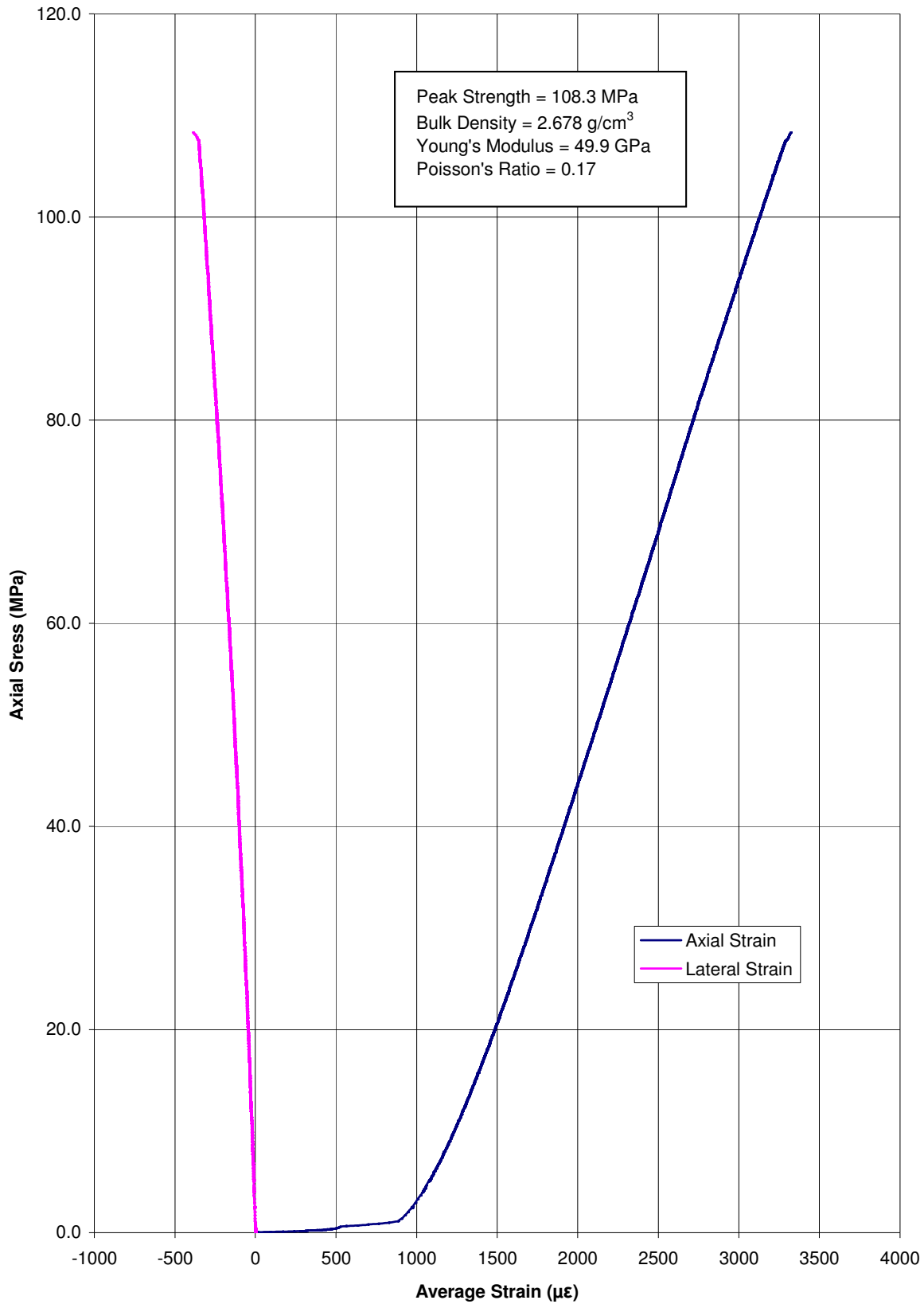
SAMPLE: MZ09-01A-02



Length: 107.28 mm
Diameter: 44.86 mm
Density: 2.678 g/cm³
Peak Strength: 108.3 MPa
Young's Modulus: 49.9 GPa
Poisson's Ratio: 0.17
Failure Cause: Intact Rock



MZ09-01A-02 Stress vs. Strain



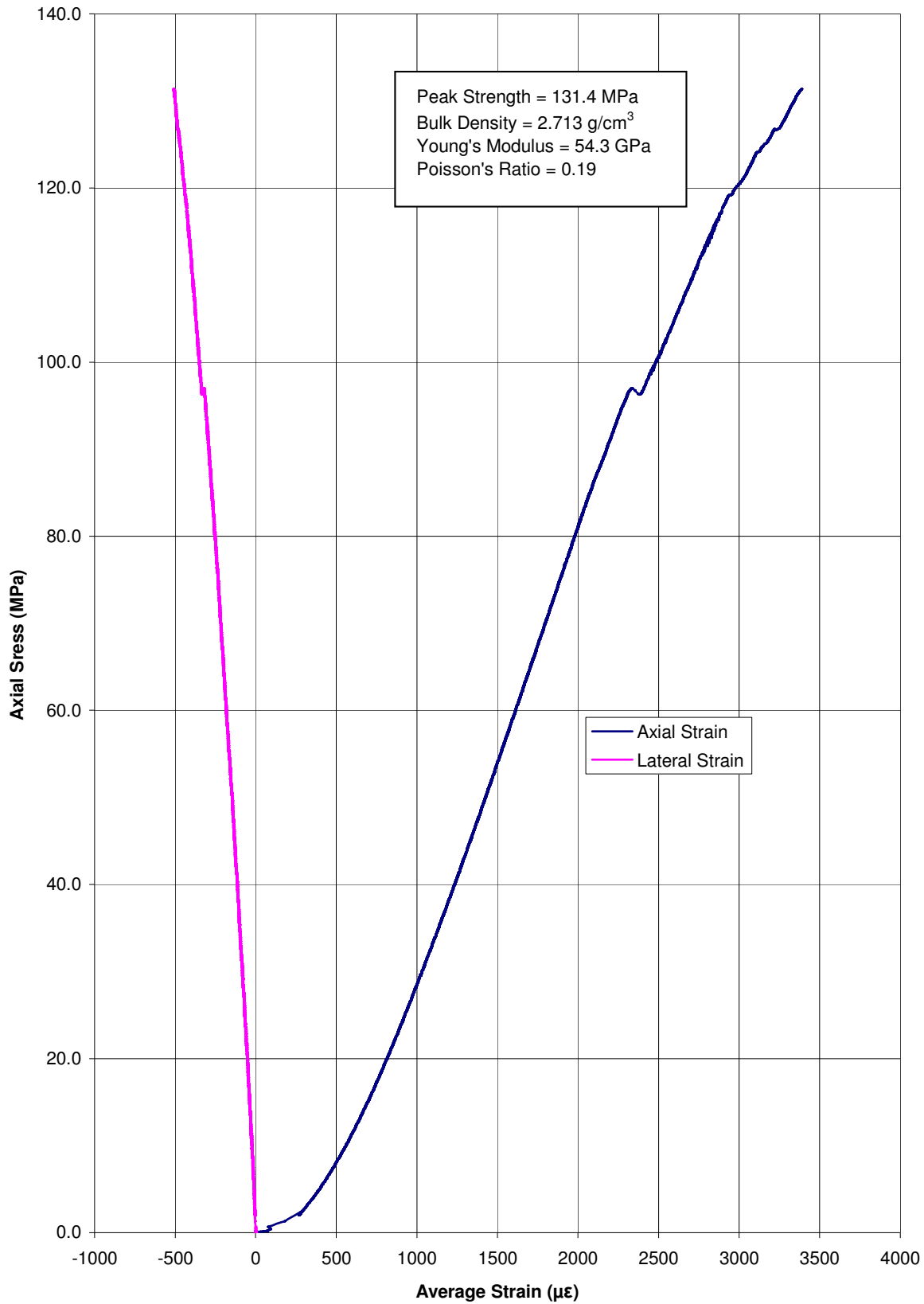
SAMPLE: MZ09-01A-03



Length: 108.29 mm
Diameter: 45.01 mm
Density: 2.713 g/cm³
Peak Strength: 131.4 MPa
Young's Modulus: 54.3 GPa
Poisson's Ratio: 0.19
Failure Cause: Intact Rock



MZ09-01A-03 Stress vs. Strain



SAMPLE: MZ09-01A-05



Length: 106.62 mm

Diameter: 44.61 mm

Density: 2.619 g/cm³

Peak Strength: 86.3 MPa

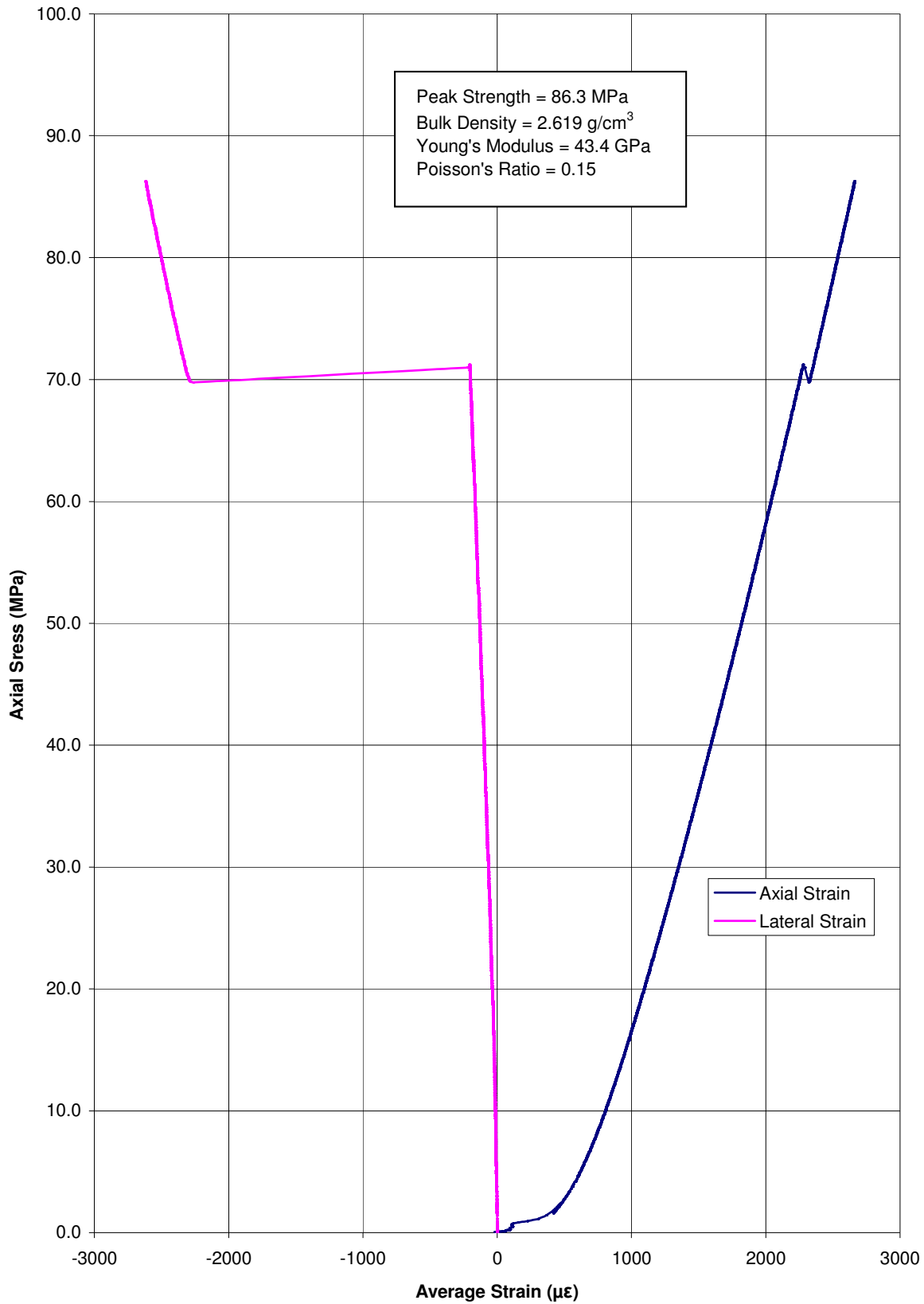
Young's Modulus: 43.4 GPa

Poisson's Ratio: 0.15

Failure Cause: Intact Rock



MZ09-01A-05 Stress vs. Strain



SAMPLE: MZ09-01A-06



Length: 109.53 mm

Diameter: 44.69 mm

Density: 2.236 g/cm³

Peak Strength: 30.0 MPa

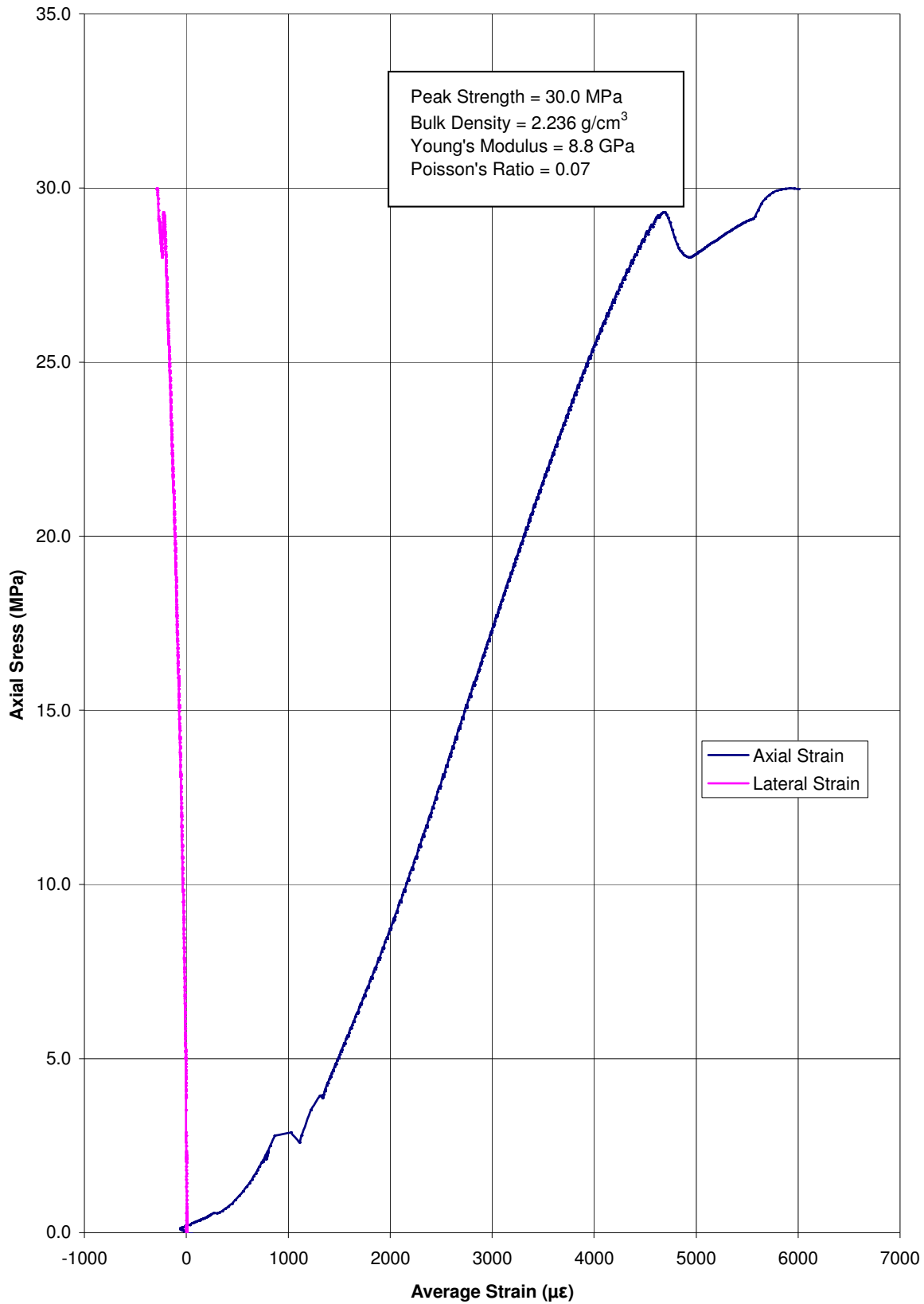
Young's Modulus: 8.8 GPa

Poisson's Ratio: 0.07

Failure Cause: Intact Rock



MZ09-01A-06 Stress vs. Strain



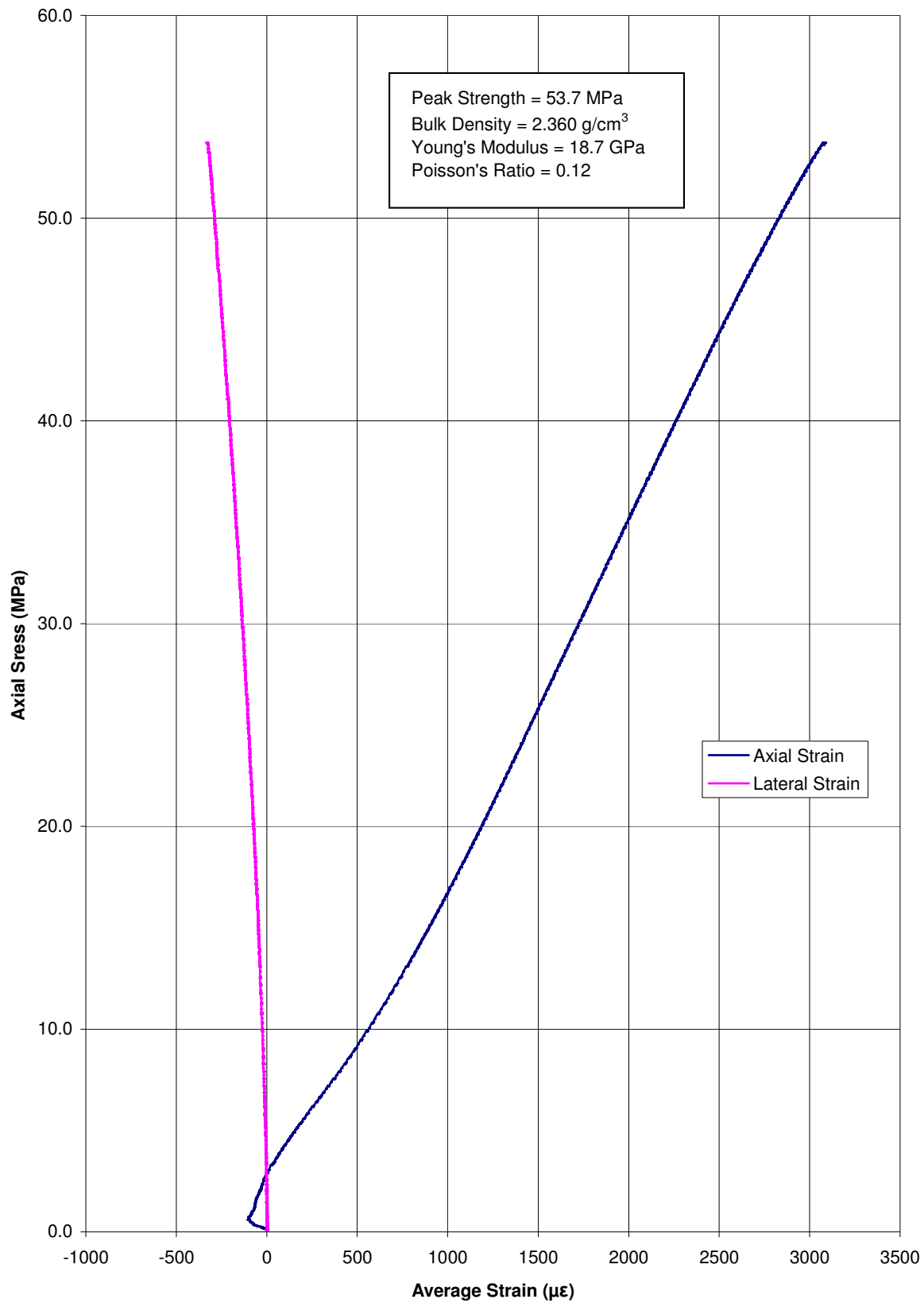
SAMPLE: MZ09-01A-07



Length: 108.02 mm
Diameter: 44.48 mm
Density: 2.360 g/cm³
Peak Strength: 53.7 MPa
Young's Modulus: 18.7 GPa
Poisson's Ratio: 0.12
Failure Cause: Intact Rock



MZ09-01A-07 Stress vs. Strain



SAMPLE: MZ09-02-01



Length: 89.15 mm

Diameter: 44.95 mm

Density: 2.367 g/cm³

Peak Strength: 21.8 MPa

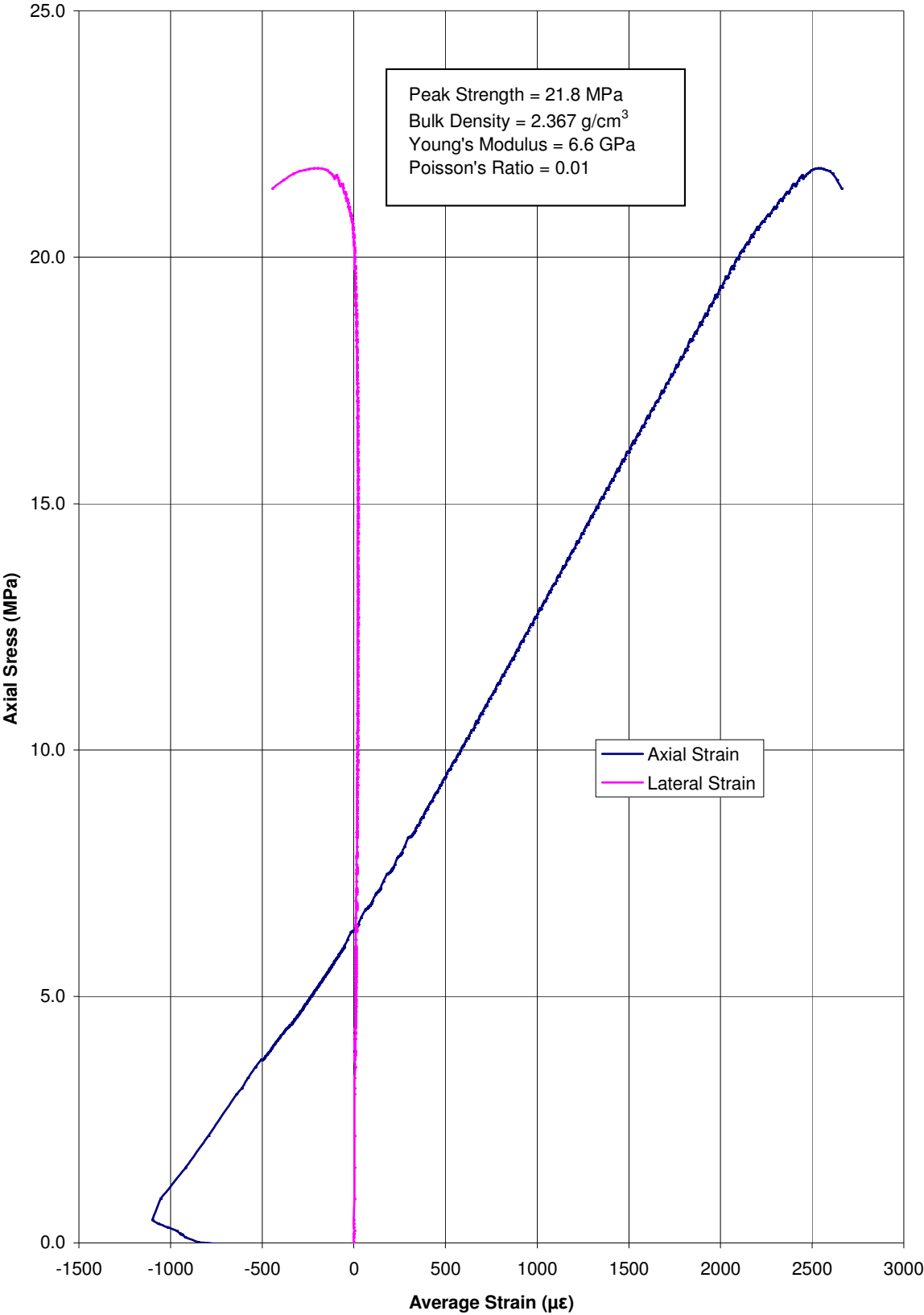
Young's Modulus: 6.6 GPa

Poisson's Ratio: 0.01

Failure Cause: Intact Rock



MZ09-02-01 Stress vs. Strain



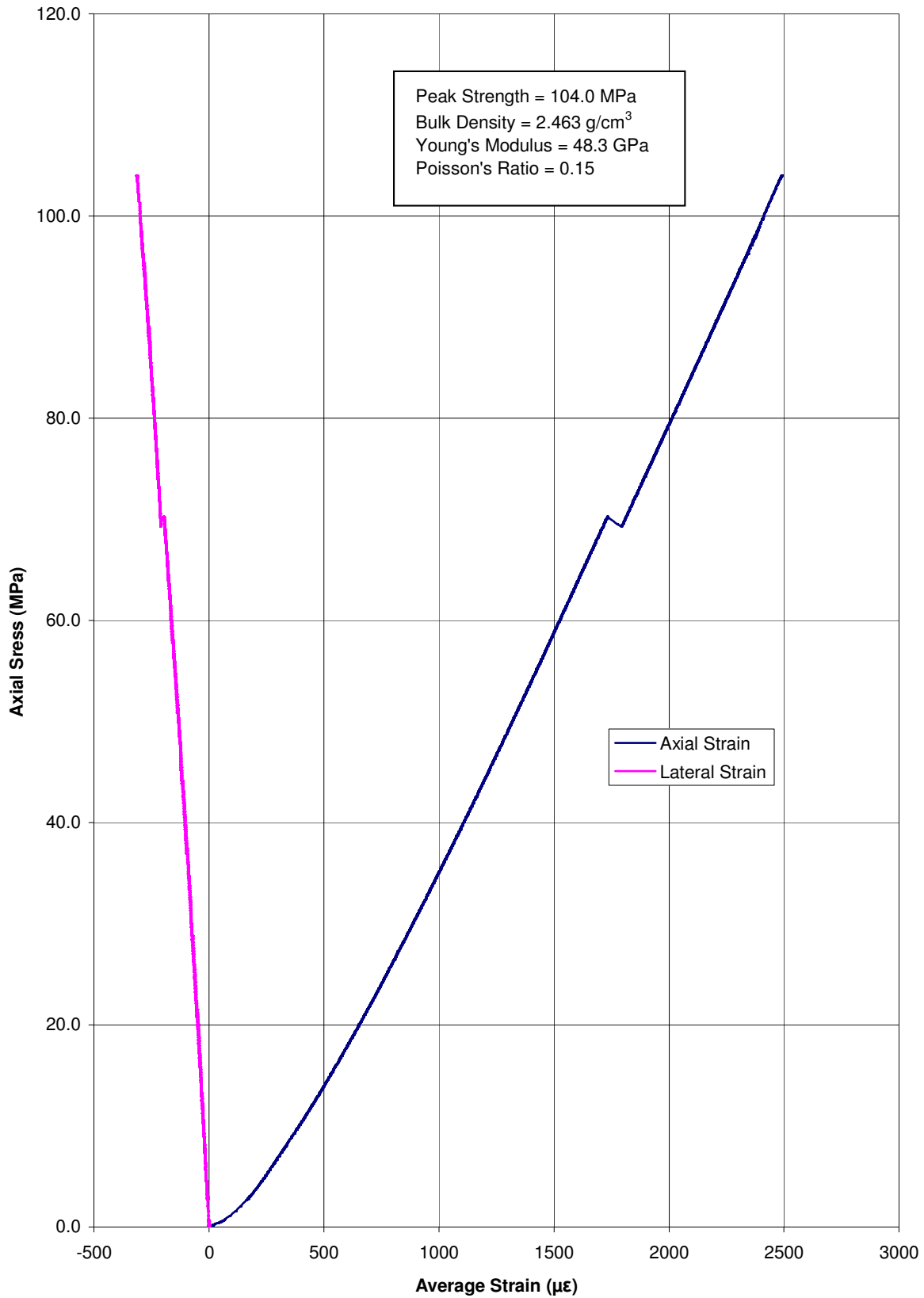
SAMPLE: MZ09-02-02



Length: 108.45 mm
Diameter: 44.78 mm
Density: 2.463 g/cm³
Peak Strength: 104.0 MPa
Young's Modulus: 48.3 GPa
Poisson's Ratio: 0.15
Failure Cause: Intact Rock



MZ09-02-02 Stress vs. Strain



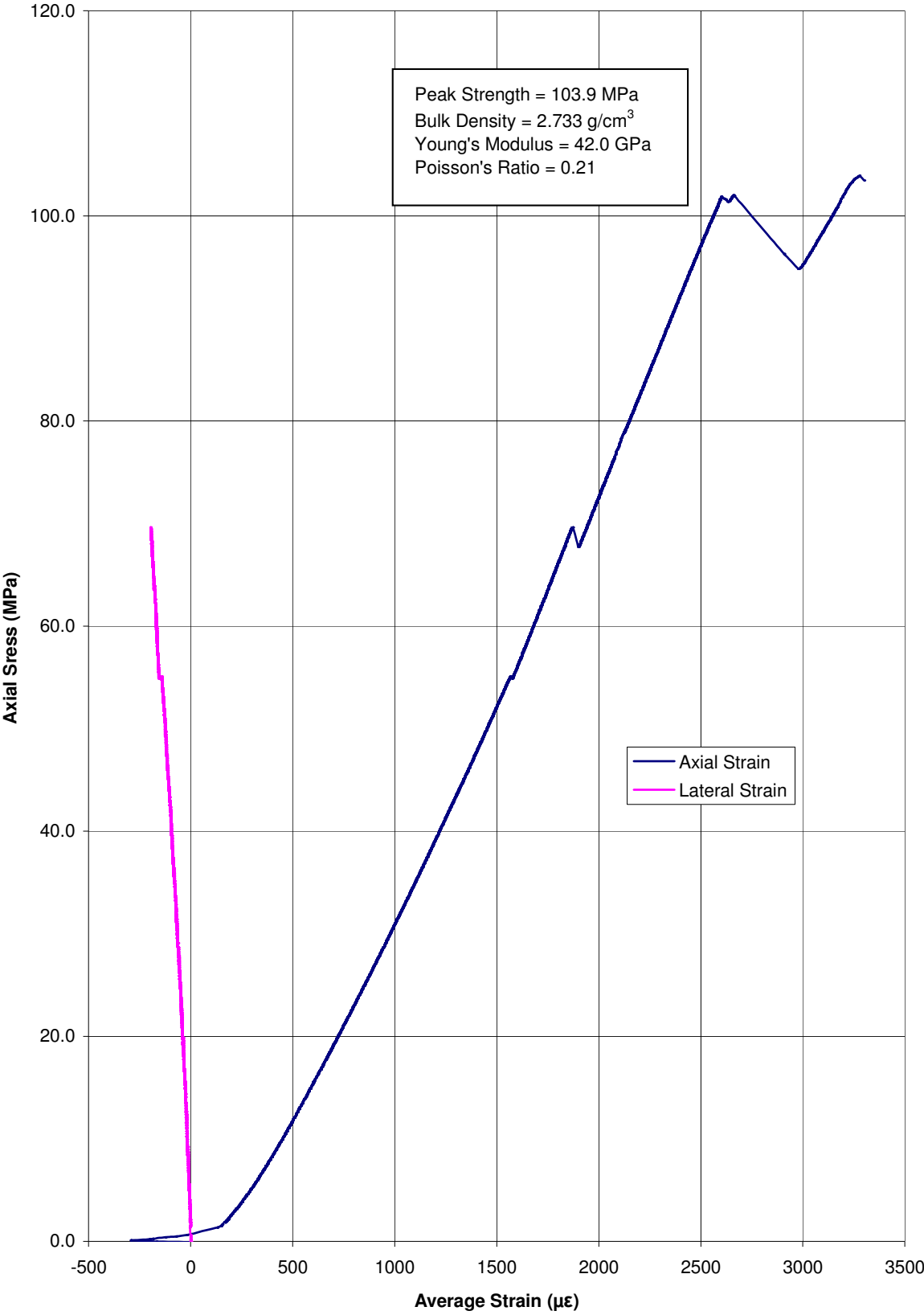
SAMPLE: MZ09-02-03



Length: 109.64 mm
Diameter: 44.85 mm
Density: 2.733 g/cm³
Peak Strength: 103.9 MPa
Young's Modulus: 42.0 GPa
Poisson's Ratio: 0.21
Failure Cause: Intact Rock



MZ09-02-03 Stress vs. Strain



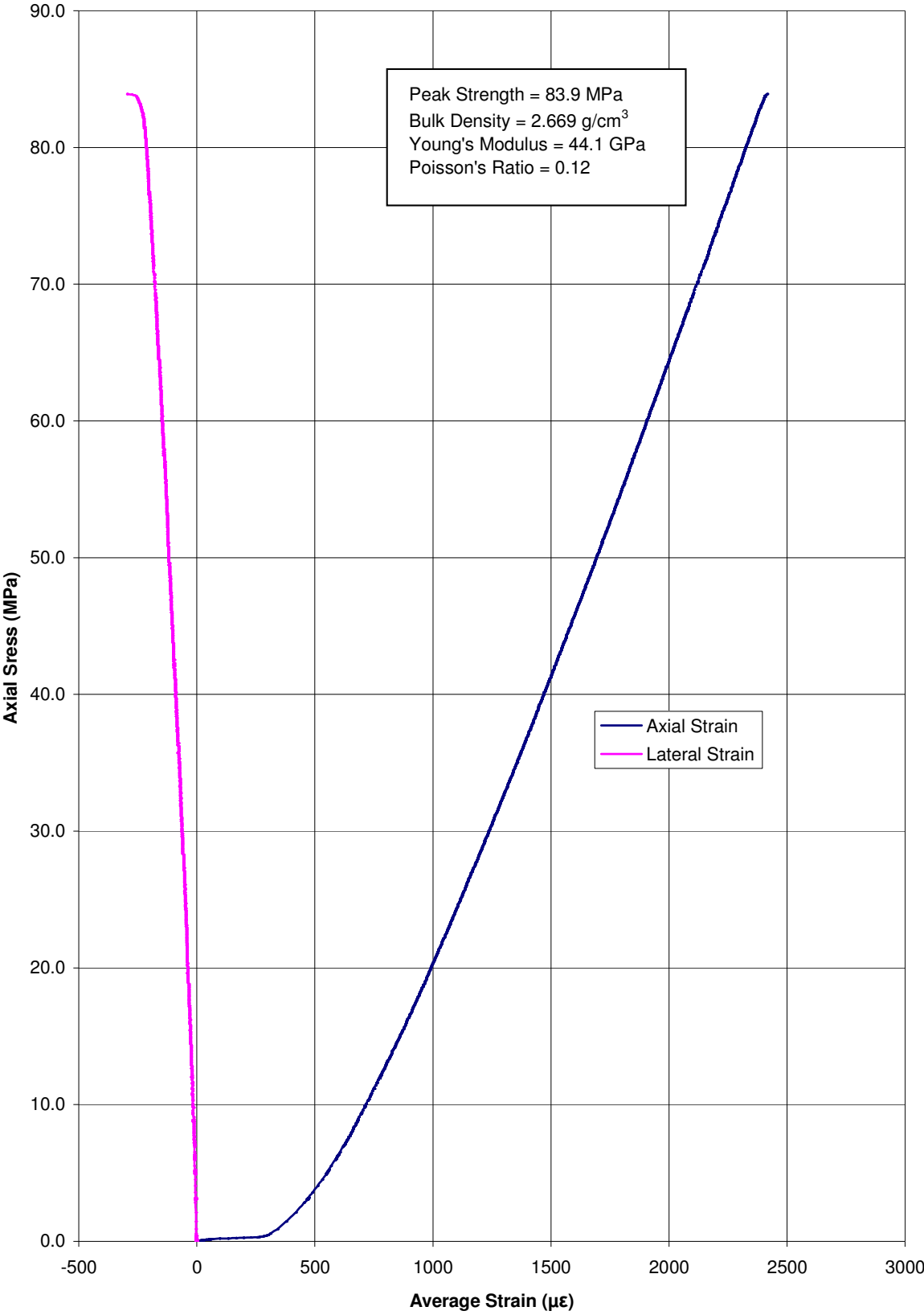
SAMPLE: MZ09-02-04



Length: 106.41 mm
Diameter: 44.98 mm
Density: 2.669 g/cm³
Peak Strength: 83.9 MPa
Young's Modulus: 44.1 GPa
Poisson's Ratio: 0.12
Failure Cause: Weakness Plane



MZ09-02-04 Stress vs. Strain



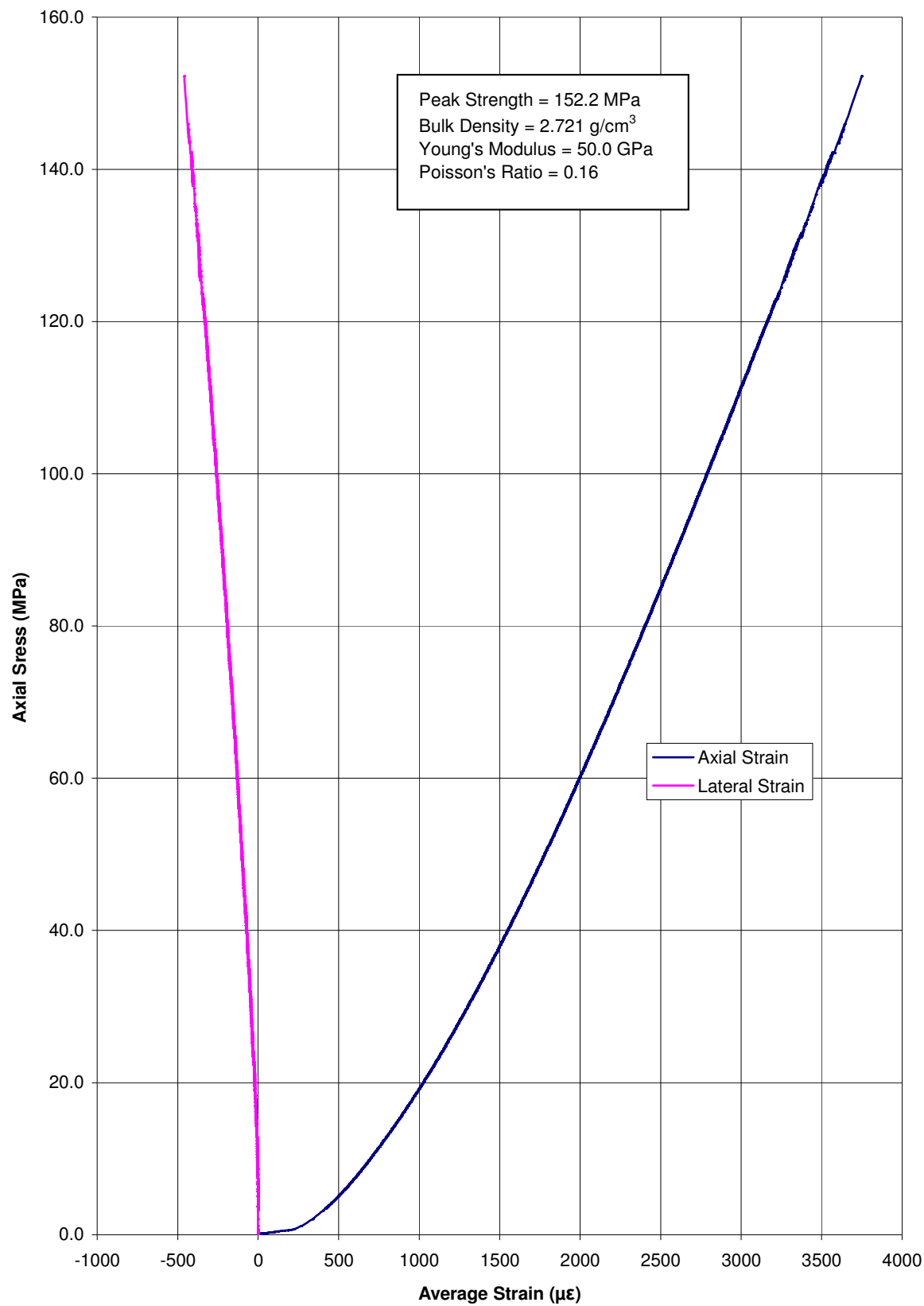
SAMPLE: MZ09-02-05



Length: 106.91 mm
Diameter: 44.91 mm
Density: 2.721 g/cm³
Peak Strength: 152.2 MPa
Young's Modulus: 50.0 GPa
Poisson's Ratio: 0.16
Failure Cause: Intact Rock



MZ09-02-05 Stress vs. Strain



SAMPLE: MZ09-02-06



Length: 109.13 mm

Diameter: 45.14 mm

Density: 2.613 g/cm³

Peak Strength: 111.1 MPa

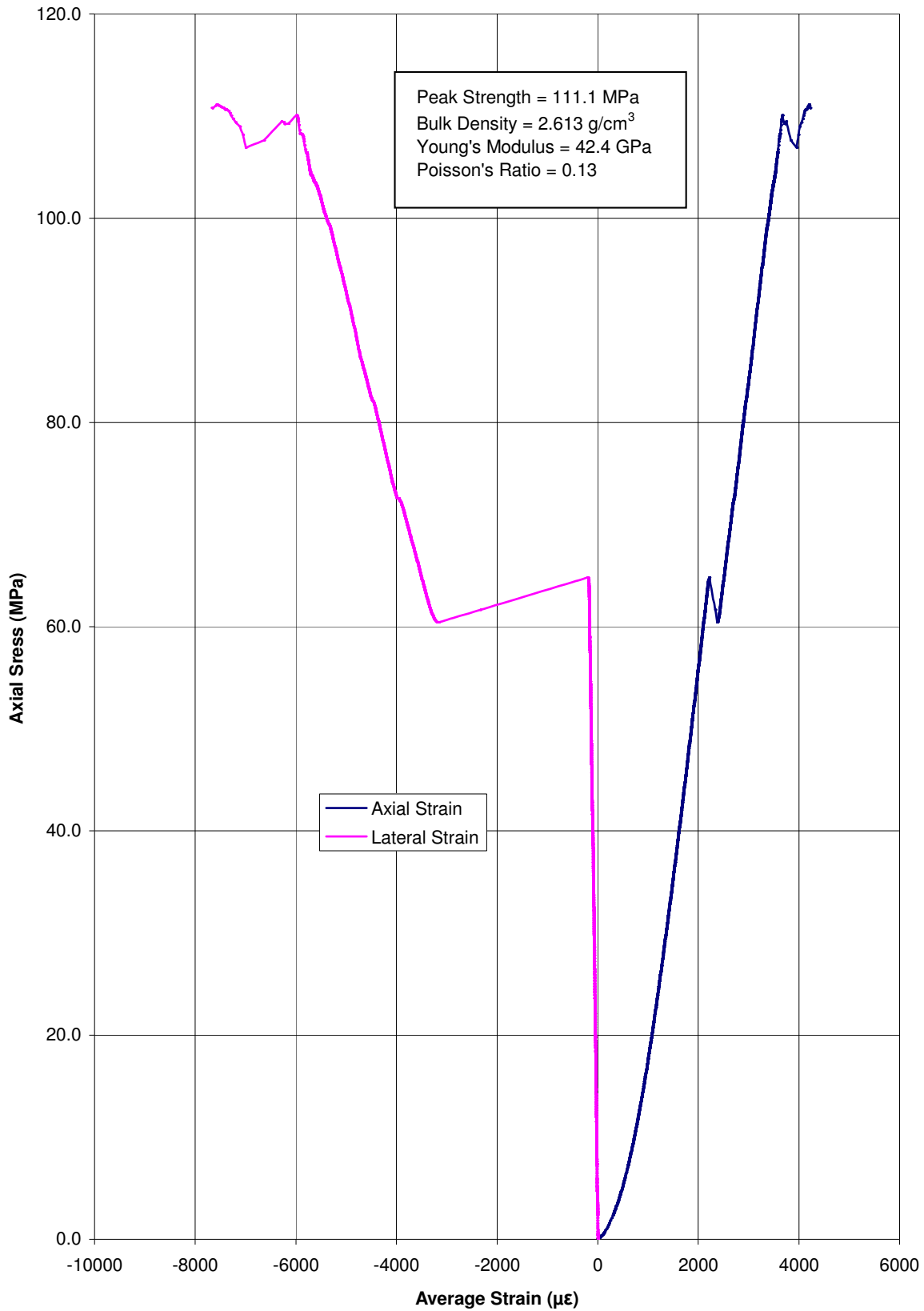
Young's Modulus: 42.4 GPa

Poisson's Ratio: 0.13

Failure Cause: Intact Rock



MZ09-02-06 Stress vs. Strain



SAMPLE: MZ09-03-03



Length: 108.46 mm

Diameter: 45.09 mm

Density: 2.697 g/cm³

Peak Strength: 101.7 MPa

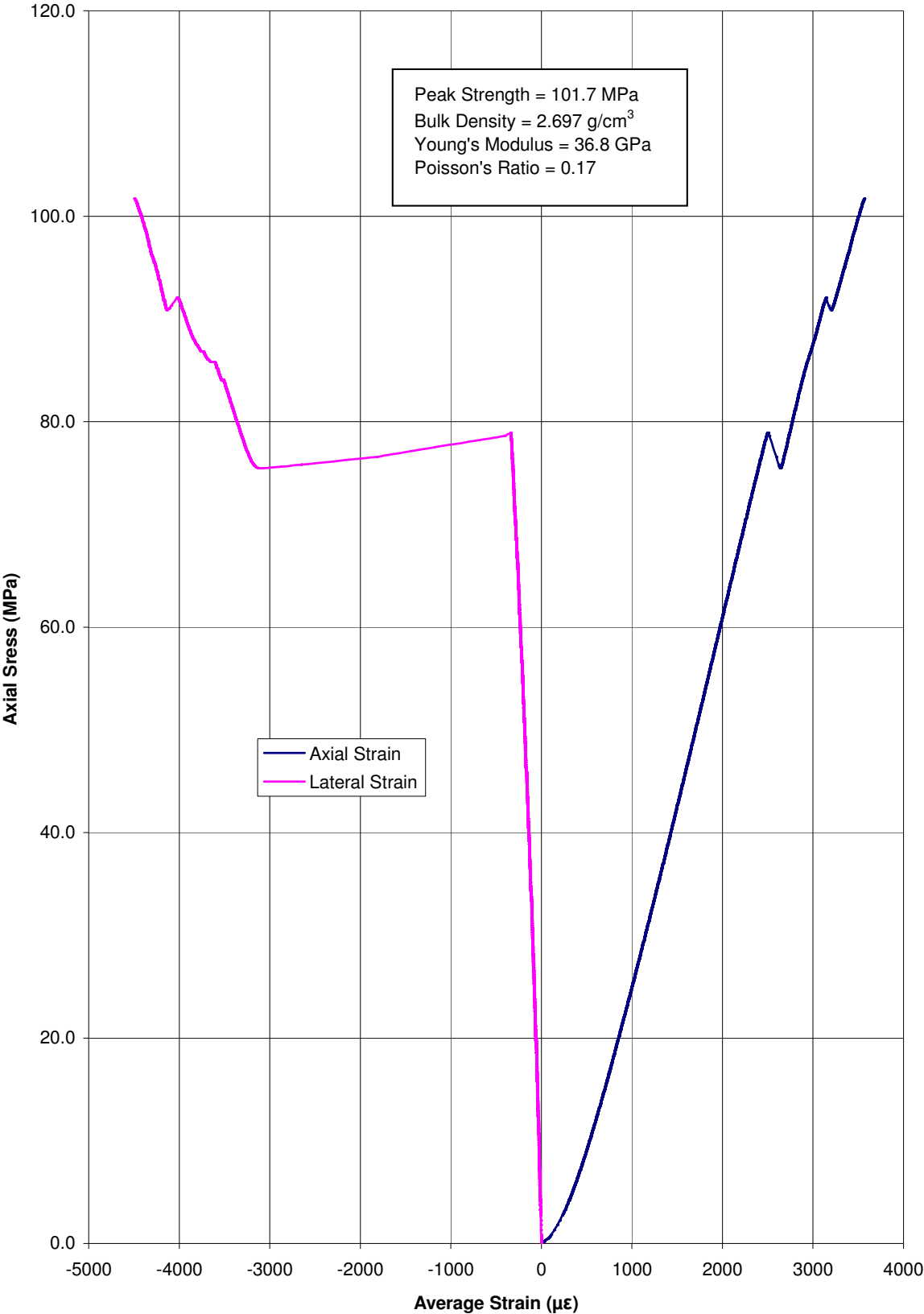
Young's Modulus: 36.8 GPa

Poisson's Ratio: 0.17

Failure Cause: Intact Rock



MZ09-03-03 Stress vs. Strain



SAMPLE: MZ09-03-04



Length: 109.51 mm

Diameter: 45.03mm

Density: 2.614 g/cm³

Peak Strength: 99.5 MPa

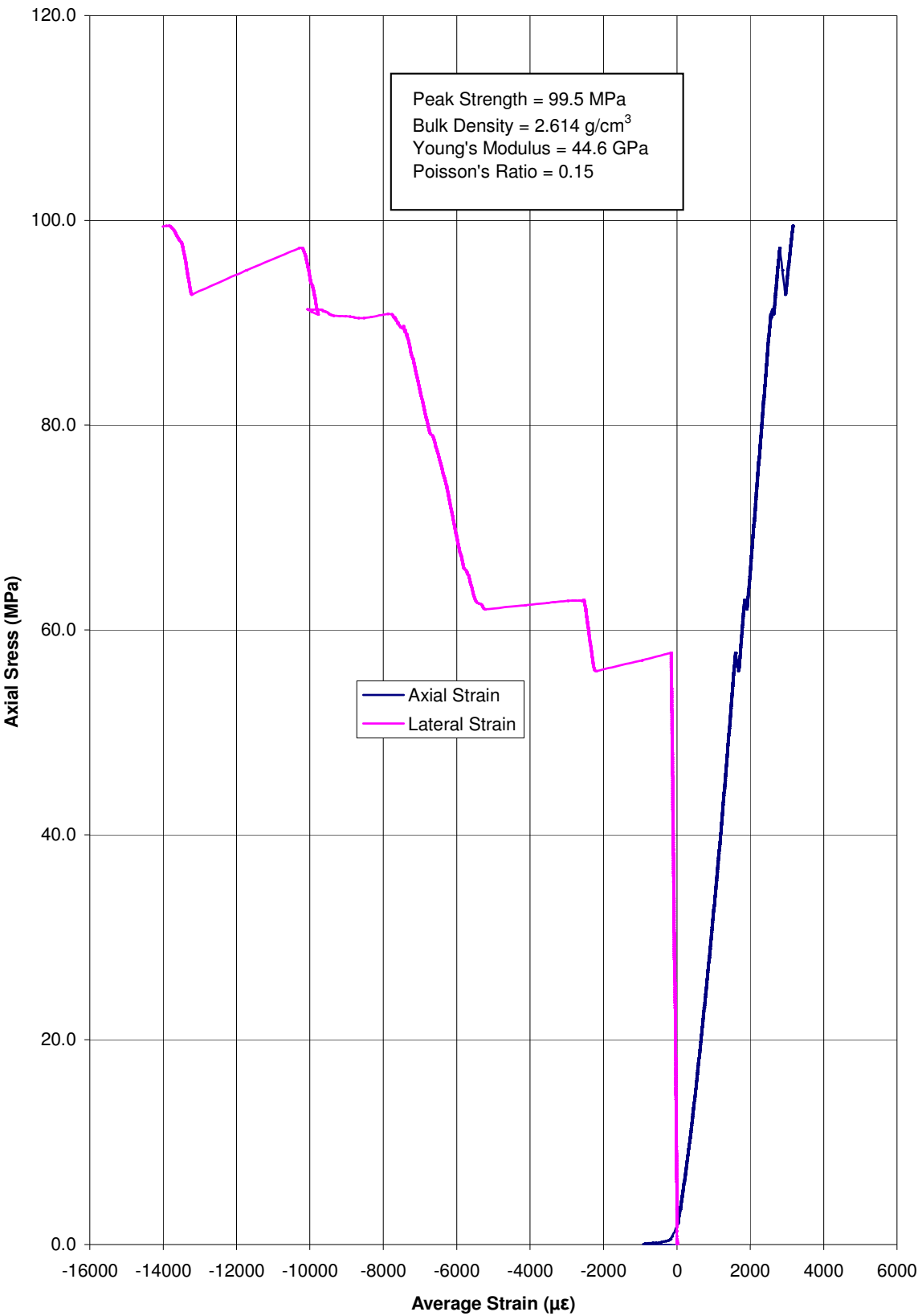
Young's Modulus: 44.6GPa

Poisson's Ratio: 0.15

Failure Cause: Intact Rock



MZ09-03-04 Stress vs. Strain



SAMPLE: MZ09-03-05



Length: 108.63 mm

Diameter: 45.03 mm

Density: 2.691 g/cm³

Peak Strength: 119.5 MPa

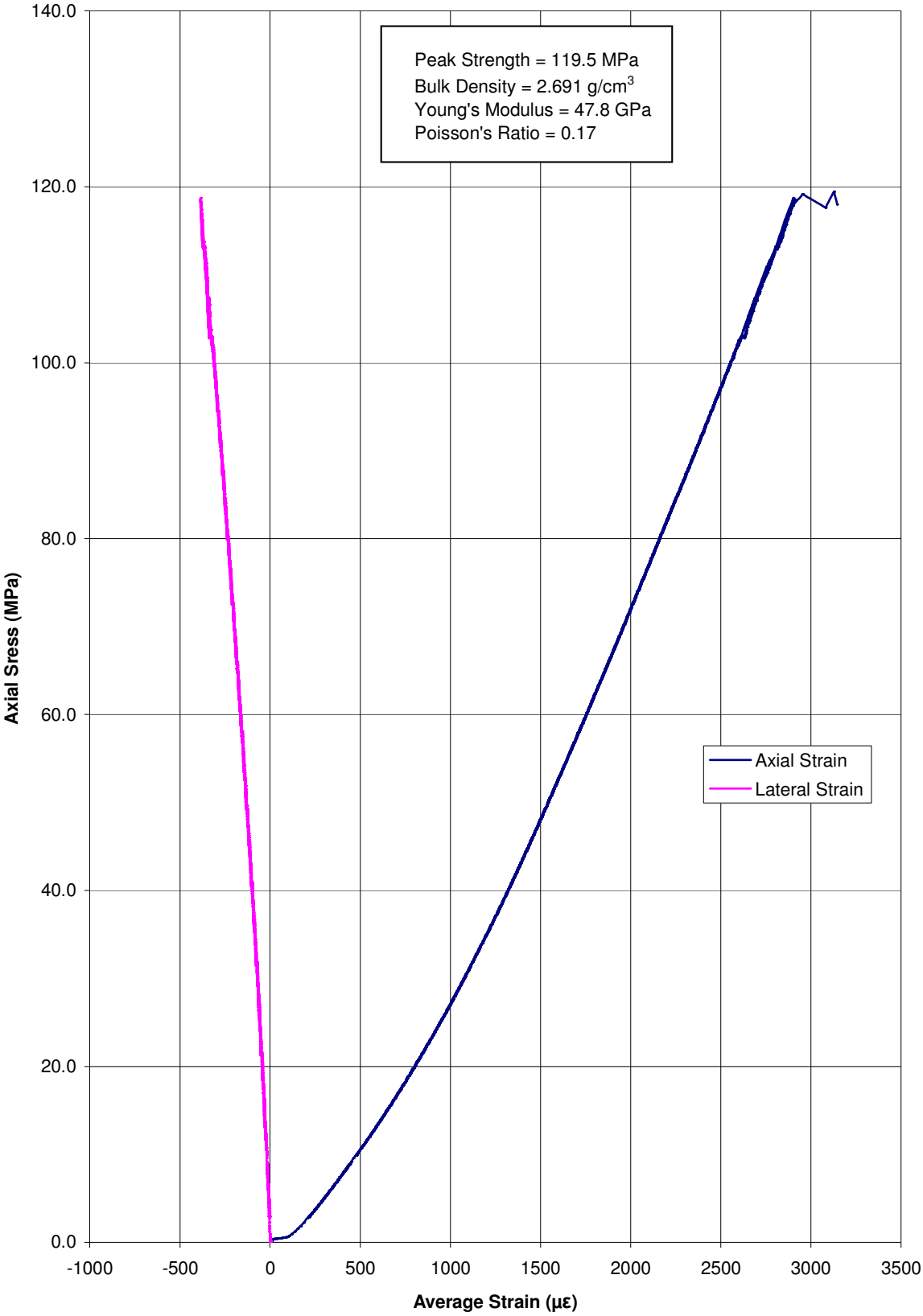
Young's Modulus: 47.8 GPa

Poisson's Ratio: 0.17

Failure Cause: Intact Rock



MZ09-03-05 Stress vs. Strain



SAMPLE: CZ09-01-02



Length: N/A

Diameter: N/A

Density: N/A

Peak Strength: N/A

Young's Modulus: N/A

Poisson's Ratio: N/A

Failure Cause N/A



SAMPLE: END09-05-02



Length: N/A
Diameter: N/A
Density: N/A
Peak Strength: N/A
Young's Modulus: N/A
Poisson's Ratio: N/A
Failure Cause N/A



APPENDIX B
RADIOACTIVE SAMPLES

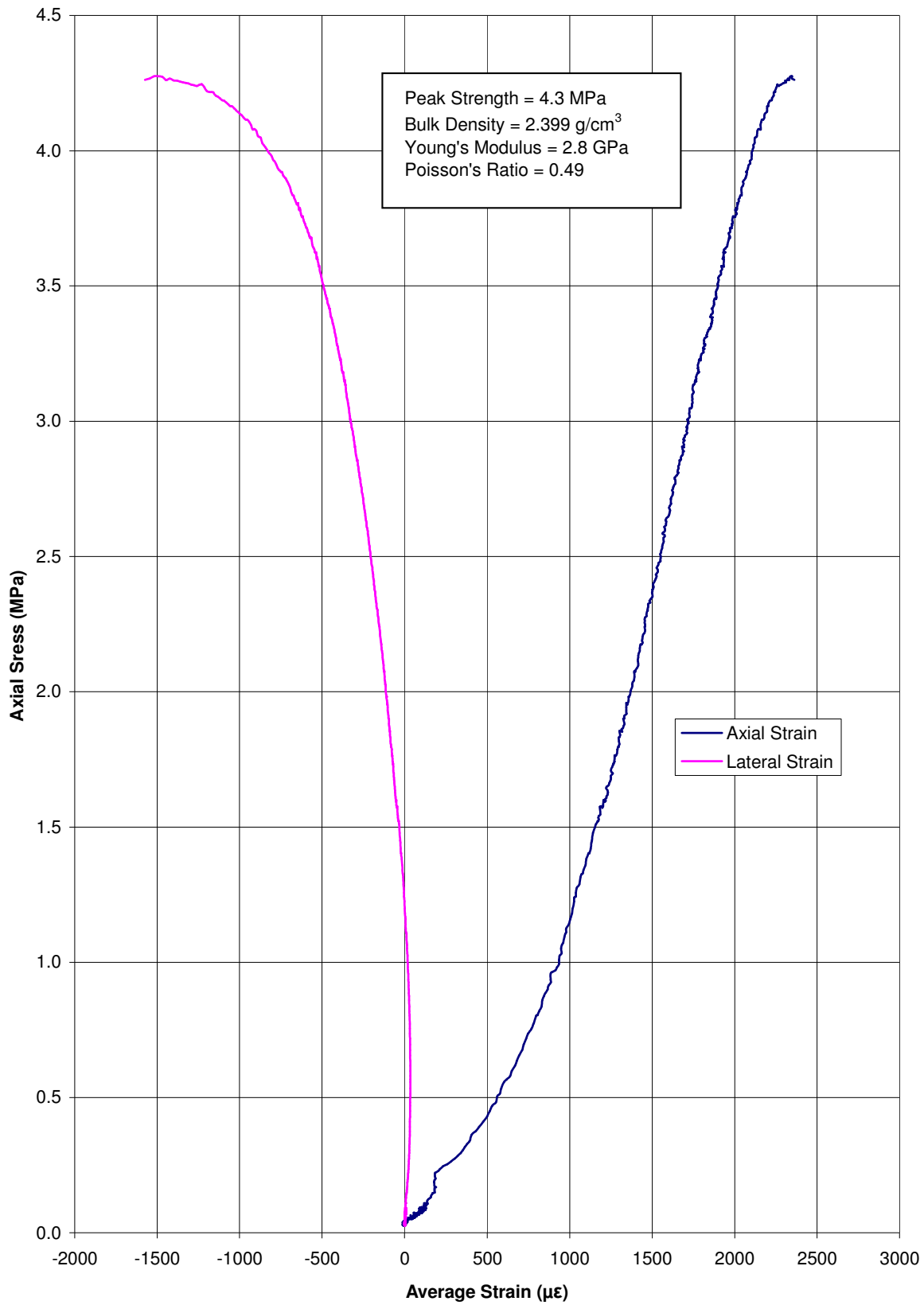
SAMPLE: END09-02_210.24-210.42



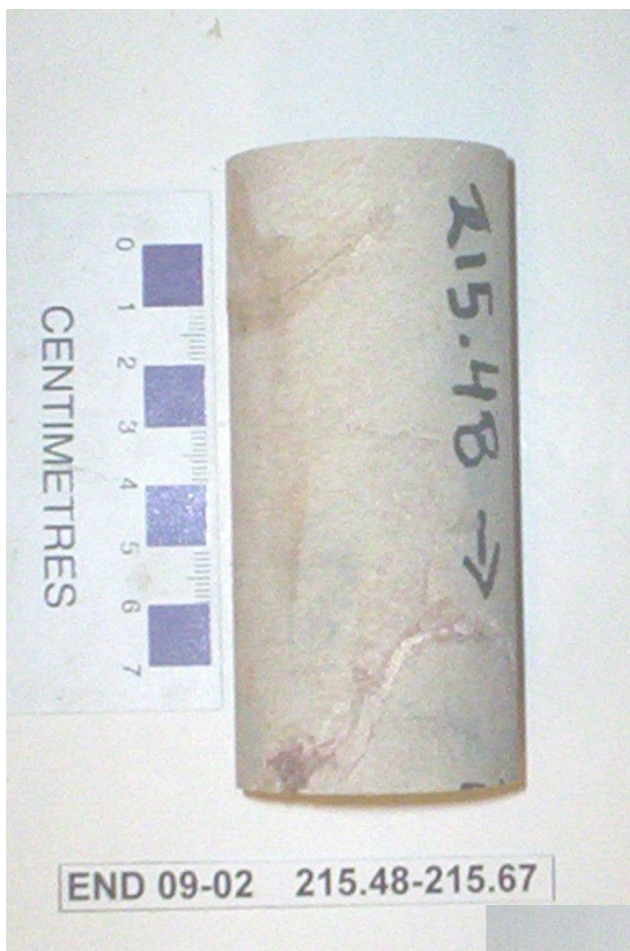
Length: 94.451 mm
Diameter: 45.02 mm
Density: 2.399 g/cm³
Peak Strength: 4.3 MPa
Young's Modulus: 2.8 GPa
Poisson's Ratio: 0.49



END 09-02 210.24-210.42 Stress vs. Strain



SAMPLE: END09-02_215.48-215.67



Length: 99.48 mm

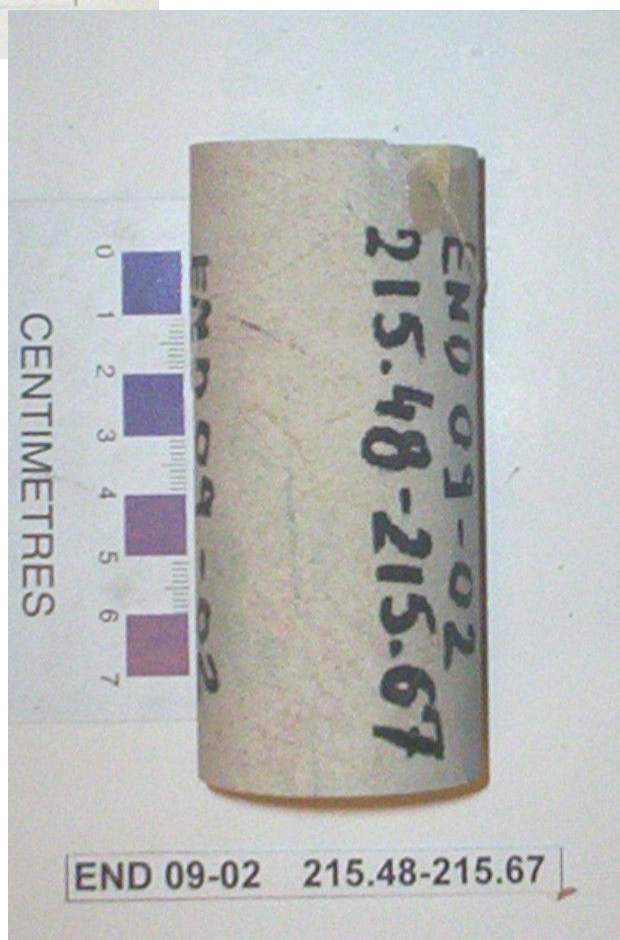
Diameter: 45.05 mm

Density: 2.352 g/cm³

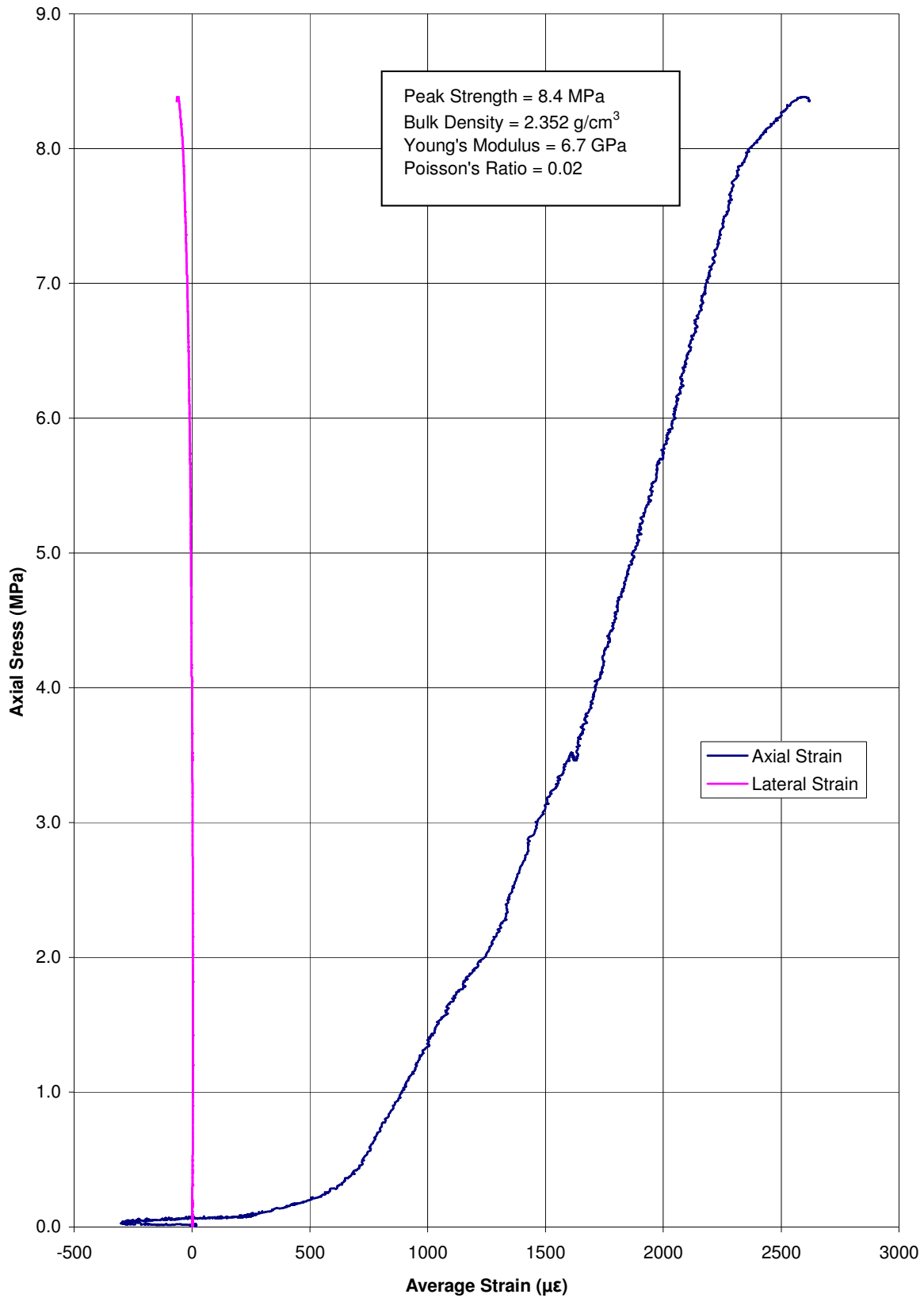
Peak Strength: 8.4 MPa

Young's Modulus: 6.7 GPa

Poisson's Ratio: 0.02



END 09-02 215.48-215.67 Stress vs. Strain



SAMPLE: END09-02_234.67-234.89



Length: 98.07 mm

Diameter: 45.12 mm

Density: 2.440 g/cm³

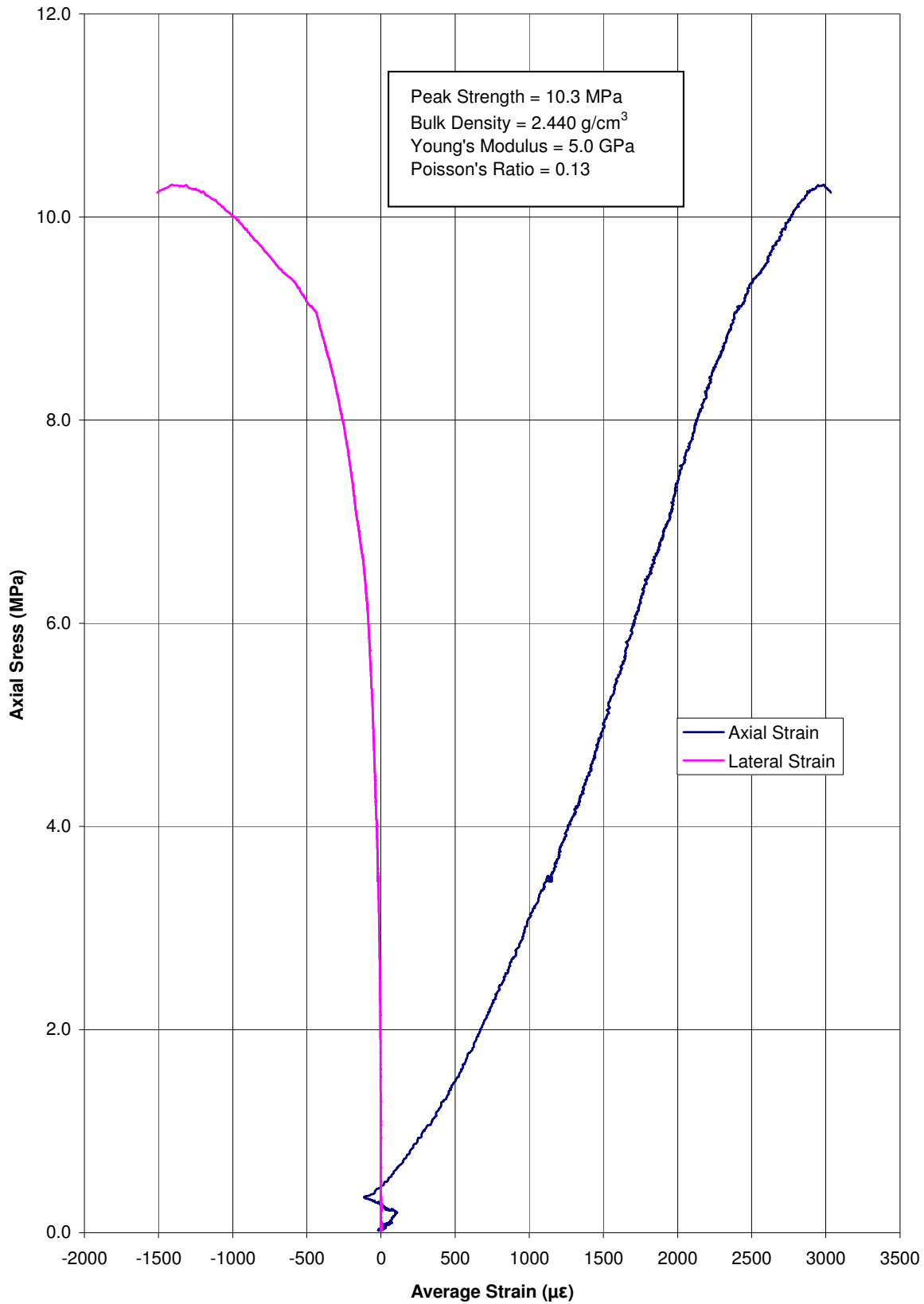
Peak Strength: 10.3 MPa

Young's Modulus: 5.0 GPa

Poisson's Ratio: 0.13



END 09-02 234.67-234.89 Stress vs. Strain



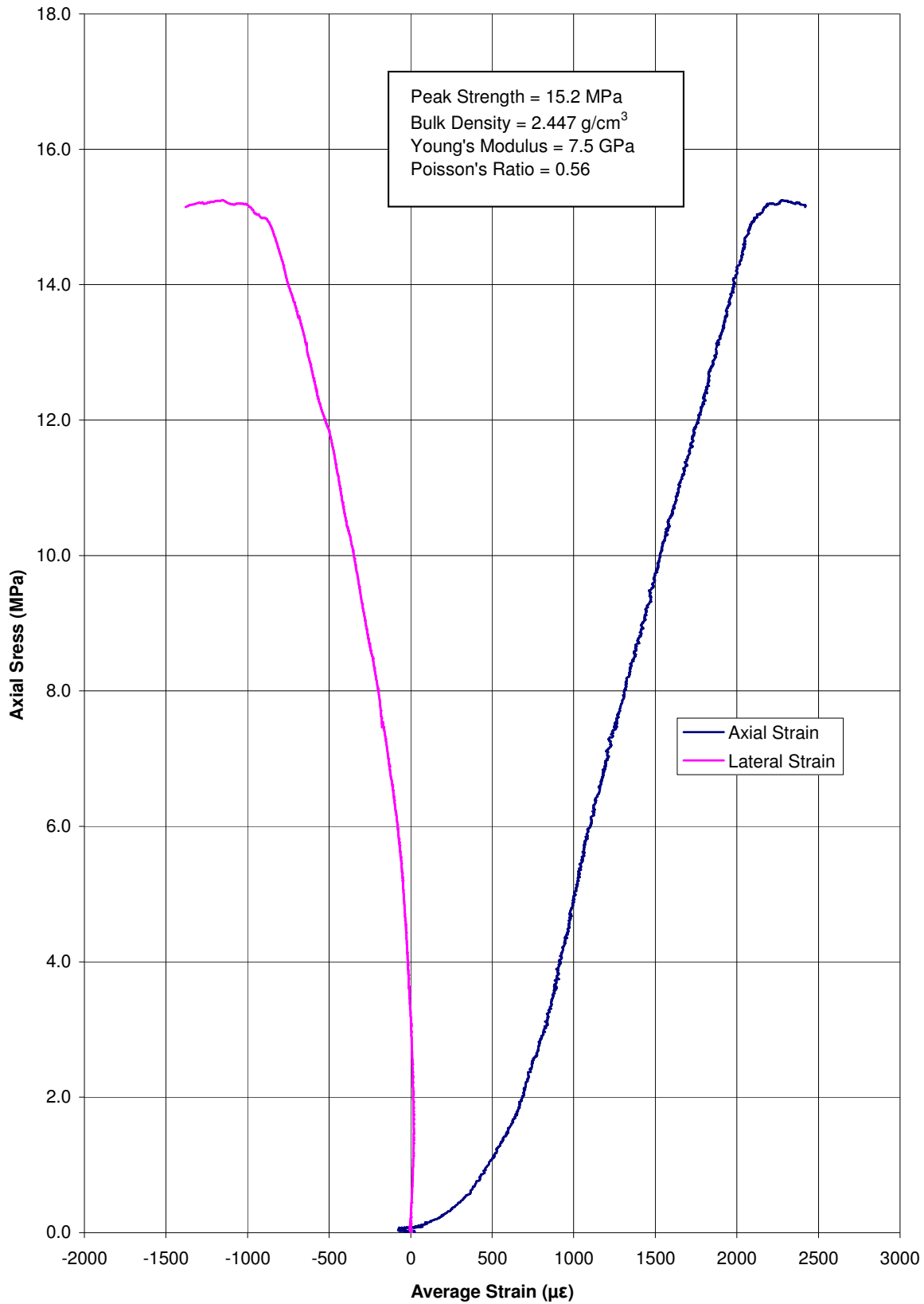
SAMPLE: END09-02_246.92-247.04



Length: 102.86 mm
Diameter: 45.05 mm
Density: 2.447 g/cm³
Peak Strength: 15.2 MPa
Young's Modulus: 7.5 GPa
Poisson's Ratio: 0.56



END 09-02 246.92-247.04 Stress vs. Strain



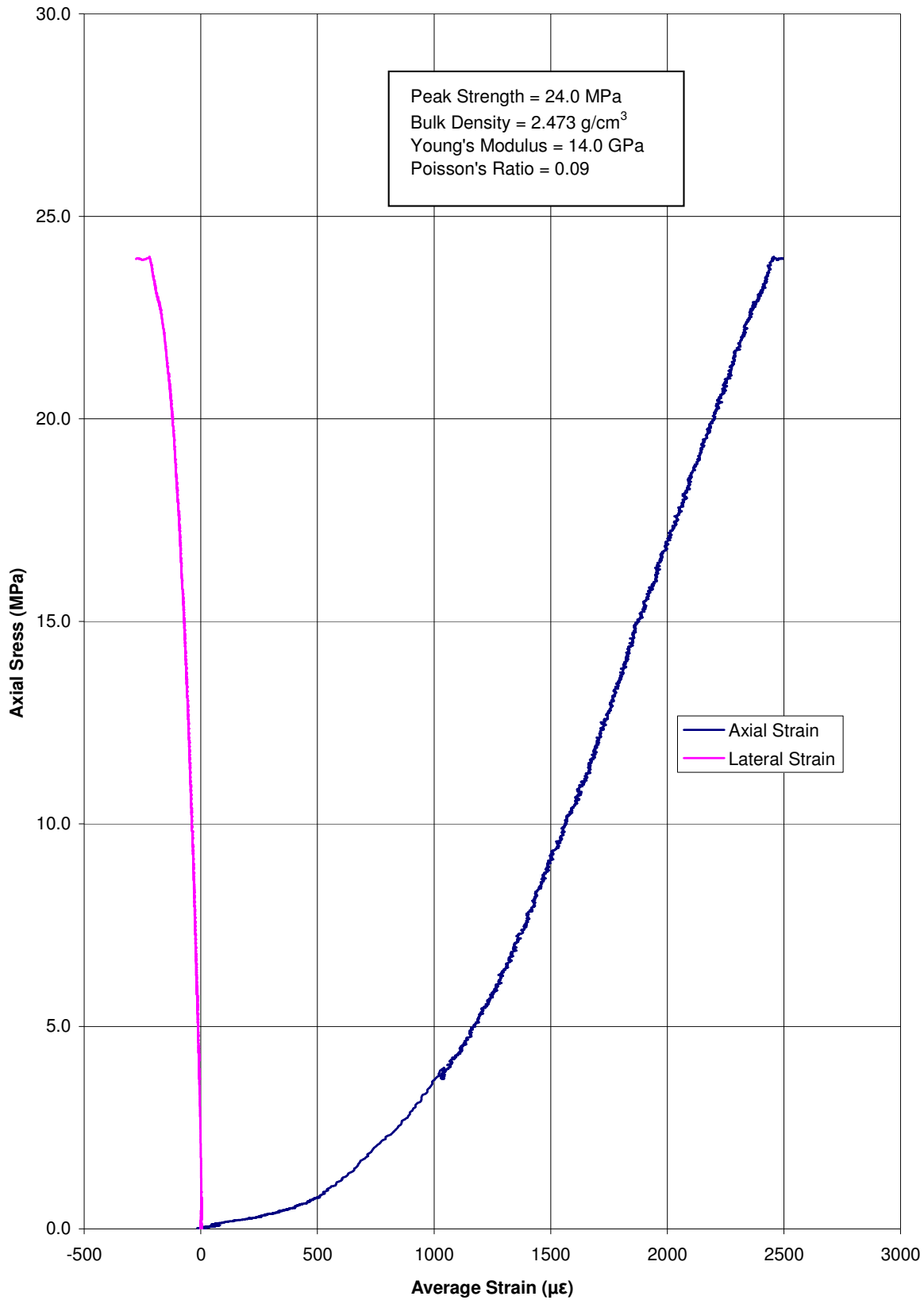
SAMPLE: END09-02_272.81-272.95



Length: 100.68 mm
Diameter: 45.03 mm
Density: 2.473 g/cm³
Peak Strength: 24.0 MPa
Young's Modulus: 14.0 GPa
Poisson's Ratio: 0.09



END 09-02 272.81-272.95 Stress vs. Strain



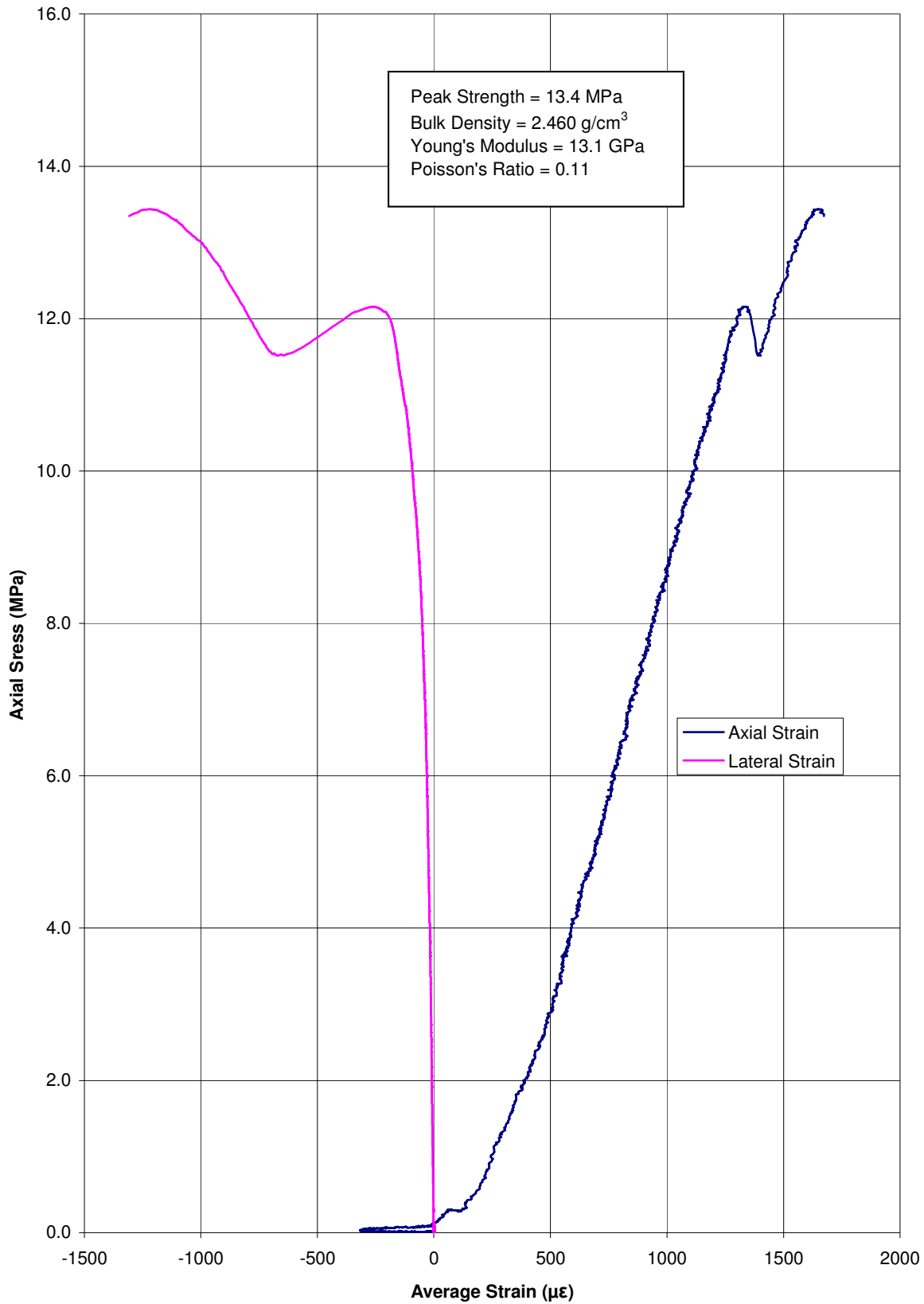
SAMPLE: END09-02_284.00-284.30



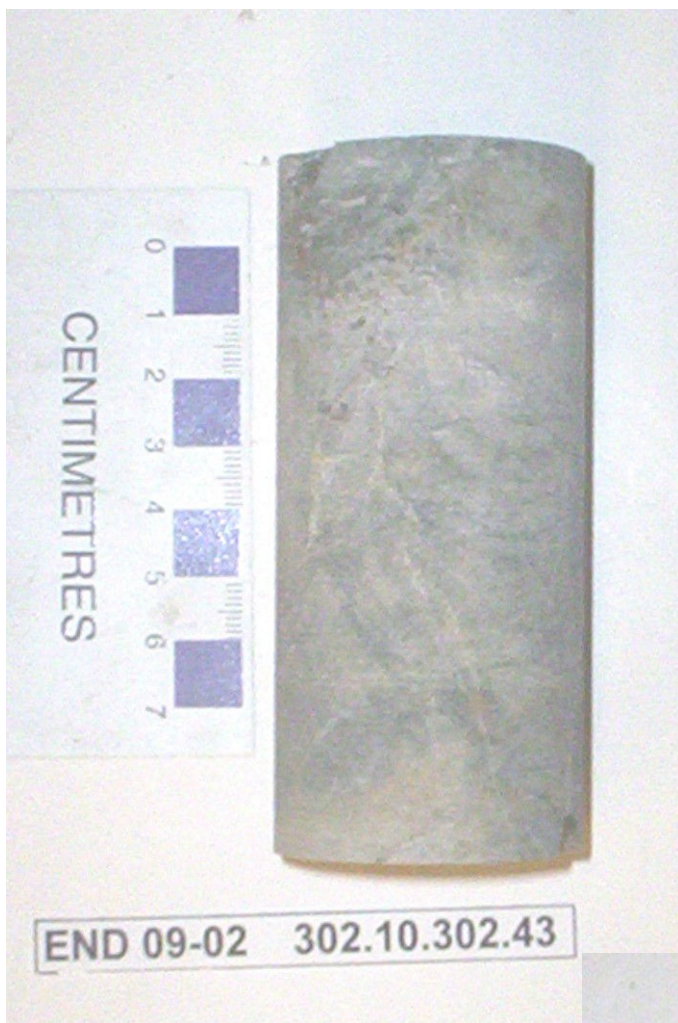
Length: 98.16 mm
Diameter: 44.96 mm
Density: 2.460 g/cm³
Peak Strength: 13.4 MPa
Young's Modulus: 13.1 GPa
Poisson's Ratio: 0.11



END 09-02 284.00-284.30 Stress vs. Strain



SAMPLE: END09-02_302.10-302.43



Length: 101.08 mm

Diameter: 45.08 mm

Density: 2.604 g/cm³

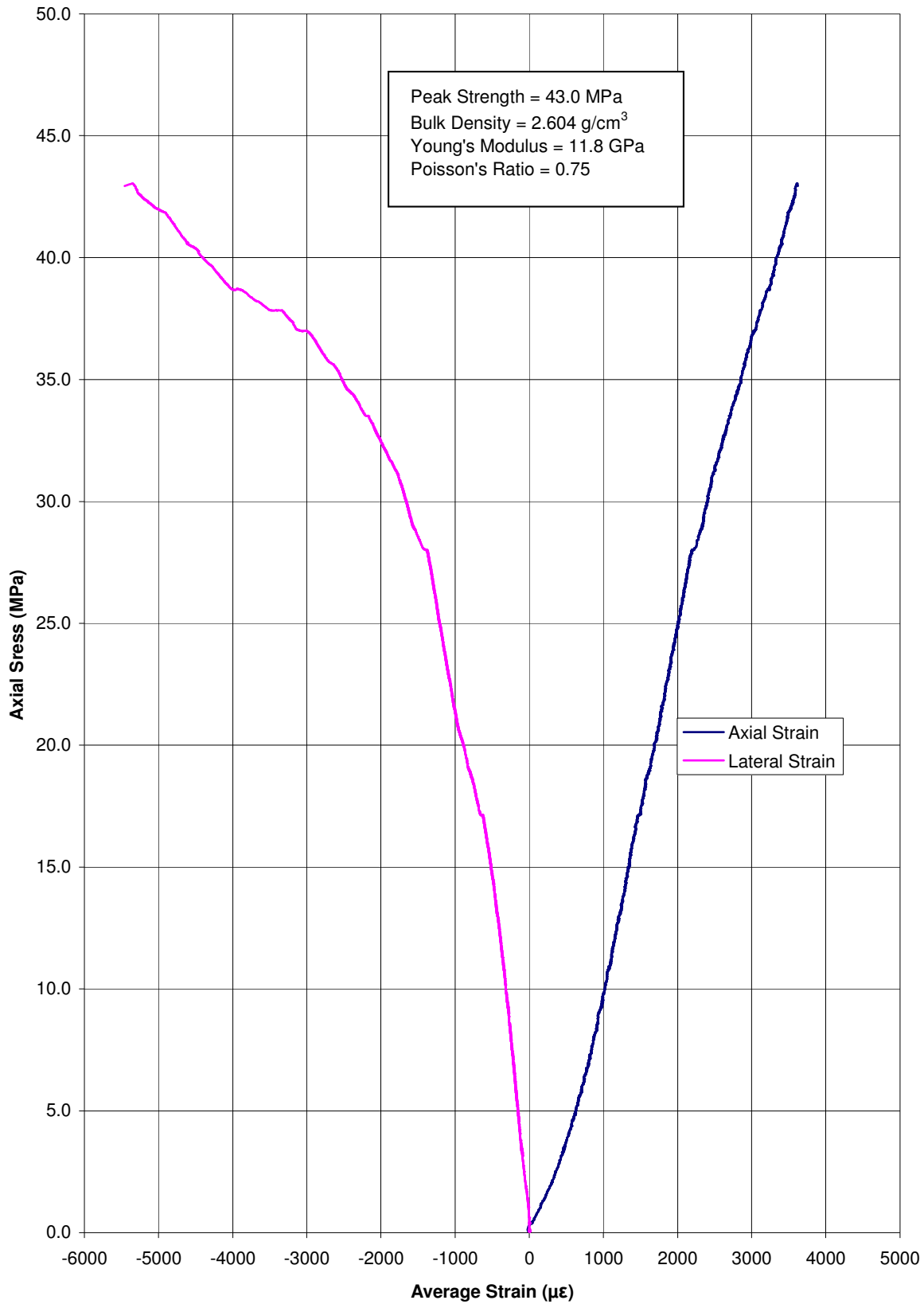
Peak Strength: 43.0 MPa

Young's Modulus: 11.8 GPa

Poisson's Ratio: 0.75



END 09-02 302.10-302.43 Stress vs. Strain



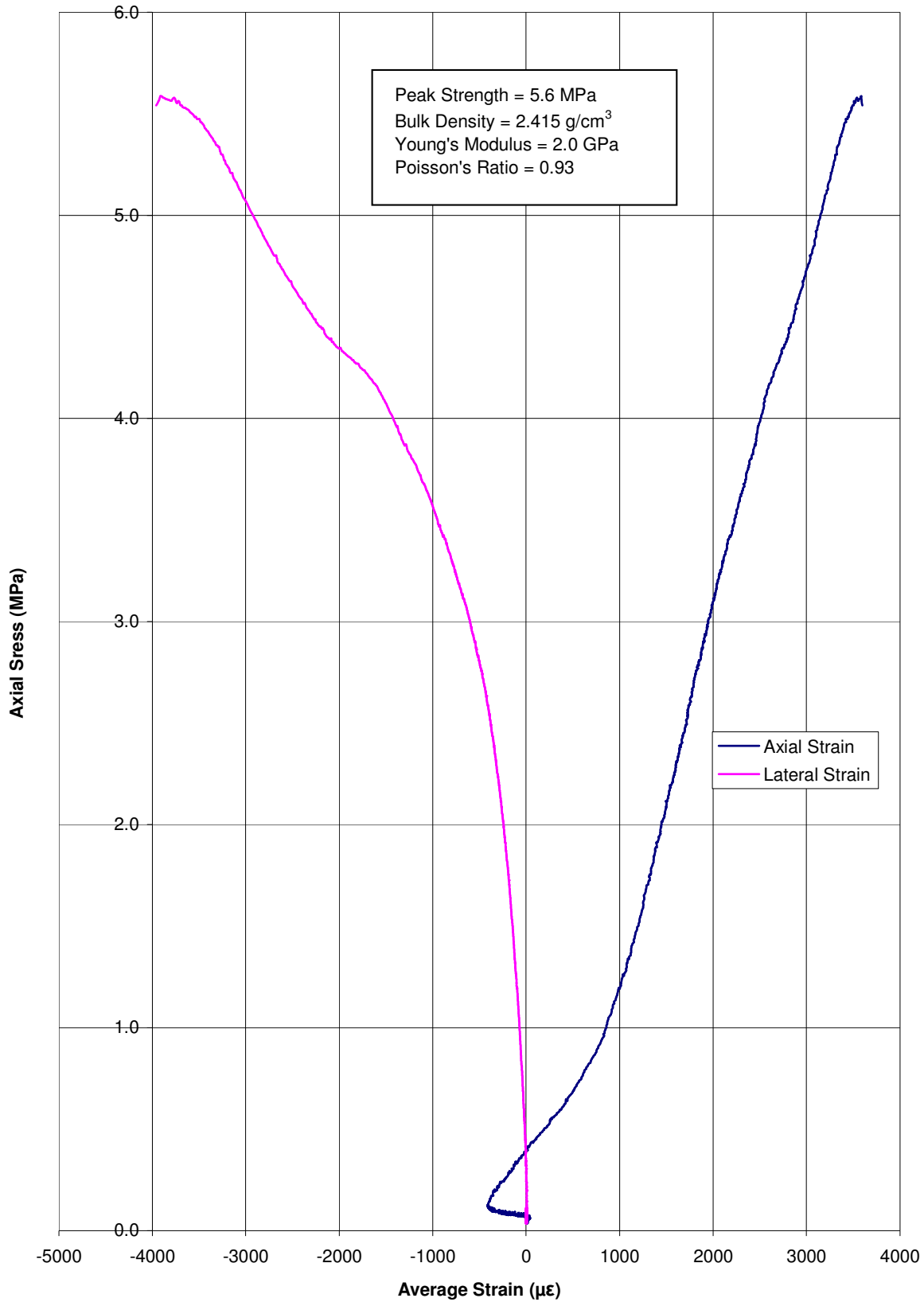
SAMPLE: END09-02_312.35-312.55



Length: 102.08 mm
Diameter: 44.95 mm
Density: 2.415 g/cm³
Peak Strength: 5.6 MPa
Young's Modulus: 2.0 GPa
Poisson's Ratio: 0.93



END 09-02 312.35-312.55 Stress vs. Strain



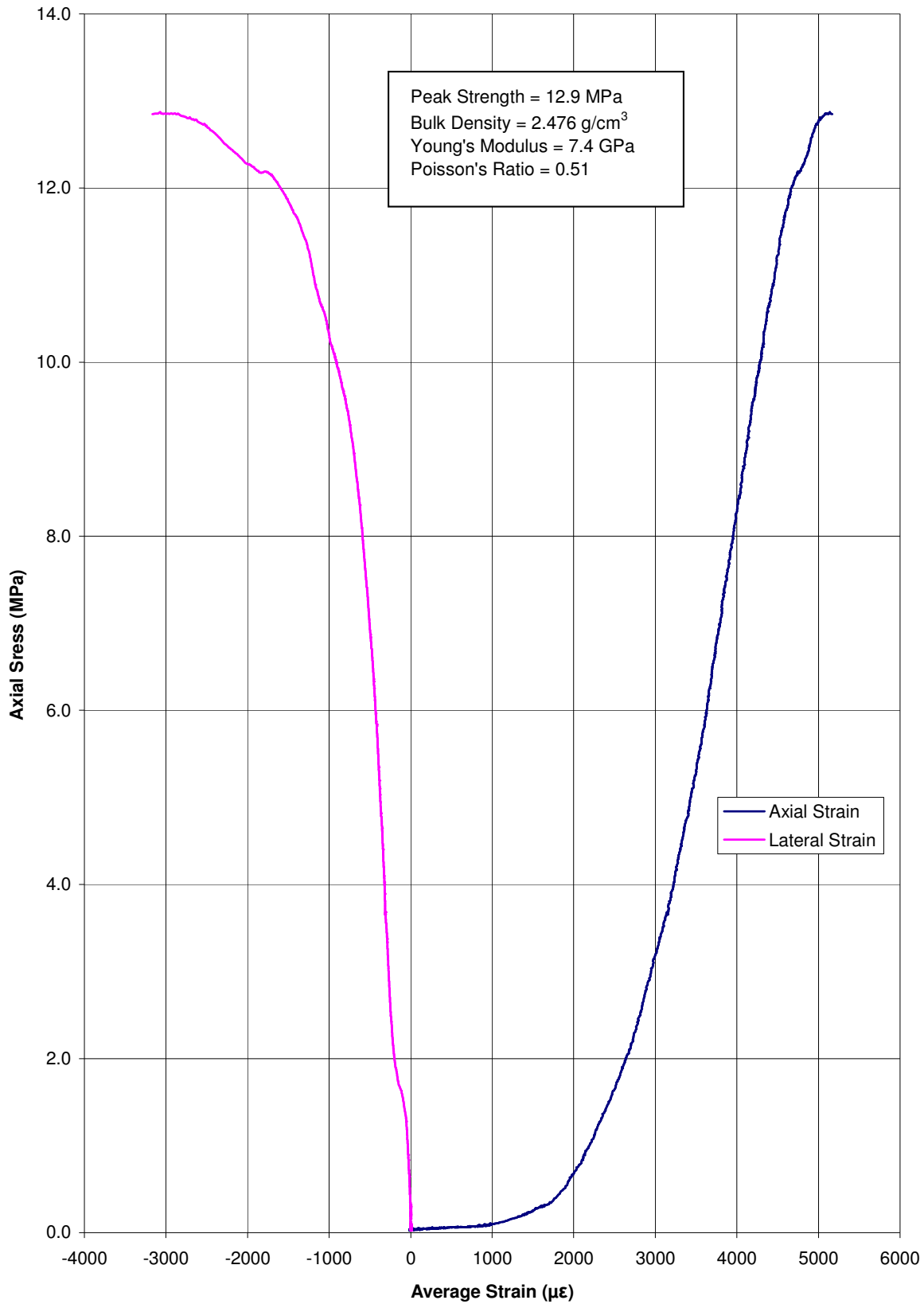
SAMPLE: END09-02_313.95-314.12



Length: 101.57 mm
Diameter: 44.97 mm
Density: 2.476 g/cm³
Peak Strength: 12.9 MPa
Young's Modulus: 7.4 GPa
Poisson's Ratio: 0.51



END 09-02 313.95-314.12 Stress vs. Strain



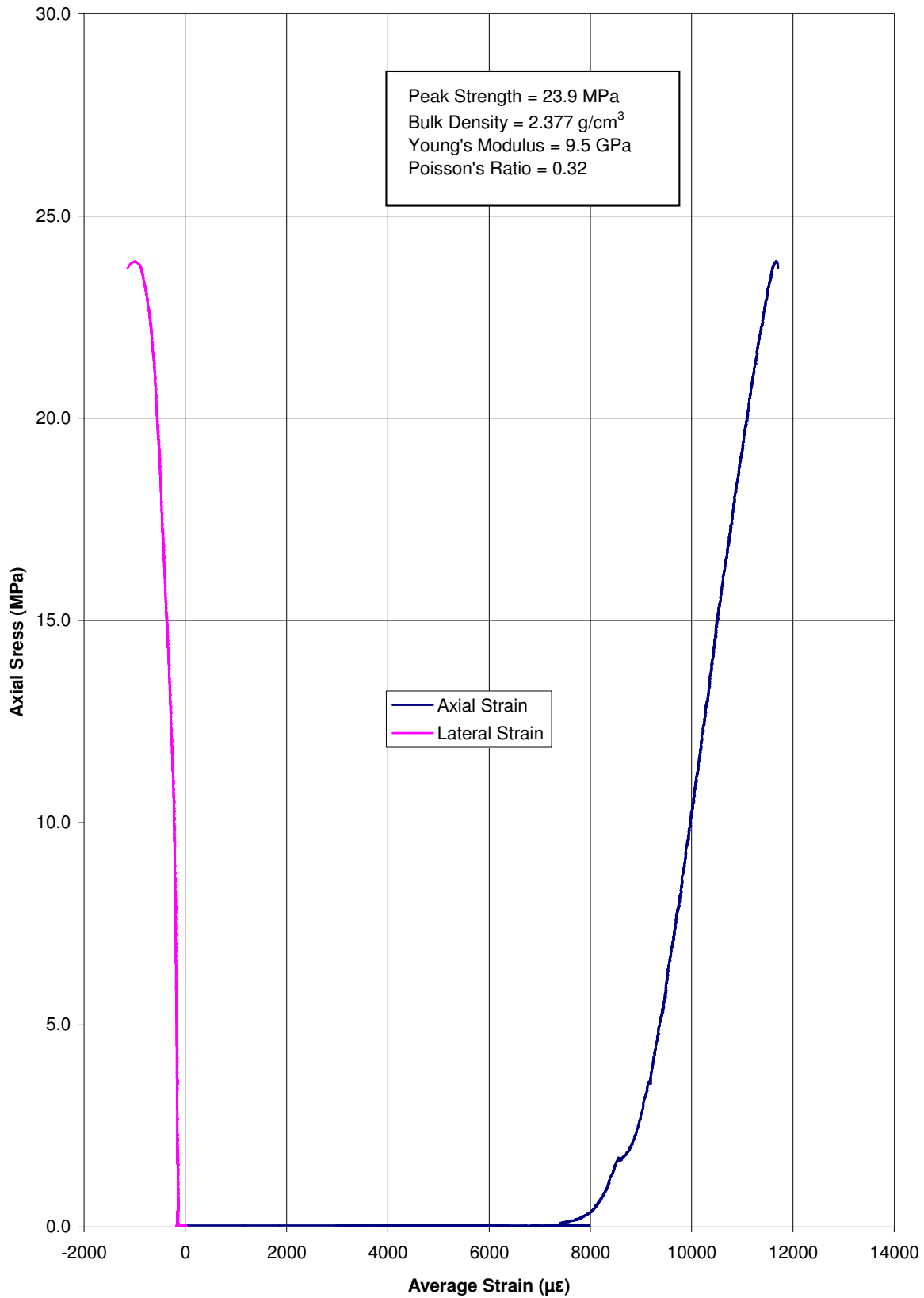
SAMPLE: END09-02_329.30-329.50



Length: 103.53 mm
Diameter: 44.97 mm
Density: 2.377 g/cm³
Peak Strength: 23.9 MPa
Young's Modulus: 9.5 GPa
Poisson's Ratio: 0.32



END 09-02 329.30-329.50 Stress vs. Strain



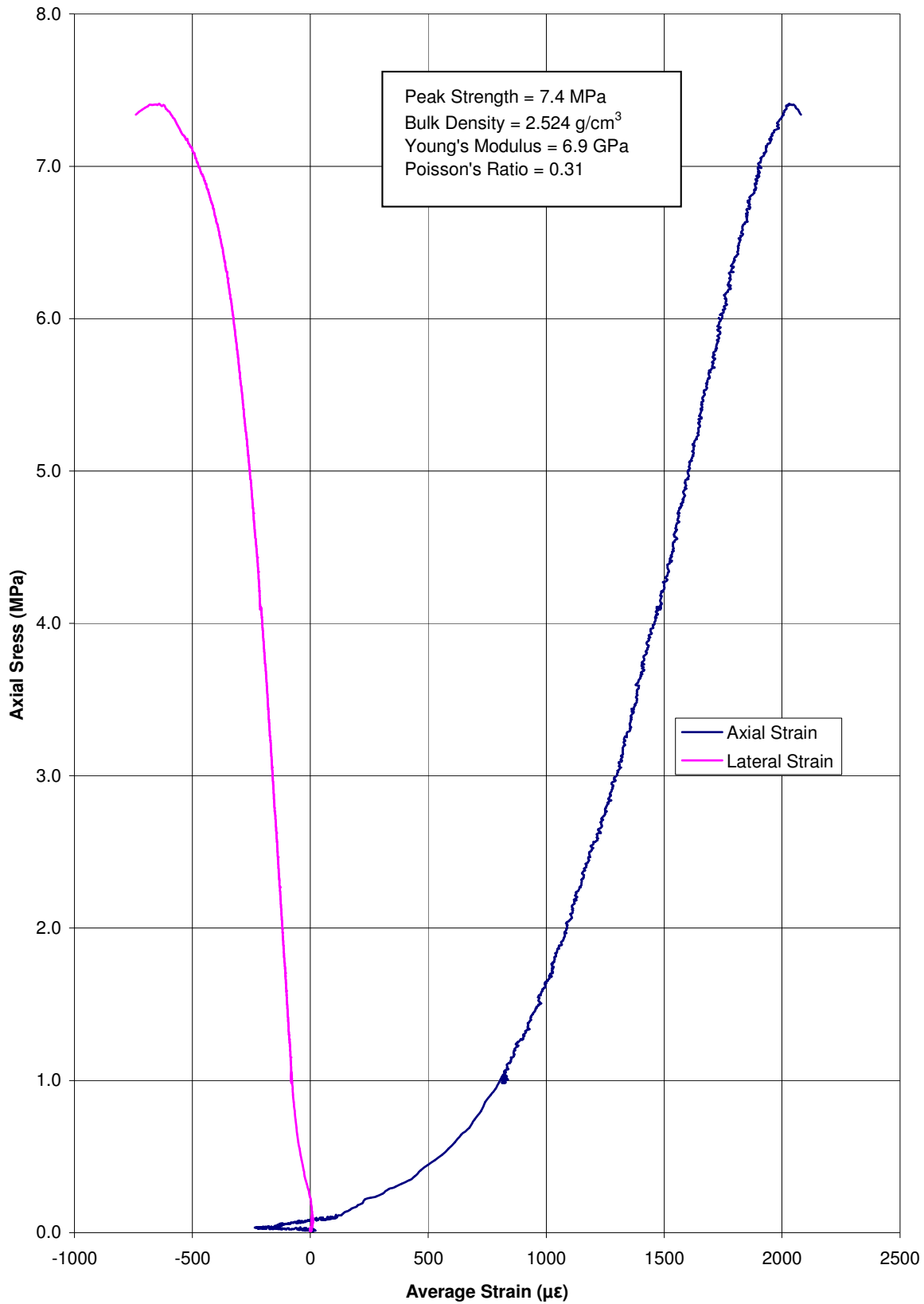
SAMPLE: END09-02_333.25-333.42



Length: 101.03 mm
Diameter: 45.13 mm
Density: 2.524 g/cm³
Peak Strength: 7.4 MPa
Young's Modulus: 6.9 GPa
Poisson's Ratio: 0.31



END 09-02 333.25-333.42 Stress vs. Strain



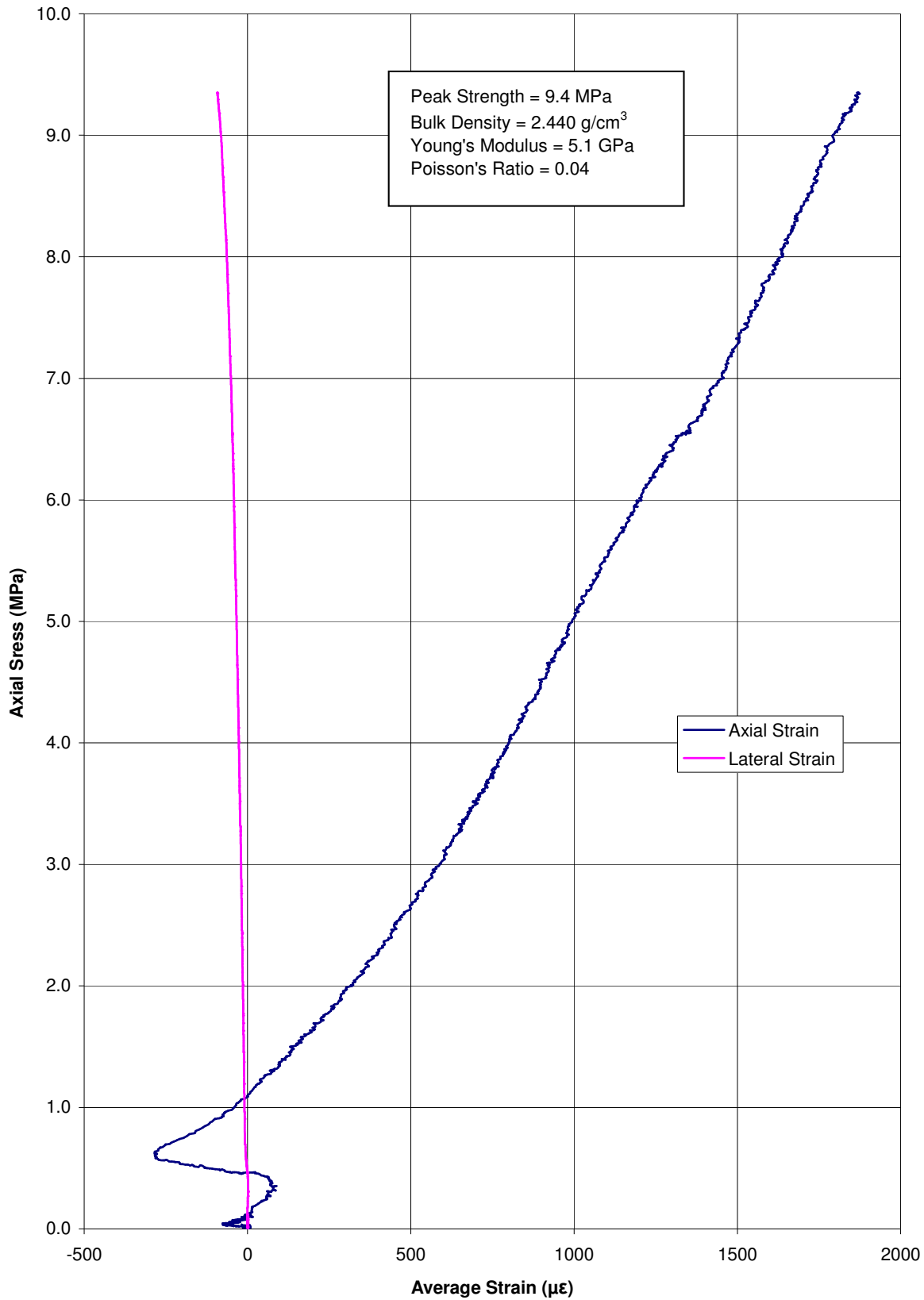
SAMPLE: END09-02_341.20-341.40



Length: 100.13 mm
Diameter: 45.05 mm
Density: 2.440 g/cm³
Peak Strength: 9.4 MPa
Young's Modulus: 5.1 GPa
Poisson's Ratio: 0.04



END 09-02 341.20-341.40 Stress vs. Strain



SAMPLE: END09-02_291.40-291.50



Length: N/A

Diameter: N/A

Density: N/A

Peak Strength: N/A

Young's Modulus: N/A

Poisson's Ratio: N/A

Failure Cause N/A

SAMPLE: END09-02_319.50-319.60



Length: N/A
Diameter: N/A
Density: N/A
Peak Strength: N/A
Young's Modulus: N/A
Poisson's Ratio: N/A
Failure Cause N/A



APPENDIX B

Rock Mass Classification



Table of Contents

1.0 INTRODUCTION.....	2
2.0 ROCK MASS CLASSIFICATION PROCEDURE	2
3.0 ROCK MASS CLASSIFICATION RESULTS.....	5
4.0 CONCLUSIONS AND RECOMMENDATIONS.....	13
5.0 REFERENCES.....	14

TABLES

Table B1: 1976 Rock Mass Rating (RMR) classification parameters (after Bieniawski, 1974).	3
Table B2: Andrew Lake – 2009 Boreholes. Summary of RMR values by borehole.	11
Table B3: Andrew Lake – 2009 Boreholes. Summary of RMR values by rock type.	12
Table B4: Andrew Lake – 2009 Boreholes. Summary of RMR values by alteration factor (Af).....	13
Table B5: Andrew Lake – Recommendations for RMR and strength parameters.	14

FIGURES

Figure B1: Andrew Lake 2009 Drillholes Rock Mass Rating (RMR) Striplogs and Strength (R)	4
Figure B2: Andrew Lake Pit Geological Sections with Inferred Alteration Zones and Lithological Domains.....	6
Figure B3: Andrew Lake Pit - Generalized Geotechnical Section (SW-NE). Inferred Fault and Mineralization Alteration Zones are Highlighted.....	7
Figure B4: Andrew Lake Pit - Geological Model of Ore Zones and Lithological Domains (SRK, 2008)	8
Figure B5: Andrew Lake Pit - Generalized Geotechnical Section (W-E). Inferred Fault and Mineralization Alteration Zones are Highlighted.....	10
Figure B6: Andrew Lake - 2009 Boreholes. Cumulative Frequency Distribution of RMR by Borehole.....	11
Figure B7: Andrew Lake - 2009 Boreholes. Cumulative Frequency Distribution of RMR by Rock Type.	12
Figure B8: Andrew Lake - 2009 Boreholes. Cumulative Frequency of RMR by Alteration Factor (Af)	13



1.0 INTRODUCTION

This appendix presents the results of the rock mass classification carried out on the 2009 geotechnical borehole data for Andrew Lake (AL). The data analysed in the rock mass classification work has been discussed in the previous appendices and the 2009 data report (Golder, 2009). In total, there was approximately 1000 m of core drilled at AL in the 2009 season.

The following appendix discusses the rock mass classification procedures, and outlines the rock mass classification results for the AL site, including interpretations for slope design.

2.0 ROCK MASS CLASSIFICATION PROCEDURE

For classification of the rock mass, the 1976 Rock Mass Rating (RMR) system was used (Bieniawski 1976). For validation of the RMR classification scheme, the Norwegian Geotechnical Institute Q-System (Barton et al. 1974) for rock mass classification was also used; however these results have not been presented herein.

Due to the variability in the rock mass quality for any particular rock lithology, the RMR was carried out at the logging interval level, meaning a separate classification was carried out on intervals ranging from 0.10 m to a maximum of once per drill run (i.e., typically 3 m of core or less). Using this approach, the RMR distribution in the borehole delineates intercepted geotechnical features, or zones in the rock mass which share similar geotechnical characteristics such as strength, fracture spacing, or alteration.

The RMR value per drilling interval is calculated as follows (on a scale of 100):

$$RMR = P_1 + P_2 + P_3 + P_4 + P_5$$

Where P_1 through P_5 represent values assigned based on the following rock mass parameters:

- *Strength of Intact Rock (P_1)*; assessed on a per run basis according to either the UCS data if available, the $PLT - I_{s(50)}$ data if available, or the field assessment of intact rock strength (R) based on the ISRM field classification. These strength parameters are discussed in Appendix A.
- *Rock Quality Designation, RQD (P_2)*; this parameter was assessed in the field for every logging interval, as discussed in the data report (Golder, 2009).
- *Fracture Spacing (P_3)*; this parameter was calculated based on the fracture frequency which was assessed in the field for every drill run of core as discussed in the data report (Golder, 2009).
- *Condition of Joints (P_4)*; this parameter was taken as the average joint condition value (J_{con}) per drill run of core for the individual discontinuities assigned in the field (Golder, 2009).
- *Groundwater (P_5)*; for the calculation of the rock mass RMR, the ground was assumed dry ($P_5 = 10$). **For stability assessment considerations, the appropriate value will have to be subtracted from the calculated RMR values to reflect in situ seepage conditions, or in the case of numerical modelling, considered separately, such as a water table.**



APPENDIX B - ROCK MASS CLASSIFICATION

The RMR classification parameters are shown on Table B1.

Table B1: 1976 Rock Mass Rating (RMR) classification parameters (after Bieniawski, 1974).

A. CLASSIFICATION PARAMETERS AND THEIR RATINGS

PARAMETER			RANGES OF VALUES						
1	Strength of intact rock material	Point load strength index	> 8 MPa	4 - 8 MPa	2 - 4 MPa	1 - 2 MPa	For this low range - uniaxial compressive test is preferred		
		Uniaxial compressive strength	> 200 MPa	100 - 200 MPa	50 - 100 MPa	25 - 50 MPa	10-25 MPa	3-10 MPa	1-3 MPa
	Rating		15	12	7	4	2	1	0
2	Drill core quality RQD		90% - 100%	75% - 90%	50% - 75%	25% - 50%	< 25%		
	Rating		20	17	13	8	3		
3	Spacing of joints		> 3m	1 - 3m	0.3 - 1m	50 - 300mm	< 50mm		
	Rating		30	25	20	10	5		
4	Condition of joints		Very rough surfaces Not continuous No separation Hard joint wall rock	Slightly rough surfaces Separation < 1mm Hard joint wall rock	Slightly rough surfaces Separation < 1mm Soft joint wall rock	Slickensided surfaces or Gauge < 5mm thick or Joints open 1-5mm Continuous joints	Soft gauge > 5mm thick or Joints open > 5mm Continuous joints		
	Rating		25	20	12	6	0		
5	Ground water	Inflow per 10m tunnel length	None		< 25 litres/min.	25 - 125 litres/min.	> 125 litres/min.		
		Ratio joint water pressure major principal stress	OR 0		OR 0.0 - 0.2	OR 0.2 - 0.5	OR > 0.5		
		General conditions	OR Completely dry		OR Moist only (interstitial water)	OR Water under moderate pressure	OR Severe water problems		
	Rating		10		7	4	0		

The calculated RMR values by drill interval for the AL 2009 boreholes are plotted on the striplogs included in Figure B1. Also shown on these striplogs are the lithology obtained from AREVA's geologists, and the ISRM strength index value (R) assessed in the field. As discussed in Appendix A, the R values agree reasonably well with the available laboratory testing. The RMR and R values have been color coded as per the legend shown on these figures. Records of Drillholes are presented in the factual data report (Golder, 2009).

Several geotechnical boreholes from 2007/2008 (SRK 2009) were also cross-checked following a similar rock mass classification approach using the geotechnical data provided by AREVA. The cross-checks showed that the calculated RMR (1976) values for the drill run intervals followed closely to previous rock mass classification carried out by SRK using the 1989 RMR system. The 2007/2008 data are not presented in this document, however some of these boreholes were used to aid the interpretation as discussed herein.

AND09-01

From	To	Geology	R	RMR
17	18	OB	0	51.7
18	20	OB	0	44.0
20	21.25	GnPsaPel	1	49.7
21.25	22.98	GnPsaPel	1	51.8
22.98	23.45	GnPsaPel	0.5	23.1
23.45	24	GnPsaPel	1	54.5
24	24.5	GnPsaPel	1	40.4
24.5	25.64	LOST	1	26.3
25.64	26	LOST	1	21.3
26	26.24	LOST	1	48.0
26.24	27	GnPsaPel	0	55.6
27	28.85	LOST	0	13.2
28.85	30	GnPsaPel	1.5	27.8
30	32.08	GnPsaPel	1.5	49.4
32.08	32.7	GnPsaPel	0.5	25.9
32.7	33	GnPsaPel	0.5	26.3
33	36	GnPsaPel	0.5	52.8
36	39	GnPsaPel	0.5	56.0
39	42	GnPsaPel	0.5	56.2
42	45	GnPsaPel	0.5	52.7
45	47.43	GnPsaPel	0.5	47.4
47.43	48	GnPsaPel	2	51.4
48	51	GnPsaPel	2.5	60.7
51	54	GnPsaPel	2.5	63.1
54	57	GnPsaPel	2.5	63.6
57	60	GnPsaPel	2.5	59.0
60	63	GnPsaPel	2.5	63.0
63	66	GnPsaPel	2.5	61.9
66	69	GnPsaPel	2.5	54.8
69	71.9	GnPsaPel	2.5	57.2
71.9	72.2	GnPsaPel	5	70.0
72.2	75	GnPsaPel	2	55.8
75	75.86	GnPsaPel	2	60.8
75.86	78	GnPsaPel	2.5	61.7
78	81	GnPsaPel	2	58.9
81	81.68	GnPsaPel	1	24.4
81.68	84	GnPsaPel	2.5	42.2
84	87	GnPsaPel	2.5	51.2
87	90	GnPsaPel	2.5	59.3
90	90.6	GnPsaPel	2	36.5
90.6	93	GnPsaPel	2.5	61.8
93	96	GnPsaPel	2	56.7
96	99	GnPsaPel	2.5	61.0
99	102	GnPsaPel	2.5	63.0
102	103.82	GnPsaPel	2.5	54.7
103.8	104.44	GnPsaPel	2	45.8
104.44	105	GnPsaPel	3	56.5
105	105.69	GnPsaPel	3	58.0
105.69	107	GnPsaPel	1	47.6
107	107.21	LOST	0	51.5
107.21	108	GnPsaPel	1.5	51.5
108	109.78	GnPsaPel	2.5	51.2
109.78	110.68	GnPsaPel	1.5	31.6
110.68	111	LOST	0	14.0
111	112.52	GnPsaPel	0	41.8
112.52	114	GnPsaPel	0	48.2
114	114.97	LAMP	0	62.1
114.97	116.22	GranT	1	60.3
116.22	117	GranT	2.5	58.7
117	120	GranT	2.5	46.9
120	122.4	GranT	2.5	49.7
122.4	123	GranT	2.5	52.7
123	124.66	GranT	2.5	52.0
124.66	126	GranT	2.5	56.3
126	126.6	GranT	3	75.8
126.6	126.9	GranT	0	40.7
126.9	127.24	GranT	3	58.6
127.24	127.65	GranT	0.5	44.8
127.65	129	GranT	3	57.9
129	132	GranT	3	63.6
132	135	GranT	1	62.6
135	135.43	GranT	1	65.1
135.43	138	GranT	3	57.2
138	141	GranT	3	66.8
141	141.3	GranT	3	58.4
141.3	141.9	GranT	2	68.3
141.9	144	GranT	3	57.4
144	146	GranT	2	67.9
146	147	GranT	2	63.9
147	150	GranT	1	56.4
150	152.59	GranT	2	57.7
152.59	153	GranT	2	52.1
153	153.3	GranT	2	56.5
153.3	155.14	GranT	2	44.8
155.14	156	GranT	1	57.1
156	159	GranT	0.5	60.0
159	161.35	GranT	0	58.1
161.35	162	LOST	0	25.4
162	162.45	GranT	0	57.1
162.45	163.35	GranT	0.5	55.9
163.35	164.9	GranT	1.5	42.2
164.9	165.93	GranT	0	60.6
165.93	168	GranT	1	62.7
168	168.3	GranT	2.5	49.5
168.3	170	GranT	2.5	57.7
170	170.84	GranT	0	61.1
170.84	171.34	GranT	2	59.2
171.34	171.9	GranT	0	58.4
171.9	173.69	GranT	2.5	51.3
173.69	174	LOST	0	24.4
174	174.8	GranT	2.5	55.7
174.8	176.68	GranT	0	51.3
176.68	177	GranT	2.5	60.0
177	179.15	GranT	2.5	53.3
179.15	180	GranT	2.5	61.3
180	183	GranT	2.5	61.7
183	186	GranT	2.5	64.0
186	186.75	GranT	2.5	57.1
186.75	187.46	GranT	2.5	56.3
187.46	188	GranT	2.5	51.9
188	189	GranT	4	66.6
189	191	GranT	4	62.5
191	192	GranT	1.5	60.4
192	194	GranT	2	59.1
194	194.6	GranT	1	59.1
194.6	195	GranT	2	51.9
195	195.3	GranT	1	55.2
195.3	196	GranT	2	69.3
196	196.4	GranT	1	56.7
196.4	197.18	GranT	2	61.1
197.18	198.25	GranT	1	59.4
198.25	201	GranT	2	56.6
201	204	GranT	2	55.8
204	206	GranT	2	58.6
206	209	GranT	2	57.1
209	209.45	GranT	0	44.5
209.45	210	GranT	2	52.0
210	213	GranT	3.5	61.9
213	216	GranT	3.5	61.3
216	219	GranT	3.5	55.4
219	222	GranT	3.5	58.9
222	225	GranT	3.5	66.1
225	228	GranT	3.5	65.3
228	231	GranT	3.5	65.7
231	234	GranT	3.5	66.4
234	237	GranT	3	62.7
237	240	GranT	3	60.4
240	243	GranT	3	55.6
243	244.77	GranT	3	49.5
244.77	246	GranT	0	47.8
246	247	FLT	1	48.3
247	248	LOST	0	30.6
248	249.54	FLT	1	56.0
249.54	249.94	GnPsaPel/FLT*	0	13.3
249.94	250.85	GnPsaPel/FLT*	1	66.0
250.85	252.4	GnPsaPel/FLT*	1	59.2
252.4	255	GnPsaPel/FLT*	2	58.7
255	258	GnPsaPel/FLT*	1	63.5
258	260.17	GnPsaPel/FLT*	1	47.3
260.17	261	GnPsaPel/FLT*	1	14.0
261	262.9	GnPsaPel/FLT*	2	57.2
262.9	265.62	GnPsaPel/FLT*	1	63.8
265.62	266.22	GnPsaPel/FLT*	1	13.8
266.22	267.5	GnPsaPel/FLT*	3	61.2
267.5	268.29	GnPsaPel/FLT*	0	26.8
268.29	270	GnPsaPel/FLT*	3	55.3
270	270.3	GnPsaPel/FLT*	1	44.6
270.3	270.6	GnPsaPel/FLT*	0	48.9
270.6	273	GnPsaPel/FLT*	1.5	39.4
273	276	GnPsaPel/FLT*	1	30.5
276	277	GnPsaPel/FLT*	1	51.0
277	279	GnPsaPel/FLT*	0	21.0
279	281.25	GnPsaPel/FLT*	0	64.4
281.25	282	GnPsaPel/FLT*	3	44.3
282	284.15	GnPsaPel/FLT*	0	13.8
284.15	285	GnPsaPel/FLT*	0	13.8
285	287	GnPsaPel/FLT*	0	13.6
287	288	GnPsaPel/FLT*	0	19.9
288	289.35	GnPsaPel/FLT*	1.5	33.5
289.35	289.7	GnPsaPel/FLT*	1	13.7
289.7	291	GnPsaPel/FLT*	1.5	44.3
291	294	GnPsaPel/FLT*	1.5	52.3
294	297	GnPsaPel/FLT*	1.5	49.9
297	300	GnPsaPel/FLT*	1.5	45.2
300	302.2	GnPsaPel/FLT*	1.5	46.1
302.2	303	GnPsaPel/FLT*	0	13.7
303	304.95	GnPsaPel/FLT*	2	50.5
304.95	306	GnPsaPel/FLT*	0	13.7
306	308.1	GnPsaPel/FLT*	2	42.8
308.1	309	GnPsaPel/FLT*	0	13.8
309	310.9	GnPsaPel/FLT*	2	46.5
310.9	312	GnPsaPel/FLT*	0	13.8
312	315	GnPsaPel/FLT*	2	50.9
315	318	GnPsaPel/FLT*	2	46.5
318	320.64	GnPsaPel/FLT*	2	45.9
320.64	321	GnPsaPel/FLT*	0	14.2
321	324	GnPsaPel/FLT*	2	42.0
324	326.65	GnPsaPel/FLT*	2	47.5
326.65	327	GnPsaPel/FLT*	0	14.2
327	330	GnPsaPel/FLT*	2	51.4
330	333	GnPsaPel/FLT*	2	46.0
333	336	GnPsaPel/FLT*	2	52.3
336	339	GnPsaPel/FLT*	2	55.5
339	342	GnPsaPel/FLT*	2	55.8

AND09-02

From	To	Geology	R	RMR
11.06	12	GnPsaPel	2	52.0
12	15	LOST	2	31.1
15	18	GnPsaPel	2	38.3
18	21	GnPsaPel	3	51.7
21	24	GnPsaPel	3	53.2
24	25.4	GnPsaPel	3	53.1
25.4	26.91	GnPsaPel	0	13.9
26.91	27	LOST	3	53.4
27	30	GnPsaPel	3	55.2
30	33	GnPsaPel	3	48.2
33	35	GnPsaPel	3	49.6
35	37	GnPsaPel	2	53.0
37	39	GnPsaPel	2	57.4
39	42	GnPsaPel	2	47.1
42	45	GnPsaPel	2	52.9
45	47.37	GnPsaPel	2	52.9
47.37	48.5	GnPsaPel	3	57.1
48.5	51	GnPsaPel	1	44.5
51	54	GnPsaPel	2	50.6
54	57	GnPsaPel	2	40.0
57	57.15	GnPsaPel	2	35.9
57.15	58.5	GnPsaPel	3	47.7
58.5	60	LOST	2	33.2
60	60.62	GnPsaPel	2	56.9
60.62	62.66	GnPsaPel	2	40.8
62.66	63	LOST	2	56.3
63	66	GnPsaPel	2	41.8
66	69	GnPsaPel	2	42.6
69	72	GnPsaPel	3	47.0
72	75	GnPsaPel	3	50.8
75	78	GnPsaPel	3	48.5
78	81	GnPsaPel	3	53.7
81	84	GnPsaPel	3	54.3
84	87	GnPsaPel	3	61.1
87	90	GnPsaPel	3	59.8
90	93	GnPsaPel	3	48.2
93	96	GnPsaPel	3	53.5
96	97.1	GnPsaPel	3	65.7
97.1	99	GnPsaPel	2	57.6
99	102	GnPsaPel	2	50.1
102	105	GnPsaPel	2	50.1
105	107.67	GnPsaPel	2	51.7
107.67	108	GnPsaPel	2	56.9
108	111	GnPsaPel	2	56.0
111	114	GnPsaPel	2	60.5
114	117	GnPsaPel	2	52.5
117	118.65	GnPsaPel	2	54.0
118.65	120	GnPsaPel	3	57.6
120	122.06	GnPsaPel	3	57.2
122.06	123	GnPsaPel	2	45.7
123	126	GnPsaPel	2	57.0
126	129	GnPsaPel	2	54.6
129	132	GnPsaPel	2	49.1
132	134.42	GnPsaPel	2	51.9
134.42	135.37	GnPsaPel	0	26.1
135.37	138	GnPsaPel	3	60.6
138	139.64	GnPsaPel	3	59.8
139.64	140	GnPsaPel	0	14.5
140	141	GnPsaPel	3	50.3
141	144	GnPsaPel	3	62.0
144	147	GnPsaPel	3	63.5
147	148.55	GnPsaPel	3	38.1
148.55	150	GnPsaPel	2.5	59.7
150	153	GnGran	2.5	63.7
153	154.06	GnGran	2.5	48.1
154.06	156	GnGran	2.5	48.2
156	159	GnGran	3	55.8
159	162	GnGran	3	63.3
162	165	GnGran	3	68.2
165	168	GnGran	3	41.6
168	169.05	GnPsa	2.5	55.5
169.05	171	GnPsa	2.5	55.0
171	174	GnPsa	2.5	46.7
174	174.64	GnPsa	1.5	36.5
174.64	177	GnPsa	2.5	59.5
177	178.42	GnPsa	2.5	60.4
178.42	178.8	GnPsa	2.5	29.6
178.8	180	GnPsa	2.5	55.5
180	183	GnPsa	3	65.7
183	186	GnPsa	3	67.4
186	189	GnPsa	3	61.1
189	192	GnPsa	3	70.5
192	195	GnPsa	3	61.4
195	197.12	GnPsa	3	51.7
197.12	198	GnPsa	3	51.6
198	201	GnPsa	3	58.1
201	204	GnPsa	3	78.9
204	207	GnPsa	3	59.9
207	210	GnPsa	3	52.1
210	213	GnPsa	3	48.6
213	216	GnPsa	3	60.6
216	219	GnPsa	3	52.6
219	221.4	GnPsa	2.5	47.6
221.4	222.86	GnPsa	2	52.9
222.86	223.86	GnPsa	2.5	53.6
223.86	224.6	GnPsa	0	25.8
224.6	225	GnPsa	2.5	46.6
225	228	GnPsa	2.5	52.3
228	228.62	GnPsa	2.5	45.4
228.62	229.13	GnPsa	2	27.1
229.13	230.34	LOST	2	41.6
230.34	231	GnPsa	2	50.9
231	234	GnPsa	3	47.3
234	237	GnPsa	3	58.0
237	240	GnPsa	3	70.7
240	243	GnPsa	3	61.9
243	246	GnPsa	3	68.2
246	249	GnPsaPel	3	66.4
249	252	GnPsaPel	3	60.5
252	255	GnPsaPel	1	48.1
255	258	GnPsaPel	2	55.2
258	261	GnPsaPel	2	41.8
261	264	GnPsaPel	2	36.2
264	267	GnPsaPel	5	74.7
267	270	GnPsaPel	5	69.4
270	273	GnPsaPel	5	74.1
273	276	GnPsaPel	5	80.8
276	279	GnPsaPel	5	73.7
279	282	GnPsaPel	5	79.8
282	285	GnPsaPel	5	71.7
285	288	GnGran	5	85.4
288	291	GnGran	5	73.6
291	294	GnGran	5	85.4
294	297	GnGran	5	80.0
297	300	GnGran	5	72.1
300	303	GnGran	5	66.4
303	306	GnGran	5	72.1
306	309	GnGran	5	90.1
309	312	GnGran	5	74.0
312	315	GnGran	5	74.8
315	318	GnGran	5	80.4
318	321	GnGran	5	84.8
321	324	GnGran	5	83.8
324	327	GnGran	5	78.3
327	330	GnGran	5	73.3



3.0 ROCK MASS CLASSIFICATION RESULTS

The 2007/2008 and 2009 geotechnical borehole rock mass rating (RMR) and rock strength index (R) values were plotted in the 3D Surpac geology model for the Andrew Lake pit. These models include the lithology, mineralization and faulting structure data provided by AREVA. On these sections, the boreholes show the R values (left bar), the lithology (middle bar), and the RMR values (right bar). Several sections were plotted across the pit boundary and some general interpretation was carried out to delineate geotechnical domains.

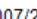

The Andrew Lake geology is complicated by the faulting and mineralization horizons which appear to coincide with mineralogical alteration, leading to weakening and reduced quality in the rock mass. Plotting these inferred fault and mineralization alteration zones on the sections tends to coincide with the lower quality zones in the borehole data. Currently, the rock mass conditions in the majority of the planned pit walls is uncertain, although it is inferred that the rock mass quality improves with increased distance away from the mineralization zones.

Figure B2 presents geological sections with the inferred alteration zones and lithological domains on the Andrew Lake pit shell.

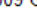
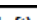
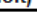
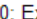

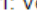
Figure B3 (from Figure B2) presents a 2D section taken SW-NE across the Andrew Lake pit. Several faults transecting the pit are shown in this section, as well as a fairly significant fault trending near parallel to the section trend. The rock associated with these faults and alteration zones tend to range from fair to good quality with some infrequent zones of poor quality, and are generally weak to moderately strong. The lithological units away from the central mineralization and faulting region are uncertain. As seen in the section, a three tier lithology arrangement has been generalized which includes; upper metasediments underlain by granitoids, underlain by lower metasediments/paragneiss. This interpretation loosely follows the geological model presented in the SRK geological model update (SRK 2008). A geological section taken from this document, showing the layout of the ore zone and lithological domains, is presented in Figure B4. Comparing Figures B3 and B4, the upper ore zones have not been clearly delineated in the AREVA geology model.

FIGURE B2














BOREHOLE

 2007/2008 Geotechnical Holes
 2009 Geotechnical Holes




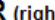

(left) STRENGTH

	R0: Extremely Weak Rock
	R1: Very Weak Rock
	R2: Weak Rock
	R3: Medium Strong Rock
	R4: Strong Rock
	R5: Very Strong Rock

simp_code

	ALT
	BC
	BX
	CLAY
	FLT
	GN
	GRA
	LC
	MSED
	OVb
	QTZ
	SCHIST
	SY

RMR (right)

 0 to 20	 60 to 80
 20 to 40	 80 to 100
 40 to 60	

The geological map displays the following features and labels:

- Geological Units:**
 - Upper Metasediments (Arevik):** Indicated by a black arrow pointing to the top left corner.
 - Upper Metasediments:** A box label for the light green area.
 - Granitoids:** A box label for the orange area.
 - Lower Metasediments:** A box label for the light blue area.
- Structural Features:**
 - Fault parallel borehole:** A black arrow pointing to a borehole location.
 - Base of Permafrost:** A horizontal blue line across the map.
 - Mineralization alteration zone:** A black arrow pointing to a yellow-shaded area.
 - Fault alteration zone:** A black arrow pointing to a yellow-shaded area.
- Geographic Coordinates:**
 - Latitude:** -100 Z, -200 Z.
 - Longitude:** 553150 E, 553250 E, 553350 E, 553450 E, 553550 E, 553650 E.
- Other Labels:**
 - ANDW-08-09-02** (purple)
 - ANDW-08-01** (purple)
 - 10-07-ANDW** (purple)
 - ANDW-08-01** (orange)
 - ANDW-08-01** (orange)



APPENDIX B - ROCK MASS CLASSIFICATION

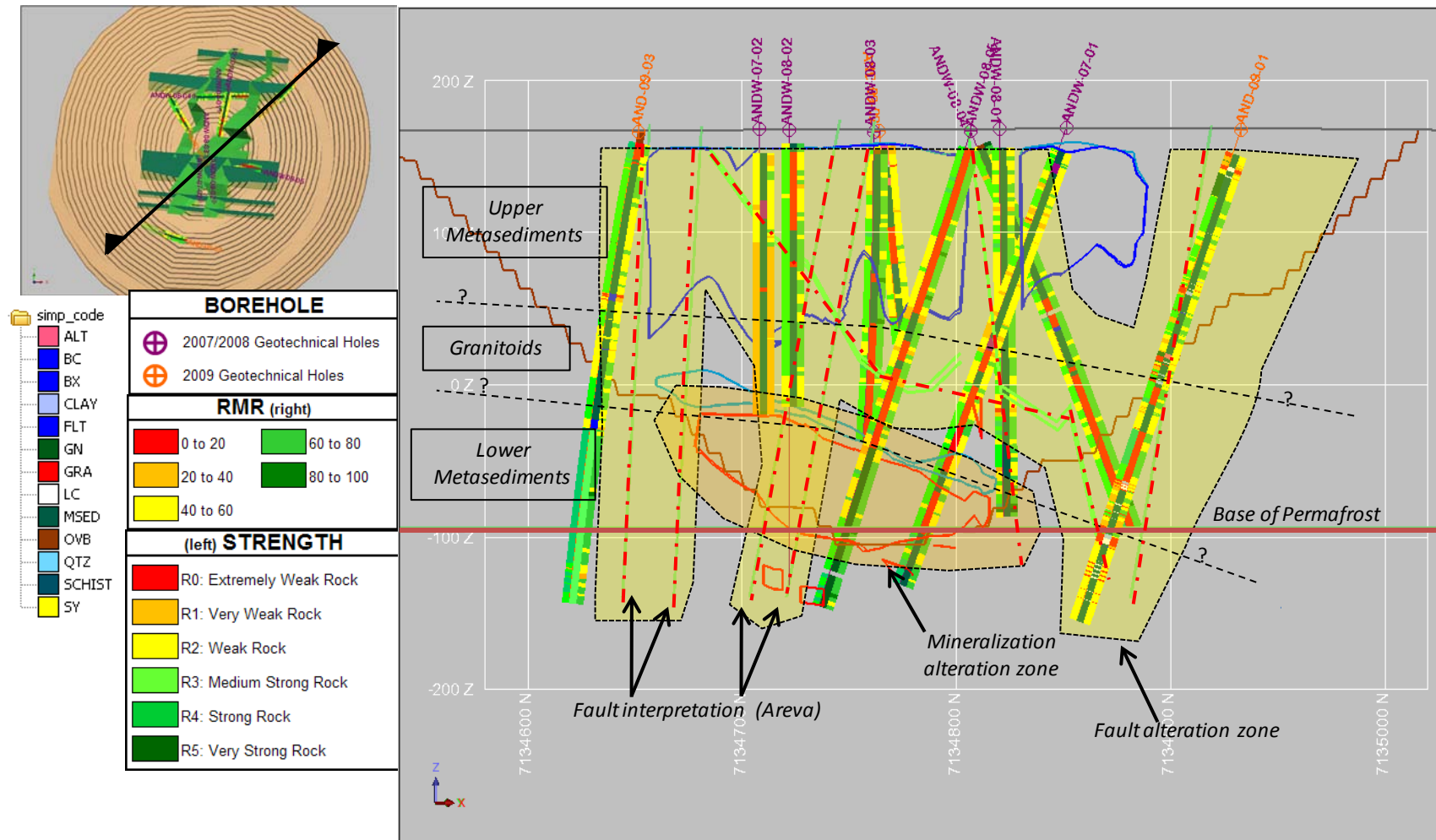


Figure B3: Andrew Lake Pit - Generalized Geotechnical Section (SW-NE). Inferred Fault and Mineralization Alteration Zones are Highlighted.



APPENDIX B - ROCK MASS CLASSIFICATION

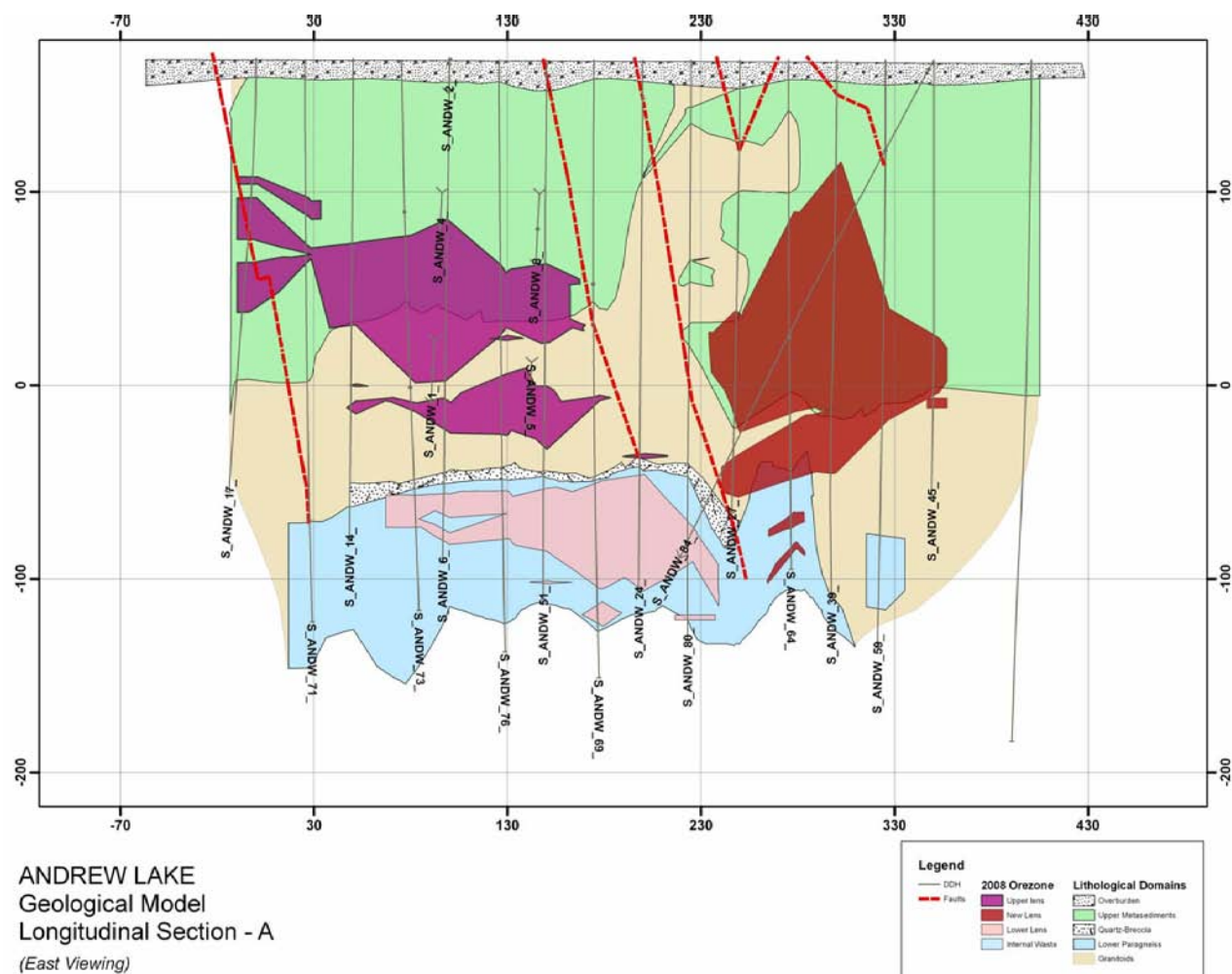


Figure B4: Andrew Lake Pit - Geological Model of Ore Zones and Lithological Domains (SRK, 2008)

Both AND09-1 and AND09-03 are plotted on Figure B3. Borehole AND09-01 appears to follow very closely to both an E-W trending fault and the major NE-SW trending Andrew Lake fault. The overall quality and strength of the rock mass intersected by this borehole are lower than the other 2009 boreholes, and rock mass conditions do not improve with depth. The poor quality of this hole is assumed to be due to the effect of alteration and faulting at close proximity to the hole.

Borehole AND09-03 shows fair quality, weak to moderately strong conditions in the initial 200 m identified as metasediments. This zone is possibly fault influenced as it trends in close proximity to the NE-SW trending fault structures. Below 200 m the rock is mainly good quality, moderately strong to strong rock identified as granitic. A lower quality zone is intersected at 300 m to 310 m, possibly associated with a second fault structure.



APPENDIX B - ROCK MASS CLASSIFICATION

Figure B5 presents a 2D section taken W-E across the Andrew Lake pit, towards the north end wall. Again the inferred mineralization appears to be associated with lower quality and weaker ground conditions. Borehole AND09-02 is plotted on this section. The upper 180 m of the borehole is shown to be generally fair quality, and generally weak, identified as metasediments. This zone is possibly fault influenced. From 180 m to 264 m, the rock shows similar fair quality with a slight improvement in strength, also identified as metasediments. The borehole appears to be trending towards an E-W trending fault in this zone. Below 264 m, the rock is predominantly good quality and strong, identified as granitic gneiss.

The 2009 Andrew Lake RMR data has been plotted in cumulative frequency distribution diagrams as shown on Figures B6 through B8. These plots were generated by summing the core lengths within given RMR ranges, and taking these sums as the statistical percentage of the overall drilled length. The RMR distributions exemplify the potential variability in rock mass conditions that could be encountered in the rock mass. The statistically significant RMR values have been taken as the Lower Bound (20% cumulative), Average (50% cumulative), and Upper Bound (80% cumulative) distributions. This provides a probable range of RMR values comprising the rock mass.

Figure B6 shows the cumulative frequency distribution of RMR values by borehole. The associated lower bound, upper bound, and average RMR values are summarised in Table B2. In general, hole AND09-01 shows the lowest relatively quality of the 3 holes, likely due to its association with the NE-SW faulting. The statistically significant range in RMR values is between 40 (fair to poor) to 68 (good), although locally RMR values are shown to range between 10 and 85. Average RMR values for the three holes are fairly consistent at between 54 and 58 (fair).



APPENDIX B - ROCK MASS CLASSIFICATION

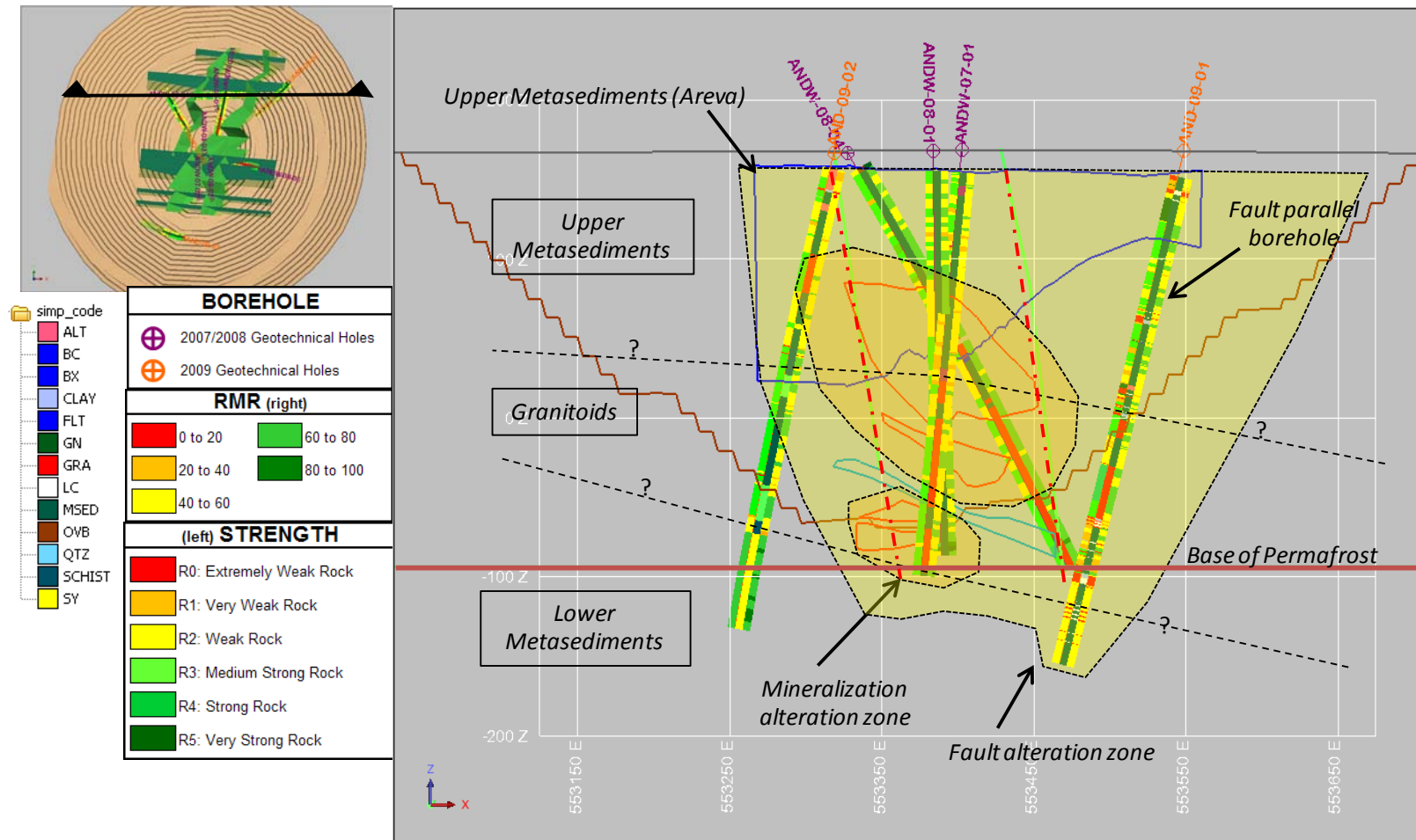


Figure B5: Andrew Lake Pit - Generalized Geotechnical Section (W-E). Inferred Fault and Mineralization Alteration Zones are Highlighted.



APPENDIX B - ROCK MASS CLASSIFICATION

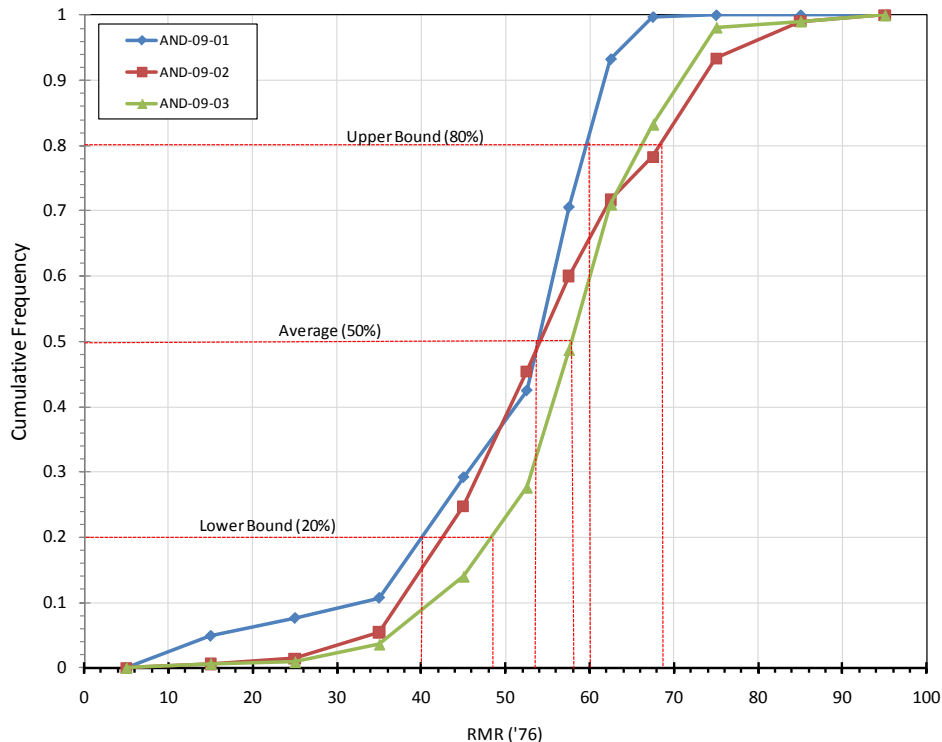


Figure B6: Andrew Lake - 2009 Boreholes. Cumulative Frequency Distribution of RMR by Borehole.

Table B2: Andrew Lake – 2009 Boreholes. Summary of RMR values by borehole.

Hole	RMR (1976)		
	Lower Bound	Upper Bound	Average
AND09-01	40	60	54
AND09-02	42	68	54
AND09-03	48	66	58

The RMR values are plotted by rock type in Figure B7, with corresponding values summarised in Table B3. The rock units have been summarised into metasediments at varying depths (less than 100 m, 100 m to 200 m, and greater than 200 m), as well as granites. It is noted that these depths are downhole depths. It is shown that the upper 200 m of metasediments shows fairly similar distribution (average RMR = 52 to 54), but for the data below 200 m, the average quality increases considerably (average RMR = 68). This increase in quality with depth is possibly both associated with the rock types, as well as increased offset from the fault and mineralization zones. A trend of increasing strength with depth below 200 m was also noted in Appendix A. The granites show slightly improved quality compared to the upper metasediments, with an average RMR of 58.



APPENDIX B - ROCK MASS CLASSIFICATION

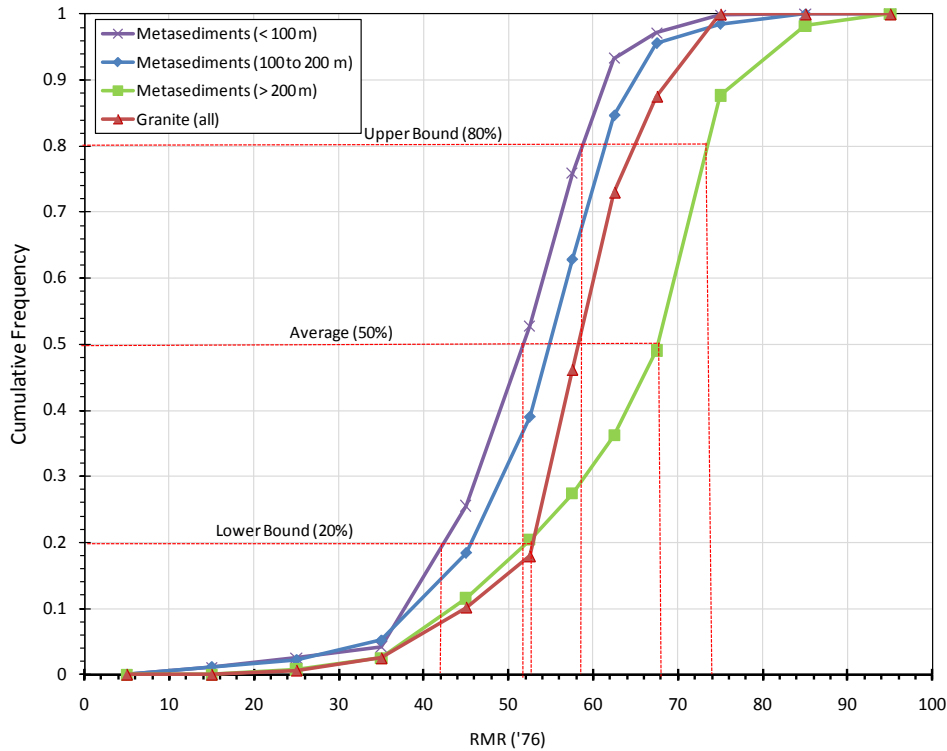


Figure B7: Andrew Lake - 2009 Boreholes. Cumulative Frequency Distribution of RMR by Rock Type.

Table B3: Andrew Lake – 2009 Boreholes. Summary of RMR values by rock type.

Lithology	Depth	RMR (1976)		
		Lower Bound	Upper Bound	Average
Metasediments (GnGran,GnPsa,GnPsaPel)	<100 m	42	58	52
	100 to 200 m	45	62	54
	>200 m	52	74	68
Granite (GranT)	all	52	65	58

GnGran, GnPsa, GnPsaPel = Granitic Gneiss, Psammitic Gneiss, Psammo-pelitic Gneiss; GranT = Granite

The Andrew Lake RMR data is again plotted by alteration in Figure B8, with RMR values summarised in Table B4. The alteration factor (A_f) has been used, which is a product of both the argillization rating ($A_{arg} = 0$ to 4) and chloritization rating ($A_{chl} = 0$ to 4) used by AREVA. The alteration factor is discussed in Appendix A. The Andrew Lake rock was divided into 3 alteration domains; nil to minor alteration ($A_f = 0$ to 1), moderate alteration ($A_f = 2$ to 3), and highly altered ($A_f \geq 4$). As expected, there is shown to be a decrease in rock mass quality with increased alteration. However, the overall range between nil to highly altered rock is not excessive, with average RMR ranging between 50 and 58. There was shown to be a more prominent variability in rock strength with increased alteration, as discussed in Appendix A.



APPENDIX B - ROCK MASS CLASSIFICATION

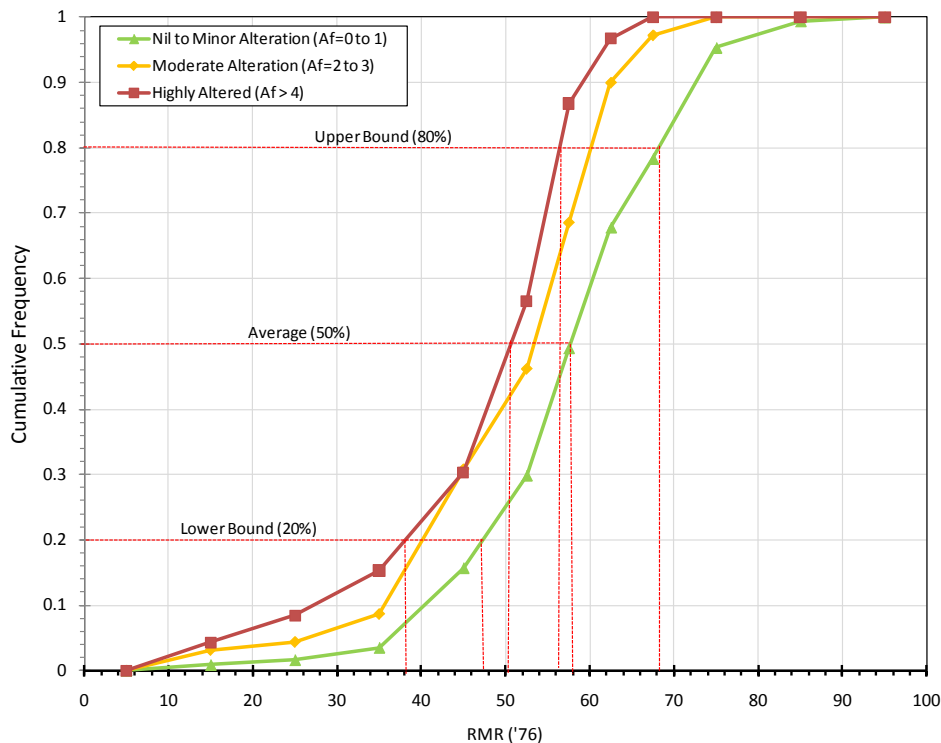


Figure B8: Andrew Lake - 2009 Boreholes. Cumulative Frequency of RMR by Alteration Factor (Af)

Table B4: Andrew Lake – 2009 Boreholes. Summary of RMR values by alteration factor (Af).

Alteration	RMR (1976)		
	Lower Bound	Upper Bound	Average
Nil to Minor (Af = 0 to 1)	48	68	58
Moderate (Af = 2 to 3)	40	60	54
Highly Altered (Af >= 4)	38	56	50

4.0 CONCLUSIONS AND RECOMMENDATIONS

The proceeding sections have presented the methodology and results of the rock mass classification work carried out for the 2009 geotechnical data for the Andrew Lake pit. Generalized interpretations were made based on the available information. Appreciably more geotechnical information should be collected to make better interpretations on rock mass quality and strength, predominantly for the final planned pit walls, where currently data is lacking.

The Andrew Lake rock mass is interpreted to be mainly comprised of metasediments, granitics, and lower metasediments or paragneiss. Mineralization and faulting related alteration halos appear to reduce the quality and strength of the rock in close proximity to this alteration. Reduced strength and quality will occur on the final pit floor, and the lower slopes of the pit walls. Potentially more significant, fault related alteration reduced strength and quality appears likely along the pit walls in various locations as shown on Figure B2.



APPENDIX B - ROCK MASS CLASSIFICATION

Recommendations for RMR and strength parameters for the main rock units at Andrew Lake are given in Table B5. Assumptions related to the recommended values are also given in the table.

Table B5: Andrew Lake – Recommendations for RMR and strength parameters.

Rock Unit	RMR (1976)	Comment	Strength	Comment
Upper Metasediments (<200 m depth)	42 to 62 (fair)	Range of RMR for lower to upper bound limits for the 2009 Upper Metasediment data. Average RMR of nil to moderately altered ground.	R2/R3 (weak to moderately strong)	Average UCS = 29.9 MPa and average $I_s(50)$ = 2.2 MPa for upper metasediments (Appendix A)
Granites (all)	52 to 65 (fair to good)	Range of RMR for lower to upper bound limits for the 2009 Granite data. Average RMR of nil to moderately altered ground.	R3/R4 (moderately strong to strong)	Average UCS = 66.5 MPa and $I_s(50)$ = 5.5 MPa (Appendix A)
Lower Metasediments/ Paragneiss (>200 m depth)	52 to 74 (fair to good)	Range of RMR for lower to upper bound limits for the 2009 Lower Metasediments data. Average RMR of nil to slightly altered ground.	R4 (strong)	Average $I_s(50)$ = 7.3 MPa (Appendix A)
Fault or Mineralization Altered Zones	42 to 52 (poor to fair)	Lower Bound RMR of all 2009 lithology data. Average RMR of 2009 highly altered data.	R2 (weak)	Average UCS = 7.4 to 24.7 MPa for moderate to highly altered rock or fault related zones (Appendix A)

5.0 REFERENCES

- Bieniawski, Z.T., 1976. Rock mass classification in rock engineering. In *Exploration for rock engineering, proc. of the symp.*, (ed. Z.T. Bieniawski) **1**, 97-106. Cape Town: Balkema.
- Barton, N.R., Lien, R. and Lunde, J., 1974. Engineering classification of rock masses for the design of tunnel support. *Rock Mech.* **6**(4), 189-239.
- Golder Associates Ltd., 2009. Draft 2009 Kiggavik Geotechnical and Hydrogeological Investigation Data Report. November, 2009. Project #09-1362-0613. November 2009.
- Hoek, E., and Brown, E.T., 1980a. *Underground excavations in rock*. London: Instn Min. Metall.
- SRK. 2008. Andrew Lake Geological Model Update. Technical Memorandum. November 27, 2008.
- SRK Consulting (Canada) Inc., 2009. Kiggavik-Sissons Updated Geotechnical Data Report 2007/2008. Project #1CA015.003. March 2009.

n:\active\2009\1362\09-1362-0613 areva kiggavik geotechnical baker lake nunavut\pit slope report\draft 2 - submitted late dec 2009\andrew lake\appendix b\app 09 dec 21 andrew lake appendix b - rock mass classification.docx



APPENDIX C

Stereonet Analysis from Oriented Core Data



Table of Contents

1.0 INTRODUCTION.....	1
2.0 CORE ORIENTATION METHODOLOGY.....	1
3.0 ASSESSMENT OF ROCK MASS FABRIC	1
3.1 Major Geological Structure	1
3.1.1 Fault Trends.....	1
3.1.2 Foliation/Bedding	2
3.2 Stereonets from Oriented Core Data	3
3.3 Definitions of Pole Concentrations.....	4
3.4 Results from Stereonet Analysis.....	4
3.4.1 Assessment of Oriented Core Data.....	4
3.4.2 Selected Discontinuity Sets.....	1
3.5 Structural Domains	2
4.0 DETERMINATION OF STRUCTURAL SETS FOR KINEMATIC ANALYSES.....	3
5.0 REFERENCES.....	4

TABLES

Table C1: Summary of Oriented Boreholes from 2007, 2008, and 2009 Andrew Lake.....	1
Table C2: Summary of Oriented Features from 2009 Boreholes at Andrew Lake.....	1
Table C3: Summary of Discontinuity sets for the 2009 Golder, 2008 (SRK), Oriented Core Data at the Andrew Lake Site.....	1
Table C4: Structural Sets for Kinematic Analysis from Andrew Lake (all sets assumed major for kinematic analysis).	5

FIGURES

Figure C1: Andrew Lake Drillhole Location Plan showing 2008 and 2009 Oriented Drillholes.....	1
Figure C2: Andrew Lake Pit Showing the Inferred Faults from the Geological Model (green) and the Regional Fault Trends (Beaudemont Faults) Cross-cutting the Pit Walls (brown and yellow).....	2
Figure C3: Andrew Lake - 2009 Oriented Core Data for Foliation (FO) and Contacts (CO).....	3
Figure C4: Andrew Lake - Oriented Core data Contoured; a) All 2009 Data; b) Moderate to High Confidence 2009 Data; and c) 2008 data (SRK)	1
Figure C5: Andrew Lake - Selected Major and Minor Sets by Borehole; a) 2008 & 2009 Sets by Golder; and b) ANDW-08-04 Sets Reported by SRK.....	2
Figure C6: Andrew Lake - Combined 2008 (SRK) and 2009 Data Contoured; a) Metasediments; b) Granites and Granitoids; and c) Gneiss (Granitic or Pelitic)	3
Figure C7: Andrew Lake - 2008 and 2009 Oriented Core Data (contoured) with Selected Structural Sets.....	6



APPENDIX C - STEREONET ANALYSIS

Figure C8: Identified Sets by Each Borehole - AND09-01	7
Figure C9: Identified Sets by Each Borehole - AND09-02	8
Figure C10: Identified Sets by Each Borehole - AND09-03	9
Figure C11: Identified Sets by Each Drillhole - ANDW-08-04	10
Figure C12: All Validated Data with Symbolic Pole Plots (Feature Type and Discontinuity Alteration Index)	11



APPENDIX C - STEREONET ANALYSIS

1.0 INTRODUCTION

This appendix outlines the methodology used to select the major and minor discontinuity sets within the rock masses at Andrew Lake.

Details of the 2009 geotechnical drilling program that was conducted at Andrew Lake have been presented in a geotechnical data report prepared by Golder entitled “2009 Kiggavik Geotechnical and Hydrogeological Investigation Data Report”. This data report outlines the drilling program conducted, and presents the data collected during the 2009 season. As reference, a total of 3 holes were oriented during the 2009 investigation at Andrew Lake. Oriented boreholes are shown on Figure C1, along with oriented boreholes logged by SRK Consulting (SRK) in 2008 for reference, and are summarized on Table C1.

Table C1: Summary of Oriented Boreholes from 2007, 2008, and 2009 Andrew Lake

Borehole #	Year Drilled ^(a)	Northing	Easting	Collar Elevation (masl)*	Azimuth	Dip	Drill Depth (mAH)	Vertical Depth (mbgs)	Bit Size
AND09-01	2009 (G)	7134927	553548	167.94	228	-70	342	321	NQ3
AND09-02	2009 (G)	7134809	553319	167.07	330	-65	330	299	NQ3
AND09-03	2009 (G)	7134574	553312	166.21	284	-70	327	307	NQ3
ANDW-08-04	2008 (SRK)	7134893	553326	168	092	-60	300	260	HQ3

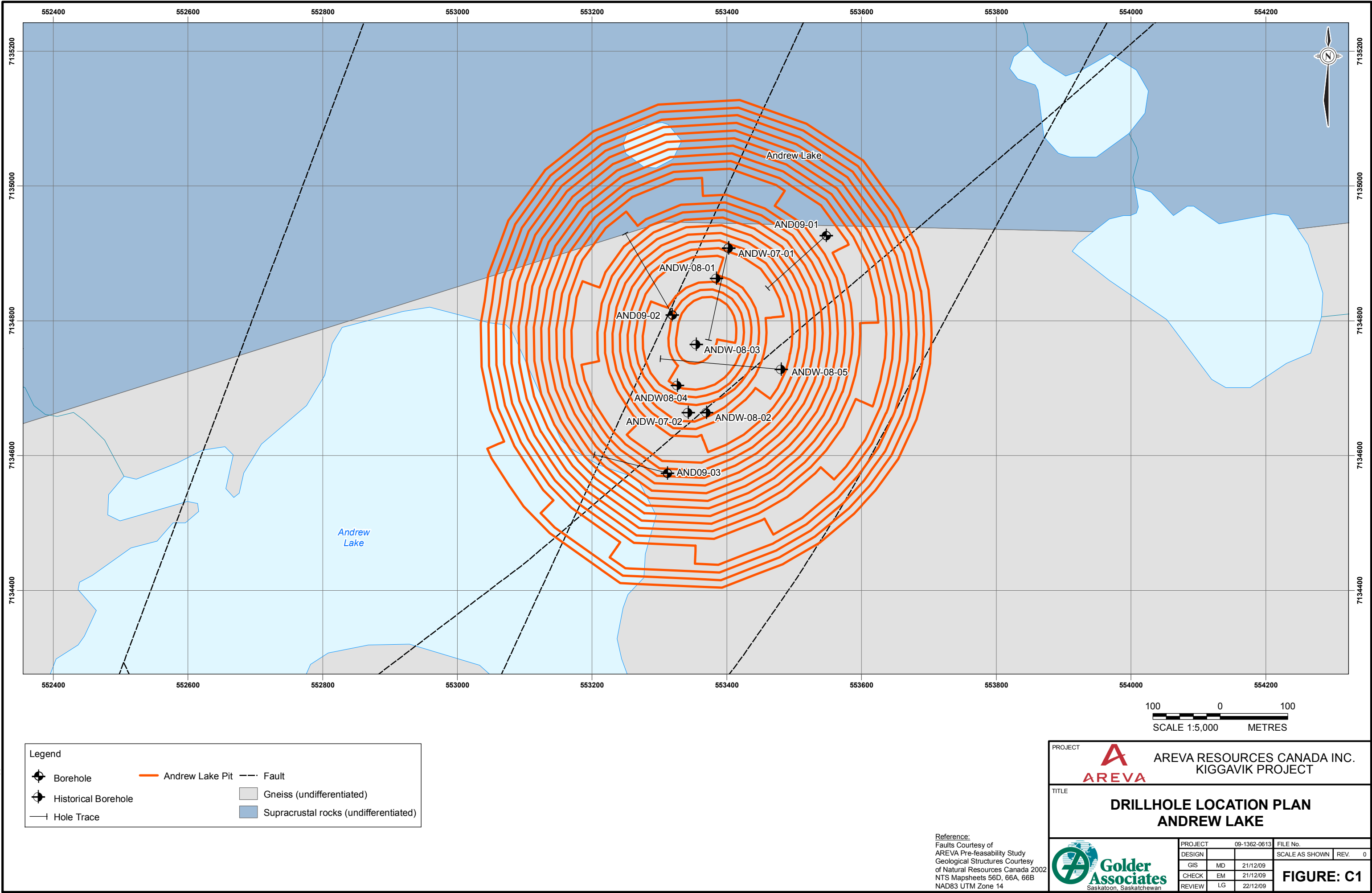
A = G = Golder (2009), SRK = SRK (2007/2008); Coordinates in UTM NAD 83 Zone 14, Collar elevation for 2009 boreholes are an estimate based on point data collected from a LiDAR survey, masl = metres above sea level; mAH = metres along hole; mbgs = metres below ground surface

2.0 CORE ORIENTATION METHODOLOGY

In 2009, core orientation was undertaken by the drilling contractor using an Ace Core Orientation Tool (ACT), made by Reflex Instruments. ACT was a fully electronic system that used accelerometers to reference the low side of the borehole (Reflex, 2009). This information was then used by the drill staff to place a reference mark at the bottom of each drill run which corresponded to the low side of the borehole.

During the core logging process, Golder personnel used the driller's reference mark to scribe an orientation line on the low side of the drill core along the length of the drill run. A good match of reference lines between consecutive drill core runs was considered valid with ‘high confidence’. When the orientation lines varied at approximately 40 to 60 degrees from one another, this data was considered valid with ‘moderate confidence’. In some cases, poor core conditions in zones of highly fractured or altered core prevented the line from being extended the length of the drill run and the core orientation line was lost. This frequently occurred for the Andrew Lake holes as the drill core was often broken and damaged in the weaker ground. When there was no match between orientation lines, or no continuity between oriented zones, the data was considered invalid or ‘low’ confidence.

G:\2009\1362\09-1362-0613-Areva Kiggavik Golder Internal Field Manual\GIS\Maps\Geotechnical\Sissons Site\GTI-09-1362-0613-GEO-Drillhole Location Plan - Current and Historical - Andrew Lake_Appendix.mxd





APPENDIX C - STEREONET ANALYSIS

Using the orientation line, alpha and beta angles were measured for each logged discontinuity. Alpha angles were a measurement of the apparent dip of the feature with respect to the core axis. These measurements were taken at the steepest part of the discontinuity, and ranged from 0 degrees (i.e., horizontal to the core axis) to 90 degrees (i.e., perpendicular to the core axis). Beta angles were the measurement of the apparent trend of the discontinuity, with respect to the orientation reference line. Beta angles were measured using linear protractors, where the zero degree mark was held on the reference line, with the measurement being taken in a clockwise direction on the “down dip” end (i.e., bottom of the discontinuity when looking downhole) of the discontinuity surface. Measurements ranged between 0 to 360 degrees. A summary of all orientation measurements taken from the 2009 boreholes at Andrew Lake are shown in Table C2. Due to the drilling conditions and relative rock mass quality, there was generally a low percentage of data which was validated for the Andrew Lake holes. The use of this data is discussed further in the following sections.

Core drilled in 2007 and 2008 was oriented using ACT in a similar manner to that used in 2009 (based on SRK, 2009).

Table C2: Summary of Oriented Features from 2009 Boreholes at Andrew Lake

2009 Borehole	# of Features Oriented	% of Features Oriented	# of Intervals Oriented	% Intervals Oriented
AND09-01	192	17%	34	17%
AND09-02	514	39%	65	48%
AND09-03	537	42%	67	49%

3.0 ASSESSMENT OF ROCK MASS FABRIC

3.1 Major Geological Structure

The major geological structures at Andrew Lake have been summarized below:

3.1.1 Fault Trends

At the Andrew Lake deposit, the regional Andrew Lake Fault, which is steeply dipping and trends northeast at 030 degrees (AREVA 2007), was assumed to lie within the footprint of the proposed pit. It is possible that four dominant north-northeast trending faults mapped from historical core data are related to the Andrew Lake fault. The four mapped fault features appear to control the lateral extents of the uranium mineralization at Andrew Lake, and strike in the same orientation as the mineralization (SRK 2008). At Andrew Lake, there is also evidence of structural features which cross-cut these faults, although there is limited drill core data to support this (SRK 2008). It is estimated that these cross-cutting features run sub-parallel to the north-northeast trending faults, and may have an influence on the mineralization at Andrew Lake (SRK 2008). It has been estimated these cross cutting features dip steeply to the southwest (SRK 2008).

The inferred faults provided in the geological model supplied by AREVA, as well as the regional fault trends for Andrew Lake are plotted on Figure C2 below. A number of fault structures are inferred to intercept the pit walls and floor at Andrew Lake, mainly trending north-south to northeast-southwest, or orthogonal to this trend striking east-west. Again there is not always agreement between the fault interpretations as given in the geological model, and the regional fault trends, which were provided by AREVA and based on geophysical anomalies identified. Future work should aim to clarify the locations and orientations of the major fault structures.



APPENDIX C - STEREONET ANALYSIS

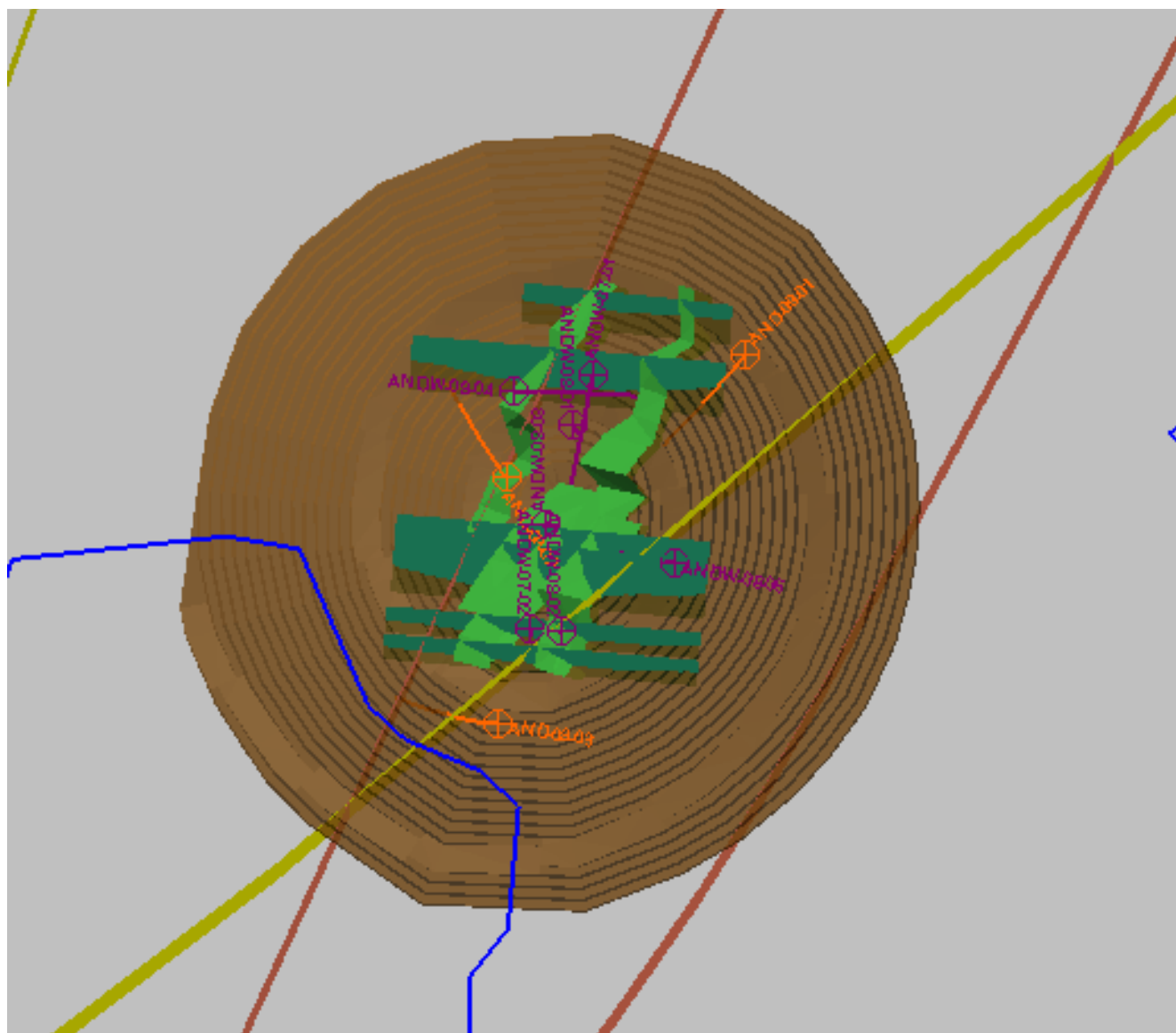


Figure C2: Andrew Lake Pit Showing the Inferred Faults from the Geological Model (green) and the Regional Fault Trends (Beaudemont Faults) Cross-cutting the Pit Walls (brown and yellow)

3.1.2 Foliation/Bedding

At Andrew Lake, the identified foliation trend dips at 20 to 50 degrees towards the east or south-east (see Figure C3). This trend, possibly related to bedding in the metasedimentary rock units, suggests a slight uplift and tilting has occurred for the lithologies at the Andrew Lake site. A single lithology contact was identified at Andrew Lake dipping at 40 degrees towards the north, although with moderate confidence in the orientation. This contact could be related to a dyke or intrusion.



APPENDIX C - STEREONET ANALYSIS

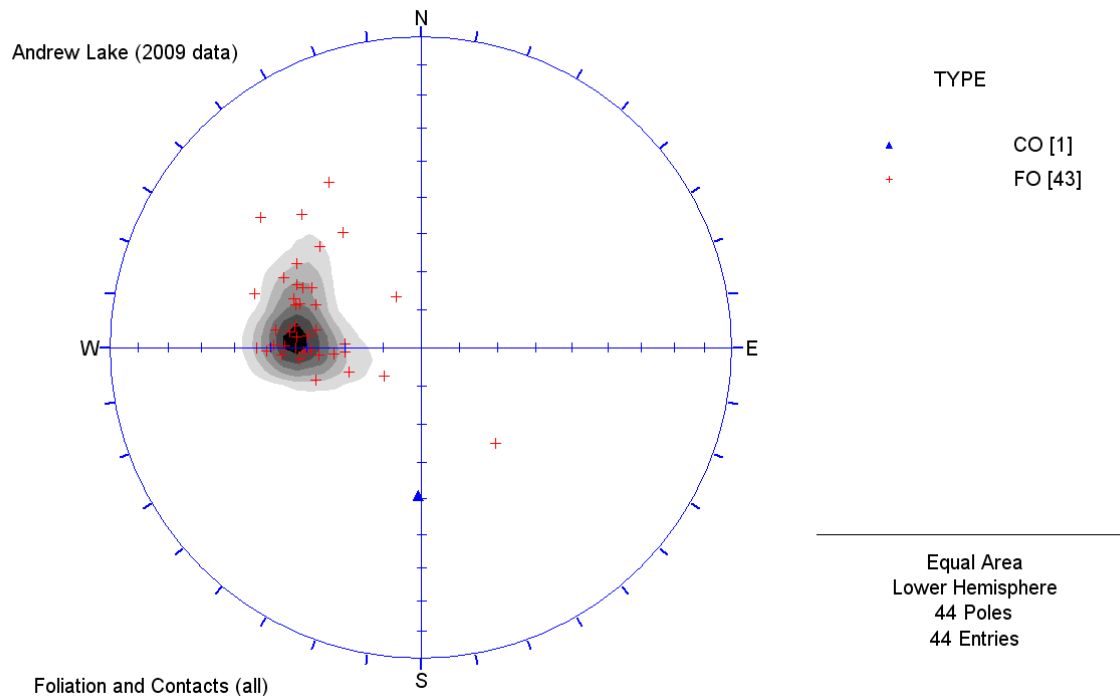


Figure C3: Andrew Lake - 2009 Oriented Core Data for Foliation (FO) and Contacts (CO)

3.2 Stereonets from Oriented Core Data

Discontinuity data was analysed statistically using the software DIPS®, distributed by Rocscience. DIPS® allows the user to analyze and visualize structural geological data using the same techniques developed for manual stereonet analysis (Rocscience 2009a). It also allows the user to contour data, analyze discontinuity statistics, and select discontinuity sets.

In order to enter borehole discontinuity data (alpha and beta angles) into DIPS®, the borehole orientation had to be input as traverses. Borehole traverses were selected based on downhole surveys that were conducted by the drilling contractor as the borehole was advanced. The downhole surveys were conducted using a Reflex EZ-Shot tool, manufactured by Reflex Instruments. These surveys recorded borehole dip and dip direction at specific depth points along the borehole, with the survey interval generally every 51 m. This survey data was entered into DIPS® as separate traverses, to which the discontinuity data was assigned. This allowed for the incorporation of any borehole deviation into the analysis of the discontinuity data. As the reflex tool provided measurements relative to magnetic north, a correction for magnetic declination was applied in DIPS®. The magnetic declination was calculated based on the Geological Survey of Canada online magnetic declination calculator, and was found to be 1.4 degrees west for the Kiggavik site.

The pole to a plane is a convenient geomechanical construction that can be used to uniquely define the inclination and orientation of the plane of a discontinuity on the stereonet projection. As each pole is located 90° from its plane, a plot of poles represent the dip and dip direction of all measured discontinuities. Thus in turn, statistical contouring allows the pole density for a given discontinuity fabric to be delineated on the stereonet, which provides a 3D representation of structural data. The analysis of the structural data from Andrew Lake was



APPENDIX C - STEREONET ANALYSIS

carried out using lower hemisphere equal area stereonet projections, and a Fisher distribution. Discontinuity sets are represented on the stereonets as areas with high pole densities or concentrations as indicated by the contours.

As much of the data was from line sources (boreholes), a bias correction (referred to in DIPS© as the Terzaghi correction) was applied to the oriented core data to help eliminate the problem of data misrepresentation. The bias correction calculates a geometrical weighting factor to each discontinuity measured, with the highest correction applied to the structures that are subparallel to the borehole orientation. Discontinuities that are perpendicular to the core axis receive the smallest weighting factor, since these features are intersected more often in the borehole, and are therefore measured more frequently during the core logging. Since the weighting function tends to infinity as the angle between the discontinuity and the borehole axis (α) approaches zero, a maximum weighting corresponding to a 15° bias angle was applied to any plane with $\alpha \leq 15^\circ$ orientation (Rocscience, 2009b).

3.3 Definitions of Pole Concentrations

For Andrew Lake, there was minimal validated orientation data. The method used for identifying major and minor sets was based on pole density. When treating data per drillhole, a pole density or concentration between 1% and 3% was selected to represent a minor discontinuity set, while a pole density greater than approximately 3% was selected to indicate major or dominant joint sets. When assessing all drillholes together, generally pole densities of 1% to 2% and greater than 2% were used to define minor and major sets, respectively. However, due to the low number of total data poles considered, consideration was also given to the continuity of the set between boreholes. If the set appeared in more than one borehole, and was apparent when all the data from all the boreholes were plotted together, it was considered a major set. If it was only apparent in one borehole, and not apparent when all the data was plotted together, then it was considered a minor set within the particular borehole it occurred in.

The discontinuity sets for Andrew Lake were selected manually by identifying the peak concentrations and recording the orientation of that point. This was done using a Terzaghi weighted contour plot of all the borehole data in DIPS© (including oriented core data from 2007/2008), using the “add plane” function.

The discontinuity sets were numbered and labelled with upper and lower case fonts representing, respectively, major and minor discontinuity sets. For example, ‘JN’ or ‘jn’ was used to differentiate major or minor discontinuity sets. Since these major and minor sets show some variations in terms of both dip and dip directions, for the kinematics analyses, these variations have been addressed by considering sub-sets, which were labelled with the letter ‘A’ (or ‘a’) and ‘B’ (or ‘b’).

3.4 Results from Stereonet Analysis

3.4.1 Assessment of Oriented Core Data

Figures C8 to C12 appended to this text show the stereographic projections for Andrew Lake. These figures show the oriented core data plotted by the individual borehole, as well as data symbolic pole plots of grouped data showing types of features logged (i.e., bedding, foliation, joints, shears, etc.) as well as the joint alteration index value referring to the degree of alteration of the joint surface (Golder 2009). Some additional comments and interpretation are included on these figures.



APPENDIX C - STEREONET ANALYSIS

As discussed previously, there was some difficulty maintaining orientation in the drilled core, particularly in zones of highly fractured or mechanically broken rock. Assessment was made in the field as to the high, moderate, and low confidence based on alignment of consecutive orientation reference lines.

For the Andrew Lake data, there is appreciably more pole scatter, likely related to the drilling and rock conditions, and the difficulties maintaining valid core orientation. All Andrew Lake 2009 data (1239 features) was compared to the moderate to high confidence data (487 features) as shown on Figure C4 below. By removing the low confidence data, much of the apparently random pole scatter is removed from the data set, therefore, only the moderate to high confidence data was used in analysing the specific discontinuity sets.

The borehole directions are also plotted on Figure C4 for comparison. Holes AND-09-01 to -03 are drilled at azimuths ranging between 225 and 330 degrees. The 2008 borehole ANDW-08-04 (119 features) was drilled in a complimentary direction, at approximately 090 degrees. This data is also plotted on a separate stereonet on Figure C4. In order to reduce potential borehole direction bias, and optimize the amount of available features for orientation, the 2008 and 2009 (validated) data was combined for analysis of discontinuity sets at Andrew Lake.



APPENDIX C - STEREONET ANALYSIS

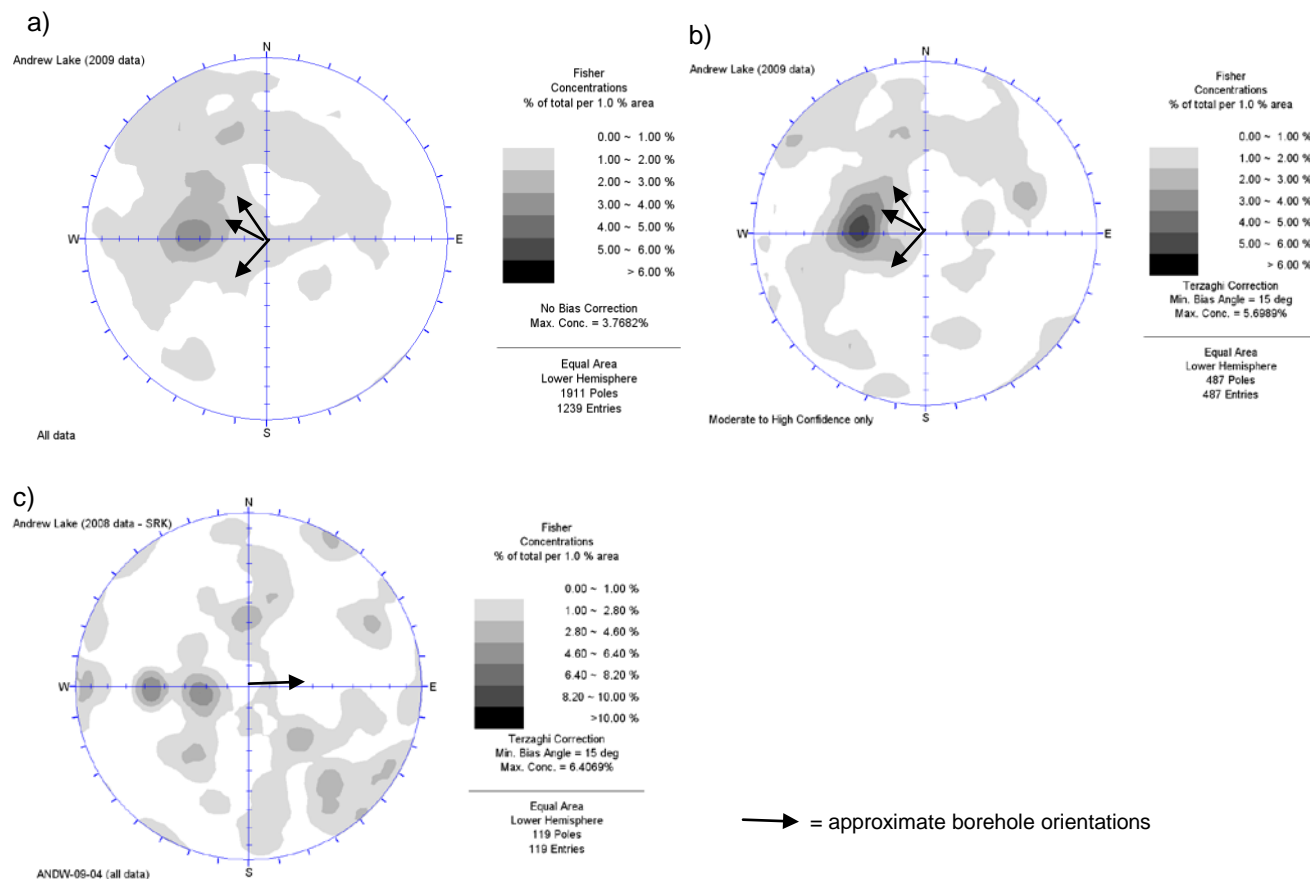


Figure C4: Andrew Lake - Oriented Core data Contoured; a) All 2009 Data; b) Moderate to High Confidence 2009 Data; and c) 2008 data (SRK)

3.4.2 Selected Discontinuity Sets

For the Andrew Lake structural data analyses, the validated oriented core data sourced from the 3 geotechnical boreholes were analysed by borehole for the identification of major and minor sets following the conventions discussed previously (major = greater than 3% pole concentration). The 2008 oriented core data from borehole ANDW-08-04 was also assessed following similar criteria. The selected major and minor discontinuity sets are summarised by trend and inclination in Table C3. Also given on this table are the summary of discontinuity sets identified by SRK (SRK, 2009) based on their assessment of the ANDW-08-04 data. Curiously, some of the discontinuity sets identified by Golder for the ANDW-08-04 were not previously identified by SRK. It is uncertain as the procedures used by SRK for selection of their reported sets, therefore some uncertainty surrounds this data.

The selected major and minor discontinuity sets by borehole are given on the stereoplots in Figure C5. There is generally considerable scatter in the selected major sets, as most of the main data trends show an association with major sets as identified in one or more boreholes. A naming convention has been developed for the set



APPENDIX C - STEREONET ANALYSIS

identification based on interpretations of the main data trends associated with bedding, foliation, or inferred fault trends, as discussed later.

Overall, 8 main discontinuity trends were identified at Andrew Lake, and some of these trends were identified with possible sub-sets or localized variations to the major trends. The sets identified as FO1, JN1, JN2, and JN5 appear to be the most representative of the overall rock mass fabric at Andrew Lake. Some interpretation of these sets is given below:

- FO1A (fo1b/fo1c) – sub-horizontal to inclined foliation or bedding set identified in all boreholes, generally dipping between 20 and 55 degrees to the east. Apparently associated with bedding in the metasediments, and possibly foliation/stress-relief in the non-bedded rock units. Identified features include mainly foliation with some veins and joints.
- JN1 (JN1A/JN1B) – inclined set, striking east-west and dipping south between 30 and 60 degrees. Possibly associated with the east-west striking faults identified in the Andrew Lake geology model. Identified as a major set in 3 of 4 boreholes. Associated features include mainly joints, with some veins and occasional shears.
- JN2 (JN2A/JN2B) – sub-vertical set, striking northwest-southeast and dipping steeply either to the northeast or southwest. Trends orthogonal to the main regional fault trends through Andrew Lake possibly associated with stress-relief. Identified as a major set in 2 of 4 boreholes. Identified features include mainly joints, with some veins and occasional shear. Considerable infilling of joints with clay noted for the sub-set JN2A trend.
- JN5 – sub-vertical set, striking near parallel to the main Andrew Lake fault trend (northeast-southwest). Noted as a major set in 3 of 4 boreholes. The main identified features include joints, with some veins and occasional shears.

The delineation of sets is based on limited valid data with only 606 oriented features. Additional structural data collection is suggested for boreholes taken at various orientations to better help define the rock mass fabric for Andrew Lake.



APPENDIX C - STEREONET ANALYSIS

Table C3: Summary of Discontinuity sets for the 2009 Golder, 2008 (SRK), Oriented Core Data at the Andrew Lake Site.

Trend	North-South				Northeast-Southwest				East-West				Southeast-Northwest				Sub-Horizontal to Shallow Inclination (dip 0° to 30°)		
Dip	Sub-Vertical (dip 60° to 90°)		Inclined (dip 30° to 60°)		Sub-Vertical (dip 60° to 90°)		Inclined (dip 30° to 60°)		Sub-Vertical (dip 60° to 90°)		Inclined (dip 30° to 60°)		Sub-Vertical (dip 60° to 90°)		Inclined (dip 30° to 60°)				
Dip Direction	Dip E	Dip W	Dip E	Dip W	Dip SE	Dip NW	Dip SE	Dip NW	Dip N	Dip S	Dip N	Dip S	Dip NE	Dip SW	Dip NE	Dip SW			
Set ID	JN6	-	fo1b/fo1c	JN4B	JN5		-	-	-	-	CJN1A	JN1A/JN1B	JN2A	JN2B	JN3	-	FO1A	CJN1B	JN4A
AND-09-01	63/072 66/055	-	54/093 44/116	54/261 56/288	-	-	-	-	-	-	57/338 69/348	46/155 52/188	79/041	-	63/072 49/056	-	-	32/359 37/336	22/270 29/252 27/290
AND-09-02	-	-	-	60/245	86/141 66/132	-	-	-	-	-	-	51/177 50/205	81/012	70/215 83/234	64/073	-	29/094	27/313	-
AND-09-03	85/078	-	-	50/250	84/123 73/143	-	-	-	-	-	50/341	61/171	70/030	85/203	62/057	-	31/091 16/059	-	-
ANDW-08-04	81/090	-	46/088	68/243	87/113	82/300 63/321	-	-	-	-	62/352	32/180 53/191	-	85/209	41/040	-	22/081	33/316	-
SRK Reported (SRK, 2009)	-	-	-	-	-	75/316	-	-	-	-	-	50/194	-	70/244	-	-	16/186	37/312	-

Upper case set names indicate major sets, lower case set names indicate minor sets. Major sets highlighted in grey. Sets given by dip/dip direction. For Dip Direction: N = North, S = South, E = East, W = West, SE = southeast, NW = northwest, NE = northeast, SW = southwest



APPENDIX C - STEREONET ANALYSIS

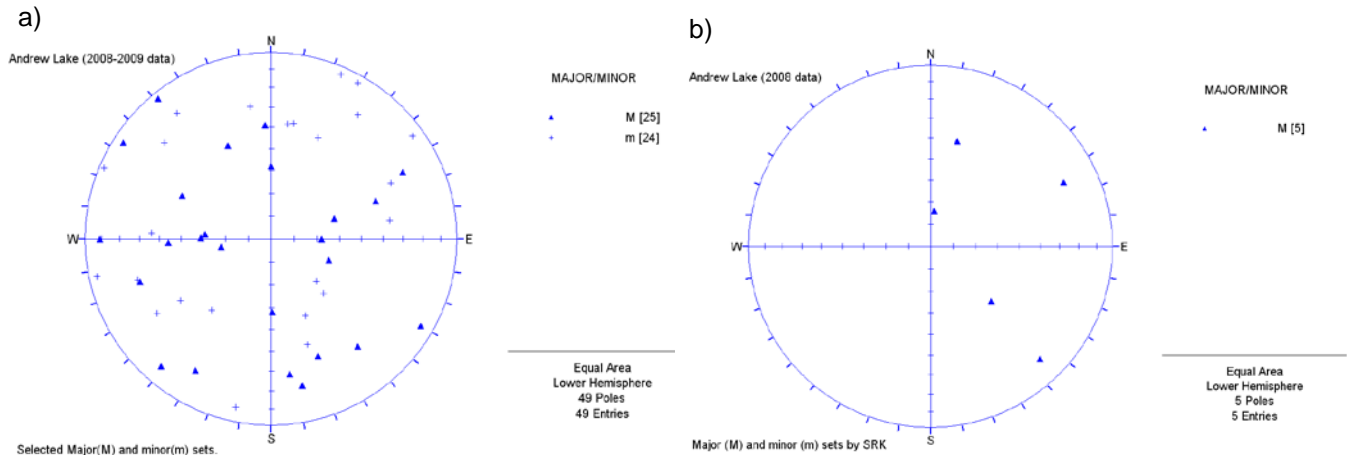


Figure C5: Andrew Lake - Selected Major and Minor Sets by Borehole; a) 2008 & 2009 Sets by Golder; and b) ANDW-08-04 Sets Reported by SRK

3.5 Structural Domains

As part of the analysis of the structural stereonet data, an assessment of structural domains that may be present at Andrew Lake was conducted. A structural domain is an area within the deposit which has different structural conditions from other areas within the deposit. This could be due to a change in rock type, hanging wall versus footwall rocks, proximity to major features, etc.

The Andrew Lake structural data by rock type are plotted in individual stereonet on Figure C6. There is generally shown to be agreement for the highest concentrations of data, representative of sets FO1, JN1, JN2, and JN5. The metasediments show more pole scatter, likely associated with the poorer drilling conditions, as well as potential variability in the rock mass structure in these weaker rock units. Sets FO1 and JN1 are shown to be particularly dominant in the granitic units. Sets FO1 and JN5 are dominant in the gneisses.

Overall it is difficult to make a solid interpretation on the various structural domains for the Andrew Lake pit, as there is a lack of data within the various rock types, as well as a lack of understanding as to the assemblage of the rock units and locations and orientations of the major fault features which might be encountered on the pit walls. For this reason, it was decided to use a single structural domain representative of all available data at Andrew Lake.



APPENDIX C - STEREONET ANALYSIS

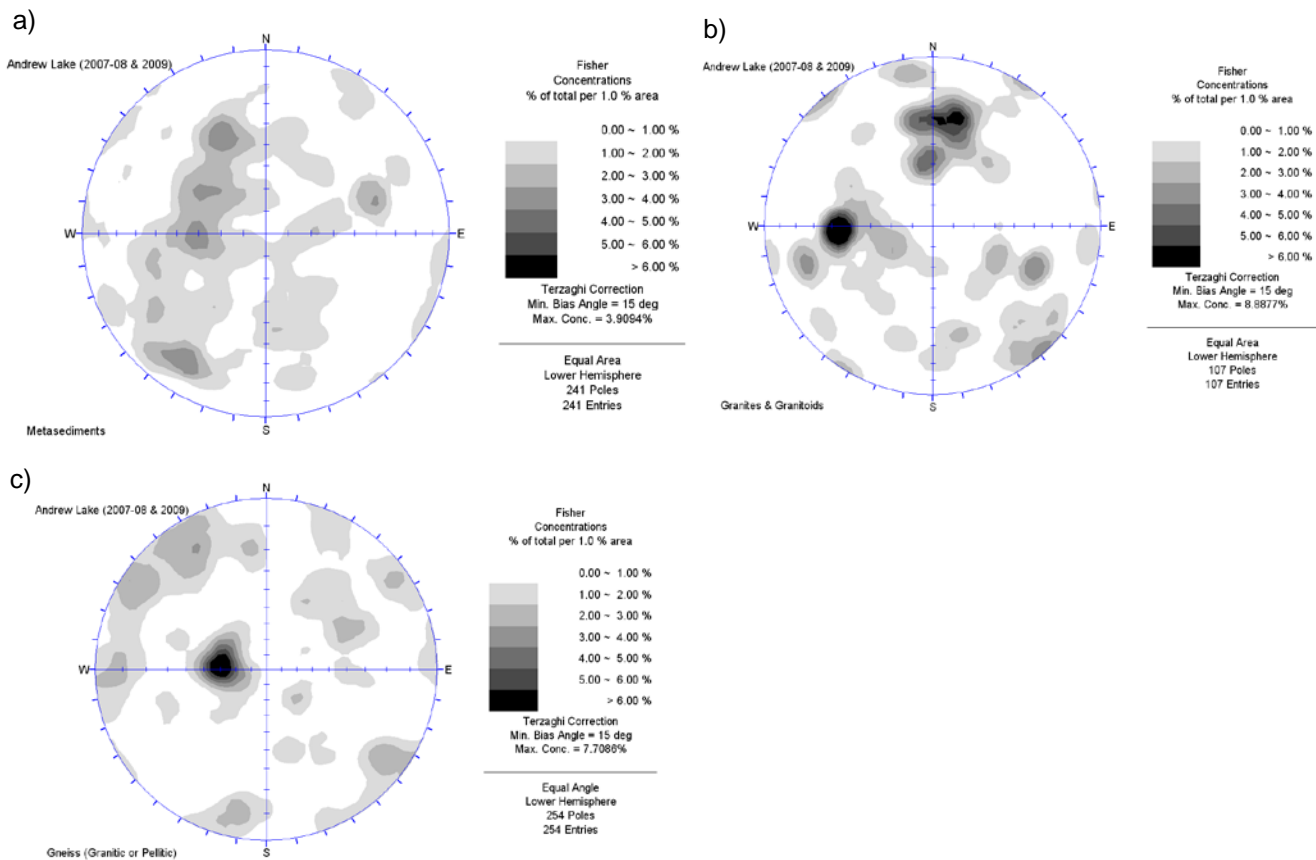


Figure C6: Andrew Lake - Combined 2008 (SRK) and 2009 Data Contoured; a) Metasediments; b) Granites and Granitoids; and c) Gneiss (Granitic or Pelitic)

4.0 DETERMINATION OF STRUCTURAL SETS FOR KINEMATIC ANALYSES

Based on the proceeding discussions related to the oriented core data obtained from the 2009 geotechnical investigation, with data supplemented from the 2008 (SRK) investigations, an assessment was made of major and minor structural sets to be used for kinematic analyses for pit slope design.

At Andrew Lake, there is a general lack of oriented core data for assessment of multiple structural domains, or for making an accurate interpretation as to the deviation of structure within the various rock units. Furthermore, the distribution of data from the oriented boreholes, as well as the data cited from previous investigations, has left some uncertainty as to the definition of major versus minor sets. Therefore all sets were assumed to have equal importance for the kinematic analyses. Additional data supplementing the 2009 investigation included regionally identified fault trends and discontinuity data identified by SRK from the 2008 oriented boreholes. It should be noted that the discontinuity information used from SRK was sourced from the geotechnical database included as Appendix E in the March 2009 version of the geotechnical data report for 20007/2008 (SRK, 2009). Several different sets based on this data were identified in a draft technical memorandum by SRK dated



APPENDIX C - STEREONET ANALYSIS

November 23, 2008. Both the reported and raw data sourced from these documents were considered in supplementing the 2009 data. The selected discontinuity sets for Andrew Lake are presented in Table C4. The selected sets are plotted with the 2008 and 2009 oriented core data (contoured) on Figure C7 for comparison.

5.0 REFERENCES

AREVA Resources Canada Inc. 2007. Kiggavik Project Prefeasibility Report – Section 5 Geology and Resources. Revision 1. Pages 5-1 to 5-4.

Golder Associates Ltd. 1989. Report to Urangesellschaft Canada Limited on the Mining Geotechnical Aspects of the Proposed Kiggavik Uranium Operations. Volume 1 and 2. Project #: 882-1421/881-1814G. August 1989.

Reflex Instruments, 2009. Brochure Reflex ACT (English).

http://reflexinstruments.com/index.php?option=com_content&task=view&id=81&Itemid=92&pmm=3.

Rocscience Inc. 2009a. DIPS Version 5.0 Product Page. <http://www.rocscience.com/products/Dips.asp>

Rocscience Inc. 2009b. DIPS Version 5.108 Manual.

SRK Consulting. 2008a. 2008 Kiggavik Sissons Geotechnical Report (Draft). Project #: 1CA015.003. November 23, 2008.

SRK Consulting. 2008b. Andrew Lake Geological Model. Technical Memorandum. Project #: 4CA005.001. November 27, 2008.

SRK Consulting. 2009. Kiggavik-Sissons Updated Geotechnical Data Report 2007/2008. Project #: 1CA015.003. March 2009.

n:\active\2009\1362\09-1362-0613 areva kiggavik geotechnical baker lake nunavut\pit slope report\final reports - february 2011\andrew lake\app clapp 11 feb 18 andrwe lake appendix c - stereonet analysis final_eam.docx



APPENDIX C - STEREONET ANALYSIS

Table C4: Structural Sets for Kinematic Analysis from Andrew Lake (all sets assumed major for kinematic analysis).

Major Fabric Trends		Structural			Type
Strike/Trend	Dip	Set	Dip	Dip Dir	
N-S	E (sub-horizontal)	FO1A	29	93	Major Foliation Set - appears as the most dominant discontinuity orientation within the Andrew Lake pit area associated with foliation/bedding in the metasediment units but also to a considerable extent in the granitoids. Data trends sub-horizontal to inclined.
E-W	S (inclined)	JN1A	46	163	Major Joint Set - perpendicular to the foliation and may related to a series of E-W striking faults which cross cut the regional fault trend in the Andrew Lake area. Shown to be particularly dominant in the granites/granitoids.
	S (inclined)	JN1B	45	200	
NW-SE	NE (sub-vertical)	JN2A	69	31	Major Joint Set - this set is trending orthogonal the to the regional Andrew Lake Fault orientation. Identified with varying concentrations in all boreholes.
	SW (sub-vertical)	JN2B	73	214	
NW-SE	NE (sub-vertical)	JN3	60	65	Major Joint Set - identified in all four geotechnical boreholes with varying degrees of persistence. Particularly dominant in the upper metasediment units possibly associated with variation on the main FO1 bedding trend.
N-S	W (sub-horizontal)	JN4A	25	257	Major Joint Set - two possible variations to this trend are sub-horizontal or inclined. It appears almost oblique to the major foliation set.
	W (inclined)	JN4B	52	247	
NE-SW	SE (sub-vertical)	JN5	84	135	Major Joint Set – strikes near parallel to the main NE-SW striking regional fault trend at Andrew Lake. Identified as a major set in 3 of 4 boreholes.
E-W	N (inclined)	CJN1A	51	344	Major Joint Set - this joint set is conjugate to JN1 and is inclined to sub-horizontal. It strikes approximately parallel to the E-W fault trend in the Andrew Lake area.
NE-SW	NW (sub-horizontal)	CJN1B	30	317	
N-S	E (sub-vertical)	JN6	82	90	Major Joint Set - this set strikes approximately parallel to the regional fault system in the Andrew Lake area if considering a N-S faulting trend. Identified in 3 of 4 boreholes.

Dip Dir = dip direction; Structural dip and dip direction shown in degrees; JN = joint, FO = foliation, CJN = conjugate joint



APPENDIX C - STEREONET ANALYSIS

09-1362-0613 Kiggavik 2009 Geotech

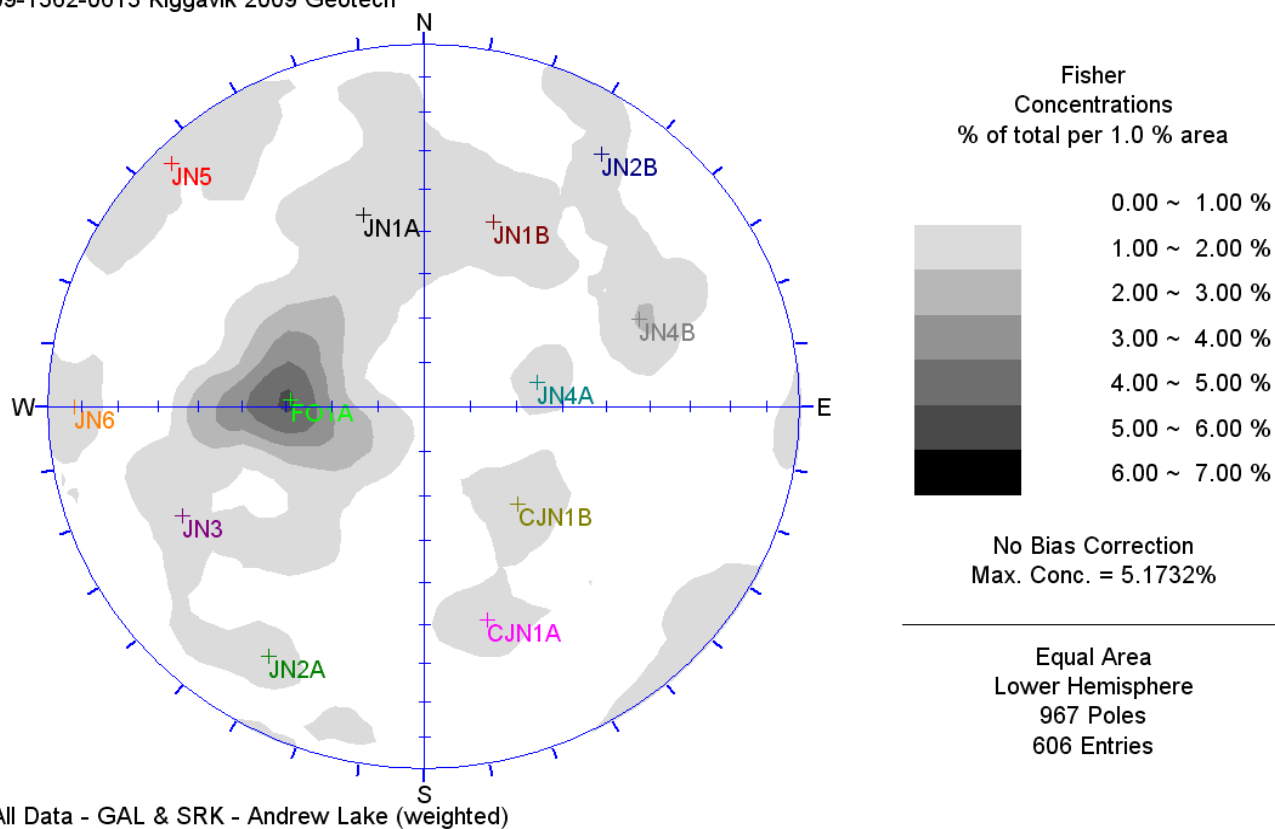
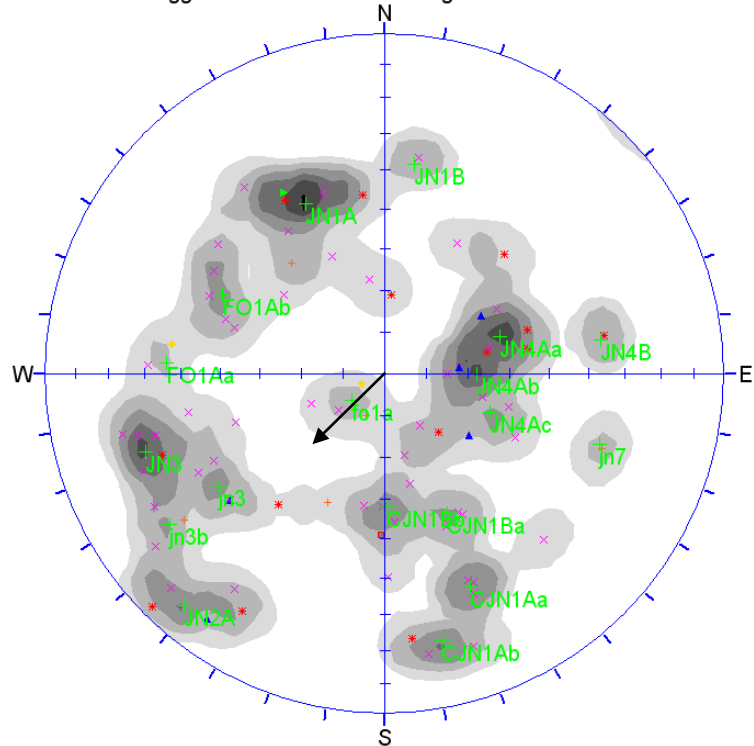


Figure C7: Andrew Lake - 2008 and 2009 Oriented Core Data (contoured) with Selected Structural Sets

Kiggavik – Andrew Lake
Identified Sets By Each Borehole – AND09-01

Figure C8

09-1362-0613 - Kiggavik 2009 Geotech Investigation



AND09-01 - Processed Data (weighted)

TYPE

- CO [1]
- FLT [6]
- FO [1]
- FR [7]
- JN [76]
- OFR [2]
- VN [23]

Fisher
Concentrations
% of total per 1.0 % area



No Bias Correction
Max. Conc. = 6.1116%

Equal Area
Lower Hemisphere
119 Poles
81 Entries

Equal Area
Lower Hemisphere
119 Poles
81 Entries

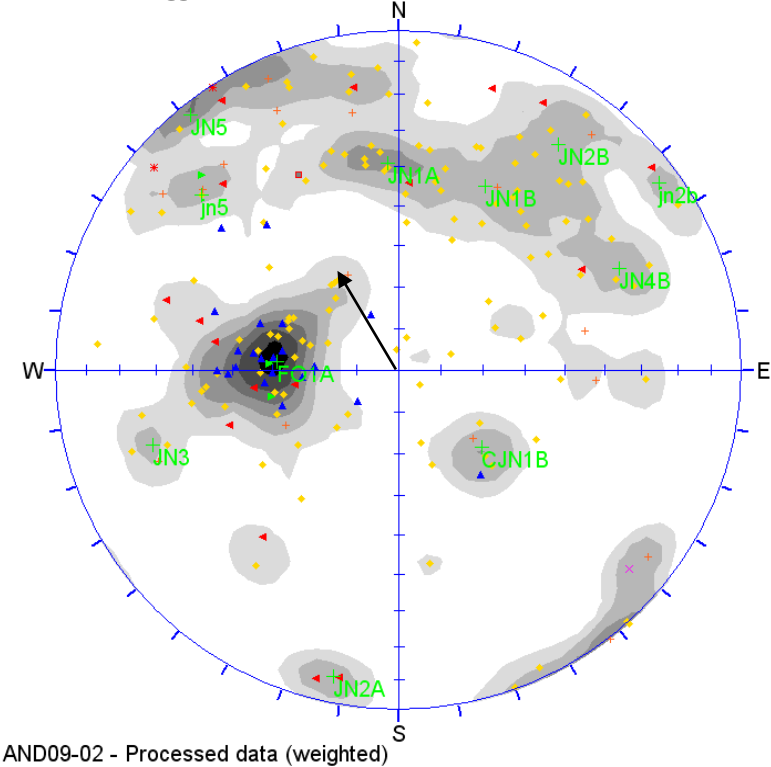
Set	Dip	Dip Dir
FO1Aa	54	93
FO1Ab	44	116
JN1A	46	155
JN1B	52	188
JN2A	79	41
JN3	63	72
JN4Aa	29	252
JN4Ab	22	270
JN4Ac	27	290
JN4B	54	261
CjN1Aa	57	338
CjN1Ab	69	348
CjN1Ba	37	336
CjN1Bb	32	359
fo1a	10	51
jn3	49	56
jn3b	66	55
jn7	56	288

- Shown are the processed data files with a Terzaghi weighting applied. The number of entries indicate the total number of data points considered, which are shown as poles in the stereonet. The number of poles shown is the Terzaghi weighted value that the Fisher concentration contours are based on.
- Upper case indicates major sets, lower case indicates minor sets
- FO = foliation, JN = joint set, CjN = conjugate joint set, Dip Dir = Dip Direction
- Orientations (Dip and Dip Direction) are based on selected peak pole concentrations, based on the Fisher Concentration contours
- Major sets were selected based on its continuity between boreholes, and its orientation with respect to regional structure
- Major sets with a lower case letter following the name (i.e., FO1Aa) indicate different peaks which were interpreted to occur within the same set due to inherent scatter within the data.
- the arrow indicates the borehole orientation

Kiggavik – Andrew Lake
Identified Sets By Each Borehole – AND09-02

Figure C9

09-1362-0613 Kiggavik 2009 Geotech



AND09-02 - Processed data (weighted)

TYPE

- FLT [1]
- FO [24]
- HFO [3]
- HJN [29]
- HVN [3]
- JN [194]
- SH [4]
- VN [33]

Fisher
Concentrations
% of total per 1.0 % area



- 0.00 ~ 1.00 %
- 1.00 ~ 2.00 %
- 2.00 ~ 3.00 %
- 3.00 ~ 4.00 %
- 4.00 ~ 5.00 %
- 5.00 ~ 6.00 %
- 6.00 ~ 7.00 %

No Bias Correction
Max. Conc. = 6.3552%

Equal Area
Lower Hemisphere
294 Poles
187 Entries

Equal Area
Lower Hemisphere
294 Poles
187 Entries

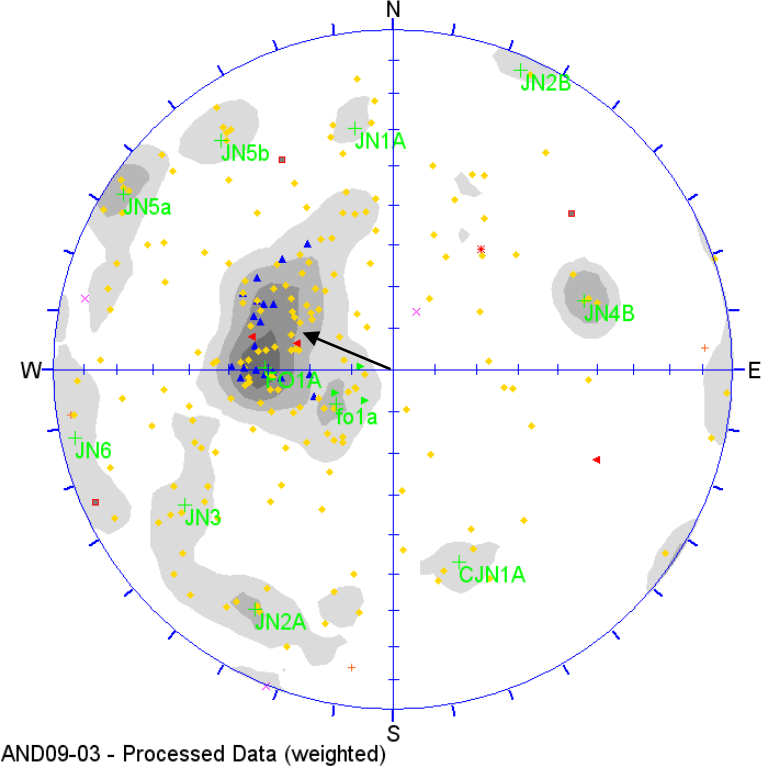
Set	Dip	Dip Dir
FO1A	29	94
JN1A	51	177
JN1B	50	205
JN2A	81	12
JN2B	70	215
JN3	64	73
JN4B	60	245
JN5	86	141
CJN1B	27	313
jn2b	83	234
jn5	66	132

- Shown are the processed data files with a Terzaghi weighting applied. The number of entries indicate the total number of data points considered, which are shown as poles in the stereonet. The number of poles shown is the Terzaghi weighted value that the Fisher concentration contours are based on.
- Upper case indicates major sets, lower case indicates minor sets
- FO = foliation, JN = joint set, CJN = conjugate joint set, Dip Dir = Dip Direction
- Orientations (Dip and Dip Direction) are based on selected peak pole concentrations, based on the Fisher Concentration contours
- Major sets were selected based on its continuity between boreholes, and its orientation with respect to regional structure
- Major sets with a lower case letter following the name (i.e., FO1Aa) indicate different peaks which were interpreted to occur within the same set due to inherent scatter within the data.
- the arrow indicates the borehole orientation

Kiggavik – Andrew Lake
Identified Sets By Each Borehole – AND09-03

Figure C10

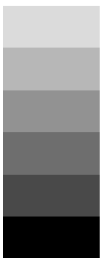
09-1362-0613 Kiggavik 2009 Geotech



TYPE

- FLT [7]
- FO [21]
- HFO [3]
- HJN [10]
- HSH [7]
- JN [287]
- SH [1]
- VN [5]

Fisher
Concentrations
% of total per 1.0 % area



No Bias Correction
Max. Conc. = 7.2320%

Equal Area
Lower Hemisphere
344 Poles
219 Entries

Equal Area
Lower Hemisphere
344 Poles
219 Entries

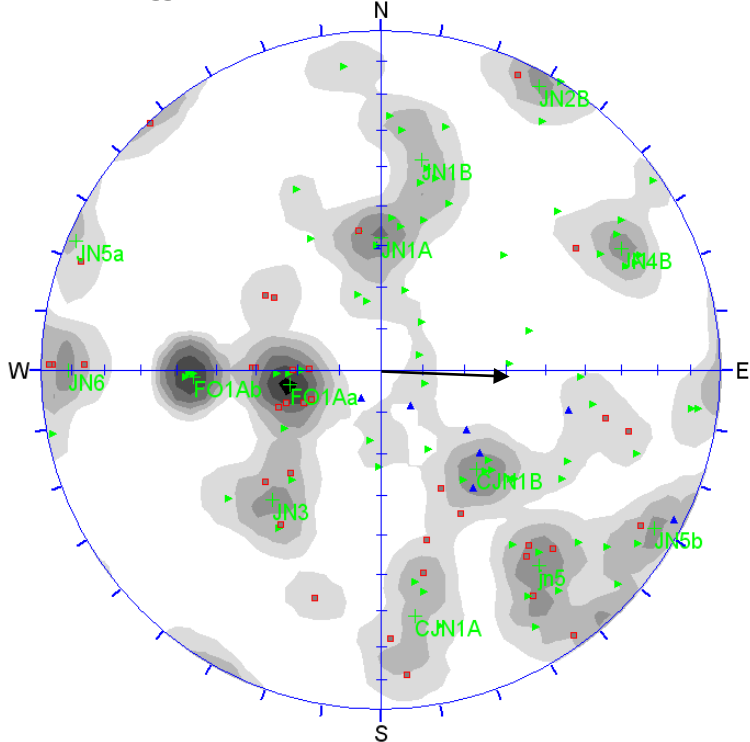
Set	Dip	Dip Dir
FO1a	31	91
JN1A	61	171
JN2A	70	30
JN2B	85	203
JN3	62	57
JN4B	50	250
JN5a	84	123
JN5b	73	143
CJN1A	50	341
JN6	85	78
fo1a	16	59

- Shown are the processed data files with a Terzaghi weighting applied. The number of entries indicate the total number of data points considered, which are shown as poles in the stereonet. The number of poles shown is the Terzaghi weighted value that the Fisher concentration contours are based on.
- Upper case indicates major sets, lower case indicates minor sets
- FO = foliation, JN = joint set, CJN = conjugate joint set, Dip Dir = Dip Direction
- Orientations (Dip and Dip Direction) are based on selected peak pole concentrations, based on the Fisher Concentration contours
- Major sets were selected based on its continuity between boreholes, and its orientation with respect to regional structure
- Major sets with a lower case letter following the name (i.e., FO1Aa) indicate different peaks which were interpreted to occur within the same set due to inherent scatter within the data.
- the arrow indicates the borehole orientation

Kiggavik – Andrew Lake
Identified Sets By Each Borehole – ANDW-08-04
(as logged by SRK Consulting in 2008)

Figure C11

09-1362-0613 Kiggavik 2009 Geotech - SRK DATA



ANDW-08-04 - Processed Data (weighted)

TYPE

CJ [72]
FO [13]
JN [122]

Fisher
Concentrations
% of total per 1.0 % area



No Bias Correction
Max. Conc. = 6.4069%

Equal Area
Lower Hemisphere
208 Poles
119 Entries

Equal Area
Lower Hemisphere
208 Poles
119 Entries

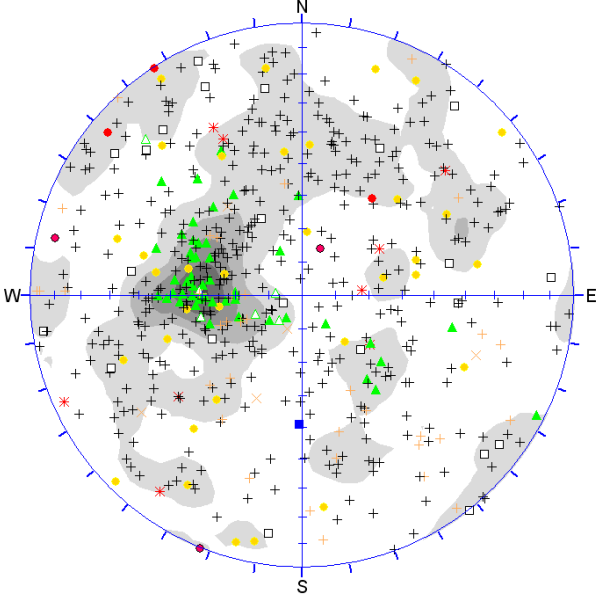
Set	Dip	Dip Dir
FO1Aa	22	81
FO1Ab	46	88
JN1A	32	180
JN1B	53	191
JN2B	85	209
JN3	41	40
JN4B	68	243
JN5a	87	113
JN5b	82	300
jn5	63	321
CJN1A	33	316
CJN1B	62	352
JN6	81	90

- Shown are the processed data files with a Terzaghi weighting applied. The number of entries indicate the total number of data points considered, which are shown as poles in the stereonet. The number of poles shown is the Terzaghi weighted value that the Fisher concentration contours are based on.
- Upper case indicates major sets, lower case indicates minor sets
- FO = foliation, JN = joint set, CJN = conjugate joint set, Dip Dir = Dip Direction
- Orientations (Dip and Dip Direction) are based on selected peak pole concentrations, based on the Fisher Concentration contours
- Major sets were selected based on its continuity between boreholes, and its orientation with respect to regional structure
- Major sets with a lower case letter following the name (i.e., FO1Aa) indicate different peaks which were interpreted to occur within the same set due to inherent scatter within the data.
- the arrow indicates the borehole orientation

Kiggavik – Andrew Lake
All Validated Data with Symbolic Pole Plots
Feature Type & Discontinuity Alteration Index

Figure C12

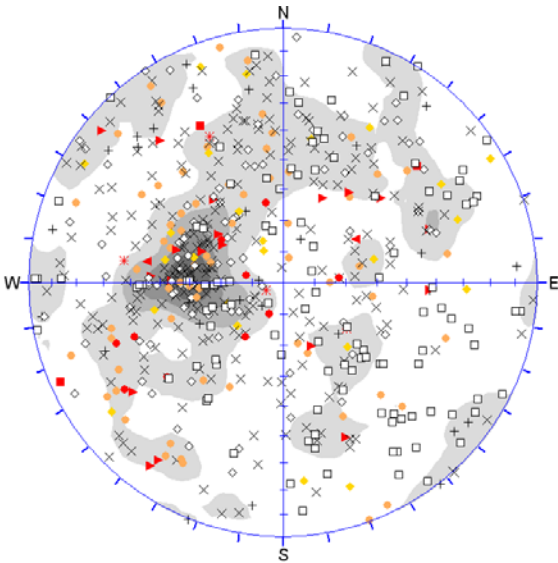
a) All valid data – Type of Feature



- TYPE
- + CJ [36] Cross-joint
 - CO [1] Contact
 - * FLT [9] Fault
 - ▲ FO [53] Foliation
 - × FR [5] Fracture
 - △ HFO [6] Healed Foliation
 - ◆ HSH [3] Healed Shear
 - + JN [434] Joint
 - SH [3] Shear
 - VN [34] Vein
 - Others [22]

Equal Area
Lower Hemisphere
606 Poles
606 Entries

b) All valid data – Discontinuity Alteration Index (Ja)



- JA
- + 0.75 [29] Healed
 - × 1 [233] Clean
 - 10 [3] Clay Infilled
 - * 15 [4] Clay Infilled
 - ◇ 2 [97] Slightly altered
 - 3 [25] Hard coating
 - 4 [65] Soft coating
 - 5 [2] Hard infilling
 - 6 [19] Clay Infilling
 - 8 [10] Clay Infilling
 - Others [119]

Equal Area
Lower Hemisphere
606 Poles
606 Entries



**GEOTECHNICAL RECOMMENDATIONS FOR THE PROPOSED
ANDREW LAKE OPEN PIT - SUPPORT DOCUMENT FOR PERMIT
APPLICATION**

APPENDIX D

Rock Mass Stability Analysis



Table of Contents

1.0 INTRODUCTION.....	1
2.0 SLOPE STABILITY ANALYSES	1
2.1 SLOPE MODEL CONFIGURATIONS.....	1
2.1.1 Generalized Rock Mass Slope Configurations.....	1
2.1.2 Material Parameters.....	3
2.1.3 Tension Cracking and Water Conditions.....	6
2.2 ANDREW LAKE PIT SLOPE STABILITY	6
3.0 FLOOR HEAVE STABILITY ANALYSES	11
3.1 METHODOLOGY	11
3.2 FLOOR HEAVE ANALYSIS RESULTS	12
4.0 REFERENCES.....	13

TABLES

Table D1: Slope Stability Analyses - Rock Mass Parameters.	4
Table D2: Andrew Lake - Recommended Maximum Slope Angles for Rock Mass Slope Stability, Full 270 m Slope Height.	10
Table D3: Permafrost depths and hydraulic heads used in the floor heave analyses.	11
Table D4: Floor Heave Analyses - Rock mass parameters.....	11
Table D5: Recommended critical depths at which remedial measures such as vertical pressure relief drains may be required to prevent floor heave – self weight and rock mass failure.	13

FIGURES

Figure D1: Andrew Lake Generalized Pit Slope Configurations for Stability Analyses	2
Figure D2: Andrew Lake Slope Stability Assessment Slide Model Configurations	5
Figure D3: Andrew Lake Slope Stability Assessment Slide Analysis Results.....	7
Figure D4: Andrew Lake Type 1 Slope - Slope Angle versus Factor of Safety for the Full Slope Altered Rock Mass Configuration	8
Figure D5: Andrew Lake Type 2 Slope - Slope Angle versus Factor of Safety for the Lower Slope Altered Rock Mass Configuration	9
Figure D6: Andrew Lake Type 3 Slope - Slope Angle versus Factor of Safety for the Non-Altered Rock Mass Configuration	10
Figure D7: General Representation of the Components Used in the Floor Heave Analysis.....	12
Figure D8: Andrew Lake - Floor Heave Analysis Results Showing Differential Pressure versus Pit Depth.....	12



1.0 INTRODUCTION

This appendix presents the results of the rock mass stability assessments carried out for the Andrew Lake pit. The stability assessments included limit equilibrium slope stability analyses, as well as floor heave stability analyses. The slope stability analyses were conducted for generalized two-dimensional rock mass slope configurations developed from the information and interpretations presented and developed in the previous appendices. Various rock mass strengths and qualities were assessed in order to estimate pit slope angles which would achieve a reasonable and representative factor of safety against deep-seated rock mass failure.

The floor heave stability analyses were developed to assess the potential for floor heave due to the high artesian water pressures acting at depths below the permafrost line within the pit floors. The floor heave stability analysis results are intended to provide a range of conservative thicknesses of pit floor above the permafrost zone at which time remedial measures such as vertical drains could be installed to depressurize the pit floor.

The following appendix presents the methodology and results of the rock mass stability assessments.

2.0 SLOPE STABILITY ANALYSES

2.1 SLOPE MODEL CONFIGURATIONS

2.1.1 Generalized Rock Mass Slope Configurations

The limit equilibrium slope stability analysis software Slide® v.5 (Rocscience Inc.) was used for assessing the stability of the design slopes against deep seated rock mass failure. Parametric trials assessing the factor of safety versus slope inclination were conducted for the various slope geometries and material configurations.

The slope configurations and engineering geology conditions used for slope stability analyses for Andrew Lake are presented in Figure D1. The material properties for the various slope configurations were inferred from the results of the rock strength (Appendix A) and rock mass classification work (Appendix B).